

Swarm

Level 1b Processor Algorithms

National Space Institute
Technical University of Denmark

DOC. No. & ISSUE: SW-RS-DSC-SY-0002, Issue 6.10c

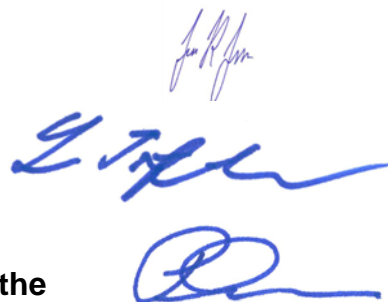
DATE: 2017-01-27

PREPARED BY: Jonas Bregnhøj Nielsen

APPROVED BY: Lars Tøffner-Clausen

AUTHORIZED BY: Poul Erik Holmdahl Olsen

CLASSIFICATION: Restricted: For use within the
ESA Swarm project only



This page is intentionally left blank

PAGE ISSUE RECORD

This Document consists of the following pages at the issues shown

| Document | Pages | Issue | File Name and Format |
|-------------------|---------|-------|---|
| SW-RS-DSC-SY-0002 | 1 - 45 | 1 | Filename: Swarm_Level_1b_Processor_Algorithms_iss_1 Format: PDF |
| SW-RS-DSC-SY-0002 | 1 - 48 | 2 | Filename: Swarm_Level_1b_Processor_Algorithms_iss_2 Format: PDF |
| SW-RS-DSC-SY-0002 | 1 - 411 | 3 | Filename: Swarm_Level_1b_Processor_Algorithms_iss_3 Format: PDF |
| SW-RS-DSC-SY-0002 | 1 - 124 | 4 | Filename: Swarm_Level_1b_Processor_Algorithms_iss_4 Format: PDF |
| SW-RS-DSC-SY-0002 | 1 – 134 | 5 | Filename: Swarm_Level_1b_Processor_Algorithms_iss_5 Format: PDF |
| SW-RS-DSC-SY-0002 | 1 – 134 | 5.1 | Filename: Swarm_Level_1b_Processor_Algorithms_iss_5.1 Format: PDF |
| SW-RS-DSC-SY-0002 | 1 – 152 | 5.2 | Filename: Swarm_Level_1b_Processor_Algorithms_iss_5.2 Format: PDF |
| SW-RS-DSC-SY-0002 | 1 – 159 | 6 | Filename: Swarm_Level_1b_Processor_Algorithms_iss_6 Format: PDF |
| SW-RS-DSC-SY-0002 | 1 – 161 | 6.1 | Filename: Swarm_Level_1b_Processor_Algorithms_iss_6.1 Format: PDF |
| SW-RS-DSC-SY-0002 | 1 – 162 | 6.2 | Filename: Swarm_Level_1b_Processor_Algorithms_iss_6.2 Format: PDF |
| SW-RS-DSC-SY-0002 | 1 – 151 | 6.3 | Filename: Swarm_Level_1b_Processor_Algorithms_iss_6.3 Format: PDF |
| SW-RS-DSC-SY-0002 | 1 – 152 | 6.4 | Filename: Swarm_Level_1b_Processor_Algorithms_iss_6.4 Format: PDF |
| SW-RS-DSC-SY-0002 | 1 – 153 | 6.5 | Filename: Swarm_Level_1b_Processor_Algorithms_iss_6.5 Format: PDF |

| Document | Pages | Issue | File Name and Format |
|-------------------|---------|-------|--|
| SW-RS-DSC-SY-0002 | 1 – 157 | 6.6 | Filename: SW-RS-DSC-SY-0002_Level_1b_Processor_Algorithms Format: PDF |
| SW-RS-DSC-SY-0002 | 1 – 157 | 6.7 | Filename: Swarm_Level_1b_Processor_Algorithms_iss_6.7 Format: PDF |
| SW-RS-DSC-SY-0002 | 1 – 157 | 6.8 | Filename: Swarm_Level_1b_Processor_Algorithms_iss_6.8 Format: PDF |
| SW-RS-DSC-SY-0002 | 1 – 157 | 6.9 | Filename: Swarm_Level_1b_Processor_Algorithms_iss_6.9 Format: PDF |
| SW-RS-DSC-SY-0002 | 1 – 157 | 6.10c | Filename: Swarm_Level_1b_Processor_Algorithms. Format: PDF |
| SW-RS-DSC-SY-0002 | 1 – 157 | 6.10c | Filename: Swarm_Level_1b_Processor_Algorithms. Format: PDF |

DOCUMENT CHANGE LOG

| Issue | Change References | Issue Date | Pages Affected | Remarks | Init. |
|-------|-------------------|------------|---|--|------------|
| 1 | | 2006-09-15 | All | Initial Issue | LTC |
| 2 | | 2006-11-01 | 9 – 35 | Added Section 4 on global processing overview. Updated figures and descriptions accordingly. Various minor updates | LTC |
| 3 | | 2007-02-05 | All | Added missing sections Major update of Sections 4 and 5 especially related to instrument transfer functions Added appendices | HF LTC |
| 4 | | 2007-04-27 | All | Updated according to Level 1b Requirements Review – in particular: Added Section 5: Level 0 Processing Replaced inclusions of documents in Appendices E through J by links | |
| 5 | | 2007-09-07 | All | Various minor changes to complete Level 1b Requirements Review. | LTC FCH |
| 5.1 | | 2007-10-05 | 38-41,43, 46,49-51, 56-57, 62-63,69, 79-83, | Updated calculation of magnetic stray fields, updated EFI CCDB parameters, added fundamental constants to CCDB, and a few minor corrections | LTC FCH |
| 5.2 | | 2008-03-10 | Many | Updated calculation of flags. Adopted changes to CCDB – in particular look-up tables and filters. Added new Appendix E with associated (and other) functions. Various other updates aimed at Operational Level 1b Procurement KO | LTC |

| Issue | Change References | Issue Date | Pages Affected | Remarks | Init. |
|-------|-------------------|------------|--|--|-------|
| 6 | | 2008-11-18 | Many | <p>Updated according to implementation plan by L1b S/W supplier.</p> <p>Updated according to changes in CCDB and Level 1b Products.</p> <p>TCF.VFM estimation data selection procedure switched to alternate method.</p> <p>ACC processing revised</p> <p>Added CurrentInfo, StateInfo, and InducedInfo and more Level 0 to Level 1a conversion description</p> <p>Updated according to revised magnetically induced field computation</p> | LTC |
| 6.1 | | 2008-12-12 | 17,21-28, 39,46, 54-55,66, 69,71-74, 77,83-84, 87,88,125 | <p>Added more Level 0 to Level 1a conversions</p> <p>Corrected and updated $B_{ambient}$ for induced stray fields, and various inconsistencies in Current/State/Induced Info description</p> <p>Added missing “.Structure” to CCDB elements</p> | LTC |
| 6.2 | | 2009-07-10 | 20, 21, 29, 41, 60, 63, 66-68, 73-75, 78-79, 83, 85-87, 94, 95, 121-123, 127-128 | <p>Updated STR processing – direction of transformation in data and aberrational correction</p> <p>Update VFM decoding and added VFM DPU identification</p> <p>Updated sample selection for TCF.VFM estimation</p> <p>Increased Mag-C sampling rate to 1 Hz and updated contents</p> <p>Updated EFI section</p> <p>Removed torque parts of Solar radiation pressure from ACC</p> <p>Added leap-second processing description</p> | LTC |

| Issue | Change References | Issue Date | Pages Affected | Remarks | Init. |
|-------|-------------------|------------|--|---|-------|
| 6.3 | | 2010-06-29 | 23-32, most pages 35-79, 109-117, 128-130, 137, 139-140 | <p>Adopted to latest structure and changes of CCDB (introduction of LIBP section, re-arrangement of parameters, update of units) including corresponding updates of in particular processing of: battery currents, AOCS torque response, and stray fields.</p> <p>Moved Level 0 to Level 1a conversions from IMDD to CCDB.TMC.</p> <p>Corrected VFM and ASM Data Conversion (Sections 5.4.7 and 5.4.8)</p> <p>Added CCDB.AOCS. Thruster_Settling_Time</p> <p>Added ASM_Freq_Dev computation</p> <p>Huber weights limited to range]0..1]</p> <p>VFM processing updated: range, temperatures, delays, and flags</p> <p>Corrected STR CHU combination.</p> <p>Updated STR flags.</p> <p>Updated ACC processing, added temperature weights</p> <p>New Tank Level1a data and temperatures computation</p> <p>Corrected description of B-spline knots and acceleration damping weights</p> <p>Corrected various typing errors and some unclear points.</p> | LTC |
| 6.4 | | 2010-12-03 | 40, 45f, 56-58, 62, 64-71, 126, 138, 152 | <p>Clarified selection and application of TCF.VFM records, a.o. changed TCF.VFM^{input} into TCF.VFM^{init}.</p> <p>Simplified VFM DPU_id handling by rejection of DPU_id-minority data.</p> <p>Modified ASM and VFM</p> | LTC |

| Issue | Change References | Issue Date | Pages Affected | Remarks | Init. |
|-------|-------------------|------------|--|---|-------|
| | | | | <p>outlier detection.</p> <p>Corrected a-priori term, added Huber weight factor (for L1bOP CDR-3), and modified convergence limit in TCF.VFM estimation</p> <p>Changed from linear to cubic interpolation of F_{ASM} for Mag-H.Flags_B computation (Table 6-8)</p> <p>Corrected small error in gap filling of Filter function</p> <p>Updated reference frame definitions (App C)</p> <p>Updated ACC document reference (App L)</p> | |
| 6.5 | | 2011-06-24 | 39, 40, 84, 110, 116-118, | <p>Clarification of $B_{ambient}$</p> <p>Harmonized units of Bus currents (changed mA to A)</p> <p>Added information on CCDB. Structure.CrossSection</p> <p>Corrected ACC timestamp (Eq. 8.3-10), centrifugal acceleration (angular velocity), and a_{GG} computations</p> | LTC |
| 6.6 | | 2012-05-08 | 22 31 36 41, 50, 51 49 68 71 79 77 | <p>Specified which products contain leap second data</p> <p>Corrected timestamping of VFM data.</p> <p>Update of HK_Source for VFM temperatures</p> <p>Corrected location of ASM.Filter from CCDB.L1BP to CCDB</p> <p>Specified timestamps (t) for ASMxAUX_1B product</p> <p>Corrected storing of W_scale values as \log_{10}.</p> <p>Specified values for dB_{AOCS} and dB_{other} in Mag-L Product</p> <p>Added Mag-L.Flags_B value 255</p> <p>Specify STR pair to use if only one pair is inconsistent.</p> | LTC |

| Issue | Change References | Issue Date | Pages Affected | Remarks | Init. |
|-------|--|------------|--------------------------------------|---|-------|
| | | | 79 88 128 130 global | Deleted last paragraph on obsolete STR flag computation Flags _q clarification and addition of values 35 and 54 Specified spherical coordinates Specified removal of knots for very short data segments Corrected XXXx_AUX1B names to XXXxAUX_1B | |
| 6.7 | | 2014-04-04 | 60, 59 93, 98 96-97 154-156 | Corrected VFM DPU_id value 1 to 2 (Section 6.3.2) SPR-245: Clarification of GPSR_r and ARP_r CCDB parameters for GPSR (Section 8.1) Clarification of calculation of pitch, roll, and yaw for GPSR processing (Section 8.1.3) Updated references to TII, LP, and GPSR algorithm documents (Appendix I, J, and K) | LTC |
| 6.8 | AI-261 SPR-39 AI-259 AI-225 | 2014-08-29 | 38 44 57 64 120 | Adjusted VFM sampling frequency to <i>approximately</i> 50 Hz (Table 6-1) Corrected condition for $I_{AOCs,VFM}$, Eq. (6.1-27b) Corrected weights for ASM B-Spline interpolation, Eq. (6.2-190) Specified rejection of initial VFM samples, Section 6.3.3 Corrected sign of acceleration corrections, \mathbf{a}_{GG} and \mathbf{a}_{centr} , Eqs. (8.3-50) and (8.3-60). | LTC |

| Issue | Change References | Issue Date | Pages Affected | Remarks | Init. |
|-------|--|------------|--|--|-------|
| 6.9 | AI-286 UPID-23 ¹ UPID-17 UPID-18 UPID-19 UPID-20 UPID-21 UPID-24 | 2014-12-09 | 31 36-37 56 76 73 79 79, 85 134 66 | Corrected EFI timestamps Added STR false leap second correction Clarified computation/ interpolation of dF_{AOCs} and dF_{other} for Mag-C and Mag-L products Corrected which VFM samples form the basis for Mag-H Added sanity-check on residual scaling in VFM sampling reduction Clarified time window for computing $Mag-L.Flags_{Platform}$ Added lower limits on attitude uncertainties Modified formula for <i>fade-out</i> B-spline knots to account for short data sequences Corrected typo (extra “(“) | LTC |
| 6.10 | UPID-25 UPID-26 UPID-2 UPID-31 | 2015-07-13 | 69-70 76 83-85 134 154, 155 | Added $d\mathbf{B}_{Sun}$ stray field Generation of Mag-C product when no ASM data Include BBO and lost-in-space STR samples B-spline knot generation for very short segments Updated versions of EFI algorithm documentation | LTC |
| 6.10a | | 2015-10-20 | 63 76 | Added $d\mathbf{B}_{Sun}$ stray field to table of outputs Added $d\mathbf{B}_{Sun}$, \mathbf{B}_{pre} , alpha and beta to table of MAG-C product elements | JBN |
| 6.10b | | 2015-12-07 | 70, 72-73 | Added s_{β} and s_{exp} to Eqs. (6.3-180), (6.3-230) and (6.3-280) | JBN |

¹ UPID refers to planned update ID's in Section 3 of SW-PL-DTU-GS-008, "Planned Updates for Level 1b"

| Issue | Change References | Issue Date | Pages Affected | Remarks | Init. |
|-------|-------------------|------------|---------------------------------------|--|-------|
| 6.10c | | 2017-01-27 | 50 76 79 135-136 | Corrected $F_{err}^{(3)}$ equation in Figure 6-4 Corrected Mag-C F_{error} description in Table 6-7 Added footnote about 1% slack in Table 6-10 at Mag-H/L $Flags_{Platform}$ values 4 and 128 Section 8.3.3.10: Corrected “min” to “max” in text. Added “if statement” and corrected “with” and “W” calculation in text and MATLAB code. | JBN |

| Table of Contents | Page |
|--|-------------|
| 1 Introduction | 14 |
| 1.1 Scope | 14 |
| 2 Applicable and Reference Documents | 15 |
| 2.1 Applicable Documents | 15 |
| 2.2 Reference Documents | 16 |
| 3 Introduction | 18 |
| 3.1 Terminology | 18 |
| 4 Processing Overview | 20 |
| 4.1 Detailed Data Flow | 22 |
| 4.2 Re-processing | 24 |
| 4.3 Time-series | 25 |
| 4.4 Corrections | 25 |
| 4.5 Timestamps | 26 |
| 4.6 Leap Seconds | 26 |
| 5 Level 0 Processing | 28 |
| 5.1 Quality and Validity Checks | 28 |
| 5.2 Data Coordination and Combination | 29 |
| 5.3 Datation of Data | 30 |
| 5.4 Conversions from Level 0 to Level 1a | 31 |
| 5.5 Level 1a Data Description | 37 |
| 6 Magnetic and Attitude Data Processing | 38 |
| 6.1 Magnetic Stray Fields | 40 |
| 6.2 Absolute Scalar Magnetometer – ASM | 46 |
| 6.3 Vector Field Magnetometer – VFM | 60 |
| 6.4 Star Tracker – STR | 80 |
| 7 Electric Field Instrument - EFI | 90 |
| 7.1 Introduction | 90 |
| 7.2 Input and Output Parameters | 90 |
| 7.3 Algorithms | 94 |
| 8 Position and Acceleration | 95 |
| 8.1 GPS Receiver - GPSR | 95 |
| 8.2 Orbit Determination | 104 |
| 8.3 Accelerometer – ACC | 119 |

Appendices

| | | |
|-----------|-------------------------------------|-----|
| A. | Abbreviations & Acronyms | 128 |
| B. | Quaternions | 129 |
| C. | Reference Frames | 131 |
| D. | B-Splines | 133 |
| E. | Miscellaneous Functions | 142 |
| F. | ASM Algorithm Descriptions | 151 |
| G. | VFM Algorithm Description | 152 |
| H. | STR Algorithm Description | 153 |
| I. | EFI-TII Algorithm Description | 154 |
| J. | EFI-LP Algorithm Description..... | 155 |
| K. | GPSR Algorithm Description | 156 |
| L. | ACC Algorithm Description | 157 |

1 Introduction

1.1 Scope

The present document is prepared as part of the Swarm Level 1b Data Processing specification. The description of the algorithms for the Level 1b processing is contained herein.

2 Applicable and Reference Documents

2.1 Applicable Documents

The documents listed below are applicable in their latest issue and revision.

- AD01 Swarm Level 0 Products
Doc. No. SW.IF.EAD.GS.00017
EADS Astrium

- AD02 Swarm Level 1b Product Definition
Doc. No. SW-RS-DSC-SY-0007
National Space Institute, Technical University of Denmark

- AD03 Swarm Level 1b Processor Characterisation and Calibration Data Base
Doc. No. SW-TN-DSC-SY-0005
National Space Institute, Technical University of Denmark

- AD04 Swarm Level 1b Processor Justification
Doc. No. SW-TN-DSC-SY-0003
National Space Institute, Technical University of Denmark

- AD05 Swarm ASM level 1B algorithms
Doc. No. AUT/ALGO1B/001
LETI, France

- AD06 Vector Field Magnetometer for the Swarm Project, Users Manual
Doc. No. SW-MA-DTU-VF-5001
Danish Technical University

- AD07 micro Advanced Stellar Compass User's Manual
Doc. No. ASC-DTU-MA-3001
Danish Technical University

- AD08 Swarm CEFI Level 1b Processor Definition
Doc. No. SW-TN-UOC-EF-003
University of Calgary, Canada

- AD09 Swarm CEFI-LP Level 1b Algorithms
Doc. No. SW-TN-IRF-EF-003
Swedish Institute of Space Physics

- AD10 Swarm Mathematical Conventions
Doc. No. SW.TN.EAD.SY.00031
EADS Astrium, Germany

- AD11 Swarm GPSR TE-12 Instrument L1b Algorithms Definition
Doc. No. SW-TN-SES-GP-0018
Saab Space AB, Sweden

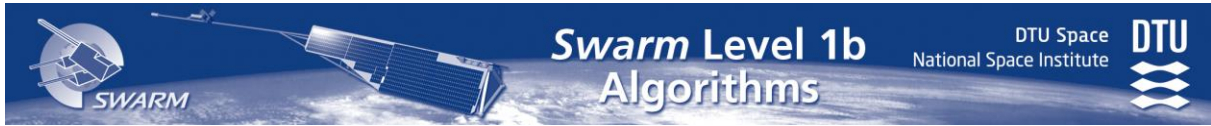
- AD12 Swarm Phase B, Level 1b Processor, MOD Processing
Doc. No. SW-TN-DSC-SY-0015
National Space Institute, Technical University of Denmark

- AD13 Accelerometer Instrument Level 1b Algorithms Definition
Doc. No. SW-DF-VZL-AC-0001
VZLU, Czech Republic

AD14 Swarm Level 1A Product Definition
Doc. No. SW-ID-GMV-GS-0003
GMV Aerospace and Defense, Spain

2.2 Reference Documents

- RD1 Calibration of the Ørsted Vector Magnetometer
Nils Olsen et.al.
Earth Planets Space, 55, 11–18, 2003
http://www.spacecenter.dk/~nio/papers/EPS_55010011.pdf
- RD2 Data Sampling Rate Reduction for the OERSTED Geomagnetic Satellite
P.B. Stark
<http://www.stat.berkeley.edu/~stark/Preprints/Oersted/writeup.htm>
- RD3 Optimal combination of quaternions from multiple star cameras
L.J. Romans
ftp://podaac.jpl.nasa.gov/pub/grace/doc/quaternion_memo.pdf
Note: The definition of quaternions used in this description differs from the one used here. Our definition has the real part as fourth component, Romans uses a definition with the real part as first component. <http://www.iers.org/>
- RD4 International Earth Rotation and Reference System Service Conventions 2003
by D.D. McCarthy and G. Petit
<http://www.iers.org/>
- RD5 Quaternion Toolbox
Jay St. Pierre
<http://www.mathworks.com/matlabcentral/fileexchange/loadFile.do?objectId=1176>
- RD6 Robust Estimation of a Location Parameter
P. J. Huber
Annals of Mathematical Statistics, Vol. 35, No. 1, pp. 73-101, March 1964
<http://links.jstor.org/sici?sici=0003-4851%28196403%2935%3A1%3C73%3AREOALP%3E2.0.CO%3B2-K>
- RD7 A Practical Guide to Splines
Carl de Boor
Applied Mathematical Sciences, vol. 27, Springer 1978
ISBN 0-387-95366-3
- RD8 Observing, Modeling, and Interpreting Magnetic Fields of the Solid Earth
Mioara Mandea and Michael Purucker
Surveys in Geophysics, vol. 26, pp. 415–459, Springer 2005
- RD9 IERS Conventions web page
<ftp://maia.usno.navy.mil/conv2000/chapter5> (Last visit 27. March, 2007)
- RD10 IAU Standards of Fundamental Astronomy software collection
http://www.iau-sofa.rl.ac.uk/2005_0901.html (Last visit 27. March, 2007)
- RD11 RINEX: The Receiver Independent Exchange Format Version 3.00
by Werner Gurtner, Astronomical Institute, University of Bern



Dated: 2006-12-19

<http://igsb.jpl.nasa.gov/igsb/data/format/rinex300.pdf>

RD12 Earth Explorer Mission CFI Software
EXPLORER_LIB SOFTWARE USER MANUAL
Doc. No. CS-MA-DMS-GS-0003
DEIMOS Space S.L., Spain

3 Introduction

The Swarm Level 1b Processor processes the Swarm Level 0 data [AD01] from each of the three satellites individually and produces the Swarm Level 1b Data Products [AD02]. This document contains the detailed description of the algorithms required for the processing.

The processing of Swarm Level 1b data falls into three groups: magnetic data, plasma data, and ephemeris (positional) data. The content of this document is as follows:

This section introduces some terminology.

Section 4 contains an overview of the overall processing and describes the concepts of spatial/temporal synchronisation and time-series.

Section 5 contains the description of the processing of Level 0 data into Level 1a data together with a description of the Level 1a data used in the subsequent sections.

Section 6 contains the description of the processing of magnetic and attitude data.

Section 7 contains the description of the plasma data processing.

Section 8 contains the description of position, velocity and acceleration (GPSR and ACC) data processing.

3.1 Terminology

The general terms and typography used in this document is listed in Table 3-1. See also the “Swarm Mathematical Conventions” document [AD10].

| | |
|-----------------------------|---|
| v | Boldfaced terms indicates vectors of any dimension (typically 3) |
| v_{frame} | A subscript of a vector is used to denote the reference frame of the vector |
| v | Length of a vector, $ v = v \cdot v$ |
| e_v | Unit vector along v , $e_v = v/ v $ |
| <u>M</u> or <u>M</u> | Double lines above terms indicates matrices – or they are not marked specifically, but it should be clear from the context, that it is a matrix |
| a | Acceleration |
| B | Magnetic field vector |
| E | Electrical field vector |
| F | Magnetic field intensity, aka scalar field |
| I | Current (electrical), often a vector (I) |
| q | Quaternion, a 4 dimensional vector defining a rotation/transformation. See Appendix B and [AD10] |

| | |
|----------------------------|---|
| r | Position |
| t | Time |
| t_{0,XXX} | Timestamp of XXX measurement in Level 0 telemetry (see Section 4.5) |
| t_{XXX} | Time of XXX measurement, $t_{XXX} = t_{0,XXX}$ corrected for delays except group delays of filtering of measurements |
| t_{out,XXX} | Time of XXX measurement adjusted for all delays, $t_{out,XXX} = t_{XXX} - \text{filter group delay}$ |
| T | Temperature |
| v | Velocity |
| ρ | Density |
| × | Matrix multiplication operator, or quaternion transformation operator. If $\mathbf{q}_{B \leftarrow A}$ is a quaternion and \mathbf{v} a 3 dimensional vector, $\mathbf{v}_B = \mathbf{q}_{B \leftarrow A} \times \mathbf{v}_A$. $\mathbf{q} \times \mathbf{v} \equiv \mathbf{q}^* \otimes \mathbf{v} \otimes \mathbf{q}$ – see also Eq. (B-20) in Appendix B. |

Table 3-1 Terms

4 Processing Overview

The overall processing of Swarm Level 1b data is outlined in Figure 4-1. The telemetry inputs in the top of the figure indicate the instrument or subsystem supplying the basic data streams for the processing. Secondary inputs such as house-keeping telemetry and auxiliary information are not shown in the figure. The outputs in the bottom of Figure 4-1 are the Level 1b Data Products (see Table 4-2) generated by the processing blocks. Some of the Level 1b data elements are fed back into other processing boxes shown by the green arrows.

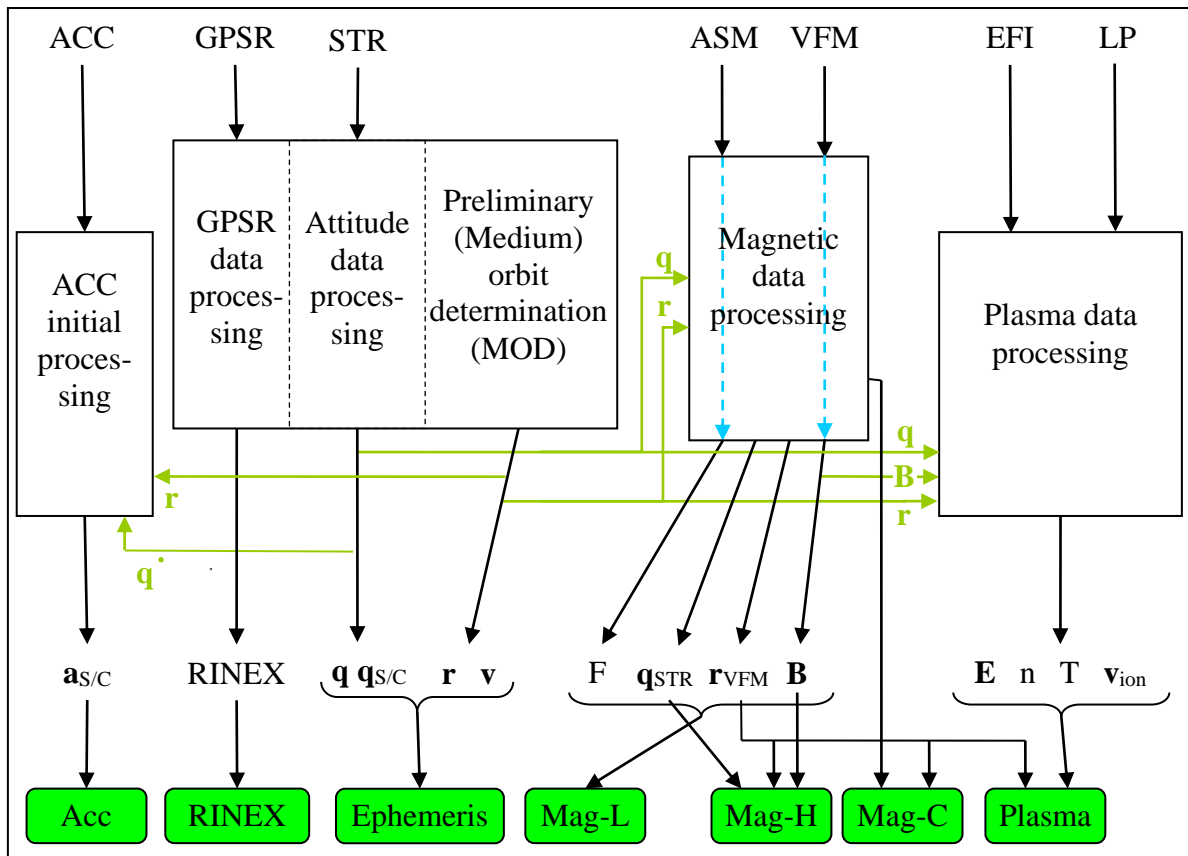


Figure 4-1 Overall Level 1b Processing

The processing sequence is as follows:

1. Process GPSR and STR data, and perform Medium accuracy Orbit Determination (MOD), cf. Sections 8.1, 6.4 and 8.2.)
2. Process magnetic (ASM and VFM) data processing, cf. Section 6.
3. Plasma data processing (Section 7)
4. ACC data processing (Section 8.3)

Note: The attitude information generated in Step 1. is being interpolated in steps 2.-4. The algorithm for this interpolation is described in Section 6.4.2.

The Level 1b Data Products are 1 day (0:00 – 24:00 UTC) in length, which fits well with the MOD and magnetic data processing, hence data are most conveniently processed in batches of one day. However, to avoid edge effects in various filter and interpolation processes the processing interval is expanded some minutes in both ends.

The basic input data streams and their data rates and cut-off (-3 dB) frequencies are listed in Table 4-1.

| Instrument | Rate | Cut-off | Comment |
|------------|-------------|------------|--|
| GPSR | 0.1 Hz | | |
| ACC | 1 Hz | TBD | To be provided |
| ASM | 1 Hz | ca. 0.4 Hz | Butterworth filter, 2 nd order, 3 in cascade |
| VFM | 50 Hz | ca. 9 Hz | Bessel filter, 4 th order, $f_0 \approx 22$ Hz |
| STR | 1 Hz | 0.44 Hz | Box-car filter, i.e. the STR provides attitudes averaged over the image integration time (1 second), 6 dB/octave |
| LP | 2 and 16 Hz | TBD | To be provided |
| TII | 2 and 16 Hz | TBD | To be provided |

Table 4-1 Input Data

Table 4-2 below provides some brief information on the Level 1b data products. To facilitate the use of the magnetic data from all three Swarm satellites the Mag-L (as well as Ephemeris) data are synchronized to integral UTC seconds.

| Product | Short Name | Rate | Comment |
|--------------------------|------------|---------------|--|
| GPSX_RO_1B GPSX_RN_1B | RINEX | 0.1 Hz | GPSR data converted to RINEX format |
| MODX_SC_1B | Ephemeris | 1 Hz | Position, velocity, and attitude from GPSR, STR and MOD |
| ACCX_PR_1B | Acc | 1 Hz | Pre-calibrated non-gravitational acceleration |
| MAGX_LR_1B | Mag-L | 1 Hz (UTC) | Magnetic vector and scalar data in VFM and NEC frames (of \mathbf{r}_{VFM}) including $\mathbf{q}_{NEC \leftarrow CRF}$ transformation quaternions and \mathbf{r}_{VFM} position. |
| MAGX_HR_1B | Mag-H | 50 Hz | Magnetic vector data in VFM and NEC frames at intrinsic VFM sampling time instants. |
| MAGX_CA_1B | Mag-C | 0.25 Hz z | Magnetic <i>calibration</i> data to monitor, verify and re-estimate CCDB.VFM.Cal and TCF.VFM parameters. |
| ASMXAUX_1B | Asm_Aux | 50 Hz | Magnetic stray fields at ASM sensor |
| VFMXAUX_1B | Vfm_Aux | 50 Hz | Magnetic stray fields at VFM sensor |

| Product | Short Name | Rate | Comment |
|------------|------------|------|---|
| EFIX_PL_1B | Plasma | 2 Hz | Provided by the EFI package, the LP and TII instruments |

Table 4-2 Level 1b Data Products, cf [AD02]

4.1 Detailed Data Flow

The detailed data flows from Level 0 and auxiliary products to the Level 1b products are shown in the following figures. The “ISP Decoding” is described in Section 5.

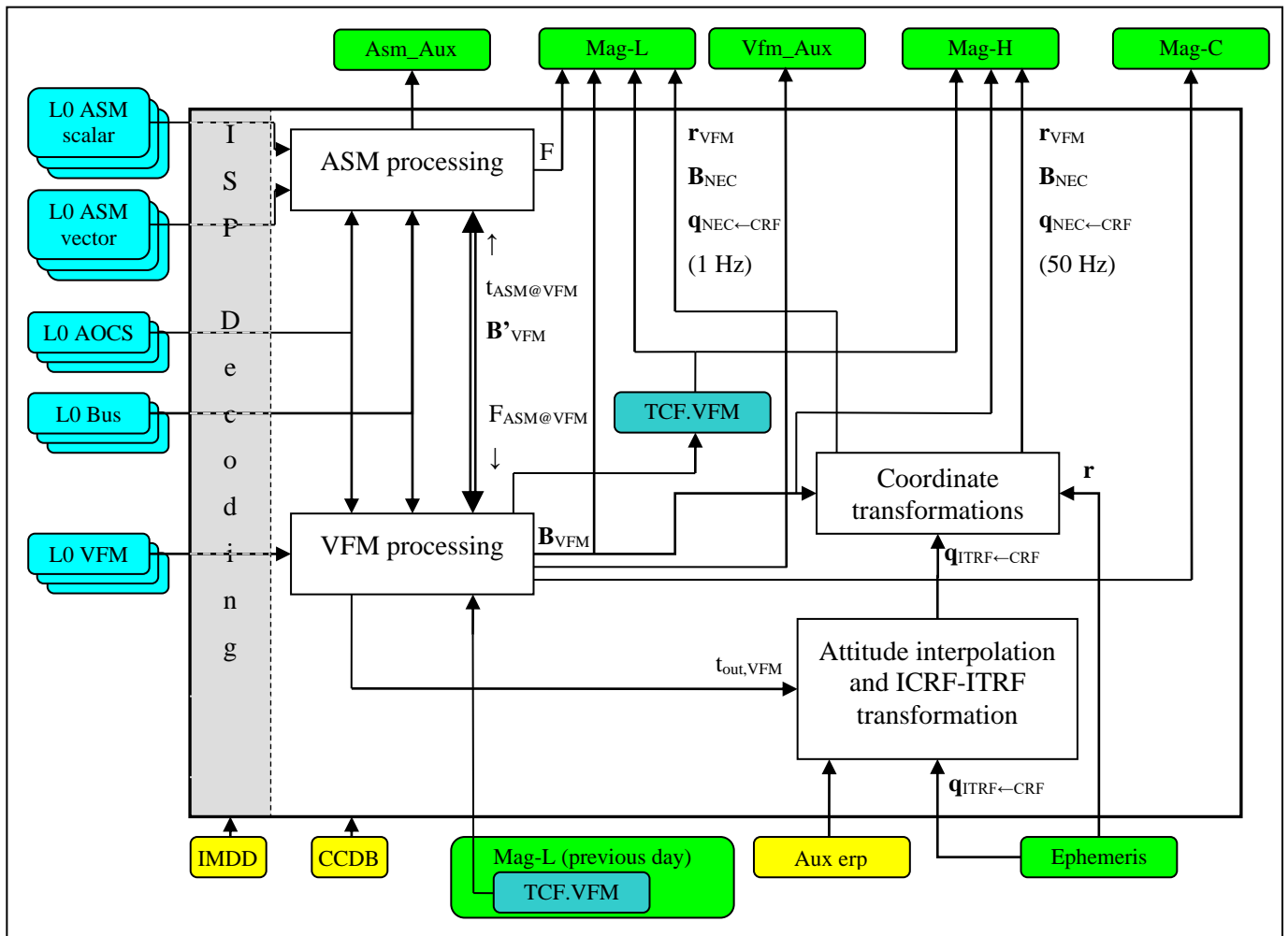


Figure 4-2 Magnetic Data Processing

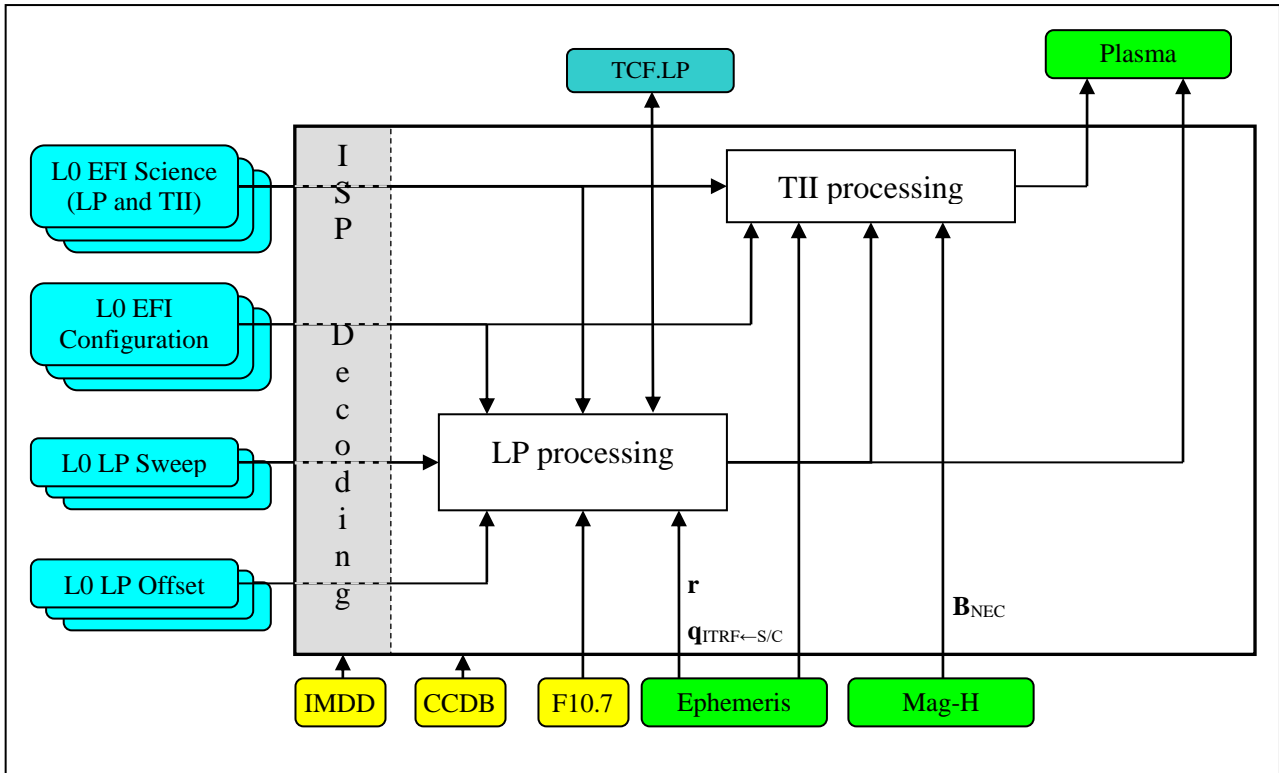


Figure 4-3 Plasma Data Processing

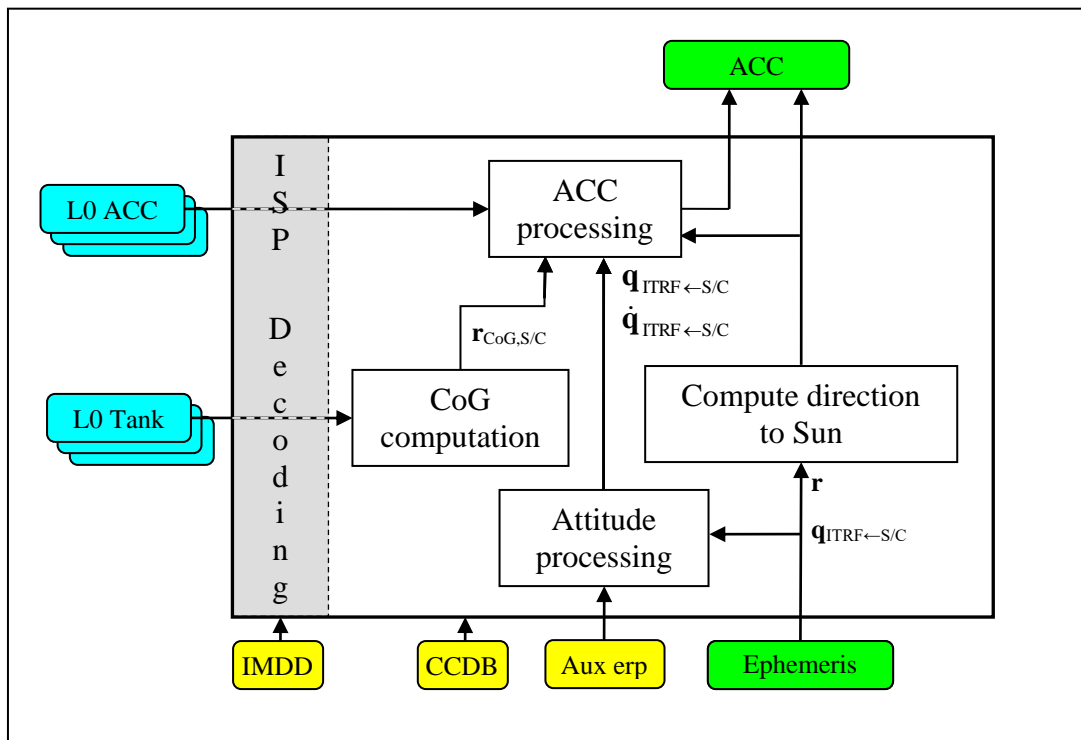


Figure 4-4 Accelerometer Data Processing

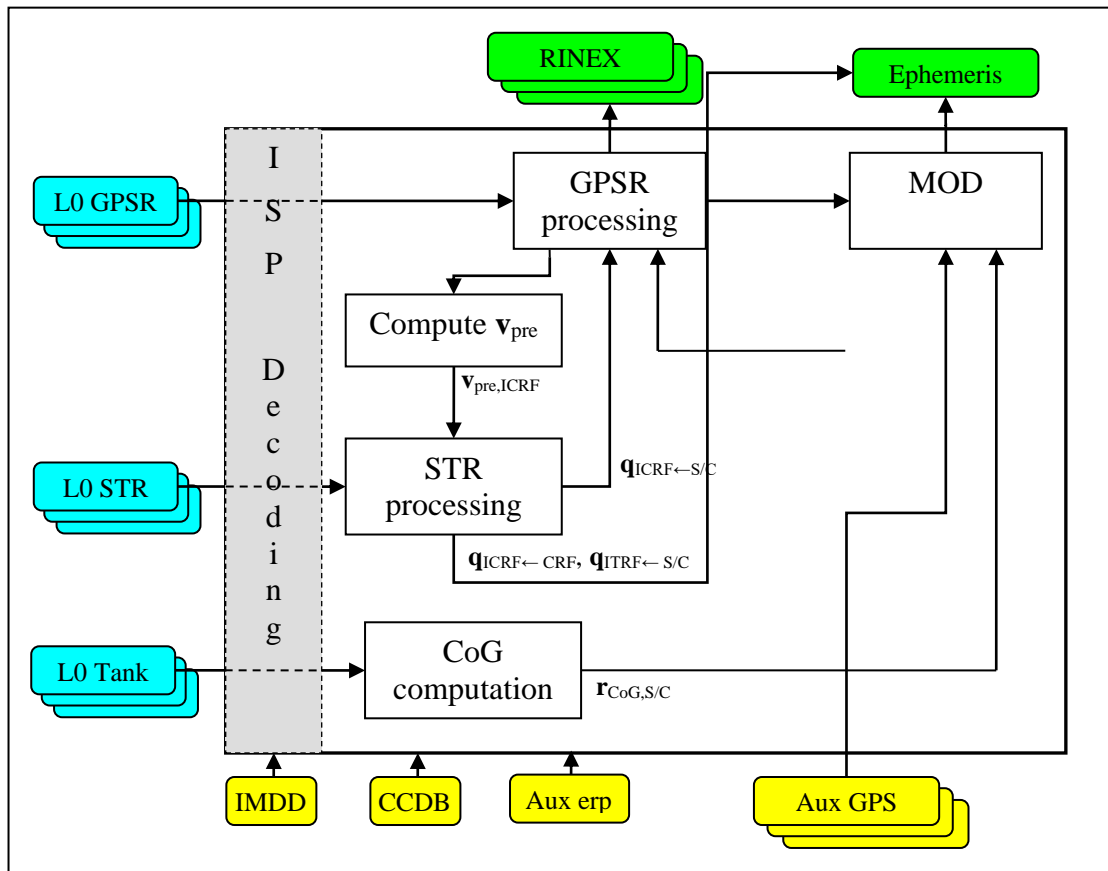


Figure 4-5 GPSR Data and MOD Processing

4.2 Re-processing

No automatic re-processing of data is foreseen. The processing steps shown in Figure 4-1 are performed only when all required telemetry and auxiliary data are available. Manual re-processing is possible for all chains and may typically be effected as a result of an update of CCDB parameters.

A dedicated re-processing chain for the magnetic data is foreseen. The CCDB.Structure.**STR_q_VFM** alignment quaternion parameter is expected to be updated 2-5 times throughout the Mission. This calls for a recomputation of the \mathbf{B}_{NEC} elements of the Mag-L and Mag-H Level 1b Products, which may be accomplished either by a full reprocessing (Figure 4-2) or by a simple recomputation of \mathbf{B}_{NEC} data as depicted in Figure 4-6 below (and described in Section 6.3.4, Eq. (6.3-420) on Page 78). This re-processing step generates new versions of the Mag-L and Mag-H Level 1b Products.

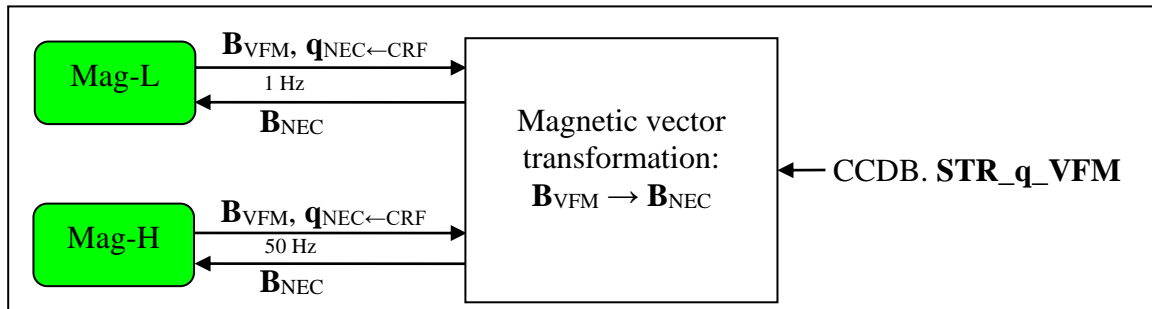


Figure 4-6 Reprocessing after CCDB.Structure.STR_q_VFM update

4.3 Time-series

The Swarm data consist of time-series, i.e. sequences of typically evenly time-spaced observations (measurements) of continuous, physical signals. The data rates and the exact time-instants of the measurements provided by the instruments do typically not match those of the final Level 1b products. This is handled by various advanced interpolation methods described in the detailed processing descriptions in later Sections.

The primary source of a given time-series is one instrument, e.g. the VFM supplies the Level 1b.Mag-H.**B** magnetic vector data – see also the dashed lines in Figure 4-1. However, the processing of the data involves the combination of the primary source with various other (secondary) time-series: e.g. several house-keeping (HK) channels such as temperatures and currents, S/C attitude, position and velocity, and possibly data from other instruments. The secondary data are typically provided at different rates and different time-instants than the primary observations, hence they need to be processed: typically interpolated and possibly filtered to the time-instants of the primary time-series. Furthermore, most of the measurements are discrete samples of continuous signals, hence the real physical signal can only be approximated. Data with a moderate requirement on accuracy and typically slow changes are linearly interpolated as this is a simple and stable solution. Scientific measurements with high accuracy demands are interpolated using higher order polynomials (position) or advanced, parameterized smoothing B-splines to achieve the most accurate re-sampled values (scalar magnetic data and attitude). Data from the magneto-torquers of the AOCS (Attitude and Orbit Control System) sub-system are processed specifically with respect to the primary data source (VFM or ASM) as the requirement on the knowledge of the AOCS signals is high and – contrary to other HK data – the AOCS signals are controlled and monitored carefully.

4.4 Corrections

The magnetic and acceleration measurements are affected by “S/C disturbances” which need to be accounted for to get the true, ambient values of these quantities. This is done by computing the actual disturbances and subtracting these from the measurements, i.e. $y_{\text{clean}} = y_{\text{measured}} - y_{\text{disturbance}}$, for any quantity y . Disturbance is sometimes also referred to as “correction”, i.e. $y_{\text{clean}} = y_{\text{measured}} - y_{\text{correction}}$, and $y_{\text{correction}} = y_{\text{disturbance}}$.

4.5 Timestamps

Telemetry data is – one way or the other – timestamped on-board the satellite. This timestamp is transmitted in the telemetry and termed *Level 0 timestamp*, $t_{0,XXX}$ (this is identical to the Level 1a timestamp). Generally, this timestamp is somehow affected by a delay compared to the true time of the measurement; the true time is referred to as t_{XXX} . $t_{XXX} = t_{0,XXX} - \text{delay}$. See Figure 4-7. Observe that this delay may be positive (the timestamp is after the actual measurement time) or negative (measurement is after timestamp). Furthermore, the measurement itself may be delayed with respect to the actual physical signal being measured. E.g. a thermistor measuring the temperature of some component may experience a delay during temperature changes while heat flows between the component and the thermistor; or a filter within the instrument may introduce a delay of the output data from the instrument – see Figure 4-7. The time of the original signal corresponding to a measurement is termed $t_{out,XXX}$; $t_{out,XXX} = t_{XXX} - \text{filter delay}$. $t_{out,XXX}$ is the timestamp used in the Level 1b data products as this most accurately² reflects the time of the signal given by the measurement.

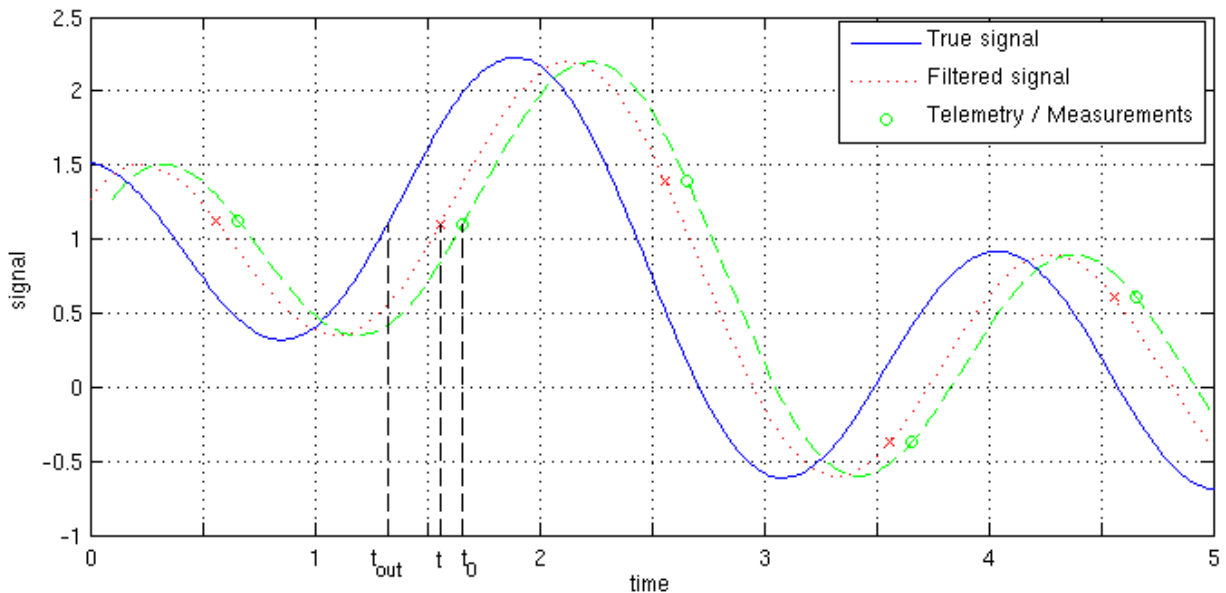


Figure 4-7 Example of timestamps

4.6 Leap Seconds

Leap Seconds are introduced to keep the time frames UTC and UT1 aligned within 1 second. They are introduced by International Earth Rotation and Reference Systems Service (IERS) when appropriate either by the end of 30 June or end of 31 December. Positive leap seconds are introduced as an extra second denoted “23:59:60”, negative leap seconds are introduced by omitting the last second of the day, i.e. “23:59:59” does not exist in this case.

When leap seconds are introduced, GPSR and MOD processing, interpolation of ASM and STR data (Sections 6.2 and 6.4) and resampling of VFM data (Section 6.3) need to account for the leap second. For all other data streams, the introduction of leap seconds may be

² The filter delay may depend on the signal frequency; however this is ignored in the Level 1b products.

ignored. GPSR and MOD leap second processing is described in the respective documents ([AD11] and [AD12]). For ASM, VFM, and STR leap second introduction is handled by assuming the length of this particular day to be 86,401 seconds (or 86,399 seconds in case a negative leap second is introduced). E.g. during the resampling or interpolation, data are time-stamped using second-of-the-day, and data from the day following the leap-second start at 86,401 (or 86,399). Similarly when processing data of the day immediately after the leap-second, data from the day of the leap-second shall be shifted 86,401 (86,399) seconds.

For products using GPS timestamps (GPSx_RO_1B, GPSx_RN_1N, and MODx_SC_1B) leap second data are preserved. For all other products, i.e. products using UTC timestamps, leap second data are omitted.

5 Level 0 Processing

The Swarm measurement data are received as Level 0 Product Files [AD01]. These files contain data sets with sequentially ordered and duplicate free Instrument Source Packets (ISP) from individual Application Processes, e.g. ASM scalar mode data. However, there may be gaps within the Level 0 files. These gaps are attempted to be covered by renewed download of the data resulting in new Level 0 files, which may contain ISPs included in previous Level 0 files. Figure 5-1 illustrates a possible scenario of four Level 0 files from a given application process. The blue bars show the periods of data (time) covered by four files; the shaded parts indicate gaps in the files. The net effect of these dumps is a small gap in the data just prior to the data in the 4th (bottom) file.

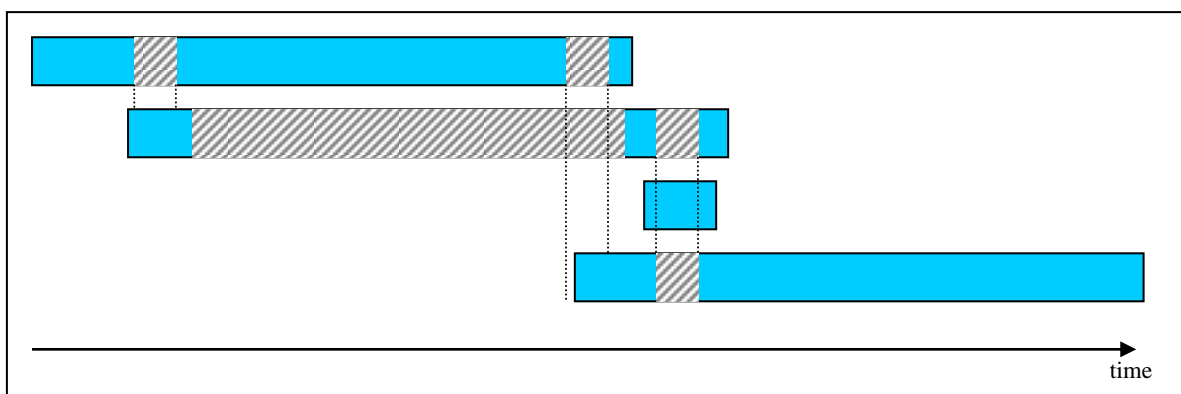


Figure 5-1 Scenario of Level 0 Products with gaps

When the Level 1b Processor is requested to process a given period of data, appropriate and available Level 0 Products containing data from the given period are provided to the Processor, hence more than one product for each Application Process may be supplied. Hence the Processor must merge the Level 0 files into a single stream of sequential, duplicate- and (as far as possible) error-free list of ISPs without gaps for each Application Process. This includes a decoding of the ISP header to identify the proper sequential order, and may further involve additional checks of error control and/or validity fields. See Sections 5.1 and 5.2.

The ISPs are decoded into Level 1a data (Section 5.4.7) using the Instrument Measurement Data Definition (IMDD) for format definition/decoding and the CCDB.TMC elements for conversion from the raw Level 0 telemetry into the units of the Level 1a data. The definitions of the ISPs can be found in [AD01]. The Level 1a data may be stored in Level 1a Product Files according to the configuration of the Level 1b Processor.

5.1 Quality and Validity Checks

The ISPs shall be checked for quality and validity. This includes checks of

- Error control code. If the check of the error control code fails, the packet shall be marked as invalid and shall be rejected.
- PPS synchronization source.
 - If the source is OBC a warning flag is to be set in the Level 1a and Level 1b Products. The processing shall be done as for GPS PPS.

- If the source is not GPS or OBC the packet shall be marked as invalid and shall be rejected.
- PPS synchronization quality
 - If only one of PPS and spacecraft O/B Time is received a warning flag is to be set in the Level 1a and Level 1b Products. The processing shall be done as if both are received.
 - If none is received the packet shall be marked as invalid and shall be rejected.
- Validity flags. If the instrument measurements are marked as invalid, the packet shall be marked as invalid and shall be rejected, if not otherwise stated in the detailed algorithms given in the later sections of this document.
- ISP fields for specific characteristics, e.g. validity boundaries. For details refer to the algorithms definitions given in the later sections of this document and the definition of the flags in the Level 1b Product Definition, ref. [AD02].

In case of gaps in the ISP stream (invalid or missing packets) there will be jumps in the Level 1a data, which are handled in the later algorithms.

5.2 Data Coordination and Combination

In addition to the simple extraction and conversion of ISP fields some further processing of Level 0 to Level 1a data is required. This includes

- Interleaving and grouping of data
- Handling of different modes
- Collection and adaptation of auxiliary data (including housekeeping and characterisation data)

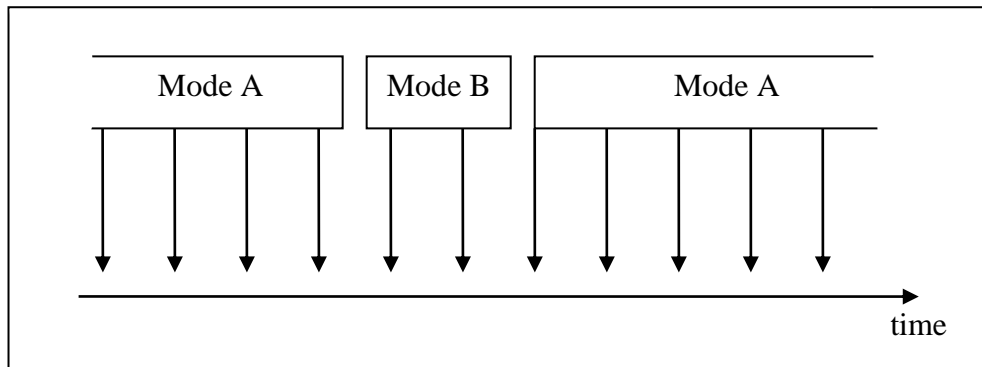
5.2.1 Interleaving and grouping of data

Packets with different Process IDs (PID) will be stored in different product types and packets with different structure may be stored in different data sets. The data from these packets need to be interleaved and grouped suitable for further processing.

5.2.2 Handling of modes

Some instruments can operate in more than one mode generating measurement data.

Some of the data are only for diagnostic purposes and can be ignored in the Level 1b processing.



Some are providing similar data. The Level 1b processing of these data is identical, where not explicitly defined as to be different. The data of these modes shall be merged. An identification shall be added to Level 1a and Level 1b products identifying the source (mode) of the measurement data.

ACC: Only Measurement Mode. Ignore Selftest Mode ISPs

ASM: Merge Scalar and Vector Mode products. Ignore Burst, SpectroMag, SpectroLaser and SpectroPowerLaser Mode products.

EFI: TBD

VFM: Merge Compressed and Uncompressed Mode ISPs.

5.2.3 Collection and adaptation of auxiliary data

For the processing of the measurement data housekeeping, characterization/calibration and other auxiliary data are needed. These have to be collected from the input files (Level 0, Level 1b and auxiliary products) as needed for the processing.

For some of the data alternative sources are available. These data shall be selected from the nominal source. Only if the nominal source is not available the data shall be read from the alternative source. Example: TCF parameter: Nominal source is Level 1b product. Alternative source is CCDB.

Several units on the satellite are redundant. The characterization and calibration parameters depend on the active configuration. Therefore the characterization and calibration parameter suitable for the active configuration have to be selected.

The housekeeping, characterization/calibration and other auxiliary data have to be selected suitably for the time instant or time interval of the measurements. This may include some minor adaptation, e.g. interpolation of data to the needed time instant.

5.3 Datation of Data

The datation of data from the various instruments and Bus house-keeping telemetry is done according to the following table:

| System | PID/SID | L0 element | L1a section | Description | t ₀ (= Level1a.t) |
|---------|--|---|------------------|---|---|
| ACC | 61/11 | dt | ACC | Delta time since PPS (unit microsecond) | t_pps + dt |
| ASM | 31/11 32/12 | dt | ASM | Delta time since PPS (unit millisecond) | t_pps + dt |
| EFI/LP | 56,57,58/- | dt | LP* | Delta time since PPS (unit 1/4096 seconds) | t_pps + dt |
| EFI/TII | 56,57,58/- | | TII | | t_pps |
| GPSR | Specific handling of time, described in [AD11] | | | | |
| STR | 80,90/ 3,4,5 | t_coi | STR | Time stamp of the centre of integration period, CDS format | t_coi |
| VFM | 41/11 41/14 | VFM _{time} VFM _{PPStime} | VFM | VFM Time of 1 st measurement respectively last PPS | t_pps + VFM _{PPStime} / 8 · 10 ⁶ |
| HK | 4/6 | t_mtg | AOCS. Mag_HK | MTQ currents 1/2/3 Command Issued (UTC) | t_mtg |
| | 4/6 | t_thruster | AOCS. Thru_HK | Thruster activate, Time Command Issued (UTC) | t_thruster |
| | 4/7 | - | Bus | | t_pps |
| | 4/8 | - | AOCS. Prop_HK | | t_pps |

Table 5-1 Datation: Level 0 to Level 1a Conversion

5.4 Conversions from Level 0 to Level 1a

This Section describes the various conversions of the Level 0 telemetry channels (*raw values*) into the Level 1a values which may be engineering units (*eu* – typically science measurements) or physical units (Volts, temperature, etc. – typically house-keeping data).

5.4.1.1 Processing of Bus State and Current Information

The extraction of the relevant state information and current measurements in the Level 0 HK data into Level 1a data suitable for the calculation of magnetic stray fields – steady as well as electrically and magnetically induced fields – is performed using the StateInfo, CurrentInfo, and InducedInfo stored in the CCDB.Bus.State, CCDB.Bus.Current, and CCDB.Bus.Induced arrays respectively. The resulting Level 1a data are listed in Section 5.5.

5.4.2 State Information – Static Stray Fields

The Level 0 state information from HK_xNOM_0_ (SID = 7) is processed into the state vector Level1a.Bus.State.States using the CCDB.Bus.State information. The purpose of this state vector is to allow state dependent remanent stray magnetic fields to be easily computed. The CCDB.Bus.State characterizes the states which change the remanent magnetic field of some instrument or subsystem, and it includes the corresponding changes in the remanent field.

CCDB.Bus.State.States is an array of type StateInfo:

| Name | Type | Description | | | | | | | | | | | | |
|-----------|--|---|------|-------------|----------|---|---------|--|-----------|--|-----------|--|--------|--|
| ID | string | Name of Level 0 Bus channel. Note: the same ID may occur several times and this may also be the ID of a heater or thruster although these states are also given in the Heater_Stat and Thru_Stat vectors of Level1a.Bus.State. | | | | | | | | | | | | |
| type | string | Specifies translation type – how to compute Level1a.Bus.State.States _i : <table border="1" style="margin-left: 20px;"> <thead> <tr> <th>type</th> <th>Description</th> </tr> </thead> <tbody> <tr> <td>'Level0'</td> <td>No translation, use value in Level0 directly: States_i = Level 0.(ID)</td> </tr> <tr> <td>'Equal'</td> <td>States_i = $\begin{cases} 1 & \text{if Level 0.(ID) = value} \\ 0 & \text{otherwise} \end{cases}$</td> </tr> <tr> <td>'Between'</td> <td>States_i = $\begin{cases} 1 & \text{if value(1) <= Level 0.(ID) <= value(2)} \\ 0 & \text{otherwise} \end{cases}$</td> </tr> <tr> <td>'Greater'</td> <td>States_i = $\begin{cases} 1 & \text{if Level 0.(ID) > value} \\ 0 & \text{otherwise} \end{cases}$</td> </tr> <tr> <td>'Less'</td> <td>States_i = $\begin{cases} 1 & \text{if Level 0.(ID) < value} \\ 0 & \text{otherwise} \end{cases}$</td> </tr> </tbody> </table> | type | Description | 'Level0' | No translation, use value in Level0 directly: States _i = Level 0.(ID) | 'Equal' | States _i = $\begin{cases} 1 & \text{if Level 0.(ID) = value} \\ 0 & \text{otherwise} \end{cases}$ | 'Between' | States _i = $\begin{cases} 1 & \text{if value(1) <= Level 0.(ID) <= value(2)} \\ 0 & \text{otherwise} \end{cases}$ | 'Greater' | States _i = $\begin{cases} 1 & \text{if Level 0.(ID) > value} \\ 0 & \text{otherwise} \end{cases}$ | 'Less' | States _i = $\begin{cases} 1 & \text{if Level 0.(ID) < value} \\ 0 & \text{otherwise} \end{cases}$ |
| type | Description | | | | | | | | | | | | | |
| 'Level0' | No translation, use value in Level0 directly: States _i = Level 0.(ID) | | | | | | | | | | | | | |
| 'Equal' | States _i = $\begin{cases} 1 & \text{if Level 0.(ID) = value} \\ 0 & \text{otherwise} \end{cases}$ | | | | | | | | | | | | | |
| 'Between' | States _i = $\begin{cases} 1 & \text{if value(1) <= Level 0.(ID) <= value(2)} \\ 0 & \text{otherwise} \end{cases}$ | | | | | | | | | | | | | |
| 'Greater' | States _i = $\begin{cases} 1 & \text{if Level 0.(ID) > value} \\ 0 & \text{otherwise} \end{cases}$ | | | | | | | | | | | | | |
| 'Less' | States _i = $\begin{cases} 1 & \text{if Level 0.(ID) < value} \\ 0 & \text{otherwise} \end{cases}$ | | | | | | | | | | | | | |
| value | vector | Value(s) for comparison, if type ≠ 'Level0' | | | | | | | | | | | | |
| dB_ASM | vector | Change in magnetic stray field vector at ASM sensor position when States _i changes from 0 to 1 | | | | | | | | | | | | |
| dB_VFM | vector | Similar to dB_ASM for the VFM sensor position | | | | | | | | | | | | |

Table 5-2 StateInfo – Elements of CCDB.Bus.State Array

5.4.3 Bus Current Measurements

The calculation of the electrically induced magnetic fields uses the information in Level1a.Bus.Curr. This is constructed from Level 0 Bus current measurements provided in HK_xNOM_0_ (SID = 7) using the CCDB.Bus.Current (and CCDB.TMC) specification, which lists the appropriate current channels and their stray magnetic field vectors. These stray field vectors are given for unit current (1 A), i.e. they are to be multiplied by the Level1a.Bus.Curr value to yield the actual stray magnetic field.

CCDB.Bus.Current consists of three arrays: I_{SP} , I_{Bat} , and I_{other} for the Solar Arrays, Batteries, and others respectively. The array elements are of type CurrentInfo:

| Name | Type | Description |
|---------|--------|---|
| ID | string | Name of Level 0 Bus channel. |
| I_xfer | Lut1d | Linear look-up table for translating Level 0 to Level 1a value: $\text{Level1a.Bus.Curr.I}_{Source} = \text{Interpol}_{Lin}(\text{I_xfer}, \text{Level 0.}(\text{ID}))$ The Interpol_{Lin} function is given in Appendix E.1 |
| dB_ASM | vector | Electrically induced magnetic stray field vector at ASM sensor position for unit current (1 A), i.e. multiply by Level 1a value |
| dB_VFM | vector | Same as dB_ASM for the VFM sensor position |
| dB_Body | vector | Same as dB_ASM for the S/C body. |

Table 5-3 CurrentInfo – Elements of CCDB.Bus.Current Array

5.4.4 State Dependent Magnetically Induced Fields

Instruments and subsystems with soft-magnetic characteristics (i.e. producing magnetically induced stray fields) are characterized by the CCDB.Bus.Static.Ind_{xxx}, CCDB.Bus.State.Induced, and CCDB.AOCS.M_{xxx} elements – for the AOCS, the M_{xxx} matrices includes both direct and induced effects. The CCDB.Bus.Static and CCDB.AOCS elements contain the properties for static soft-magnetic properties as well as *default* state properties for equipment with non-static characteristics. The characteristics of state dependent soft-magnetic properties are stored in the CCDB.Bus.State.Induced array of InducedInfo (Table 5-4), which is used to generate Level1a.Bus.State.IndStates.

| Name | Type | Description | | | | | | | | | | |
|-----------|--|---|------|-------------|----------|--|---------|---|-----------|--|-----------|---|
| ID | string | Name of Level 0 Bus channel. Note: the same ID may occur several times | | | | | | | | | | |
| type | string | Specifies translation type – how to compute Level1a.Bus.State.IndStates: <table border="1" data-bbox="454 1550 1362 2056"> <thead> <tr> <th>type</th> <th>Description</th> </tr> </thead> <tbody> <tr> <td>'Level0'</td> <td>No translation, use value in Level0 directly: $\text{IndStates}_i = \text{Level 0.}(\text{ID})$ </td> </tr> <tr> <td>'Equal'</td> <td> $\text{IndStates}_i = \begin{cases} 1 & \text{if Level 0.}(\text{ID}) = \text{value} \\ 0 & \text{otherwise} \end{cases}$ </td> </tr> <tr> <td>'Between'</td> <td> $\text{IndStates}_i = \begin{cases} 1 & \text{if value(1)} \leq \text{Level 0.}(\text{ID}) \leq \text{value(2)} \\ 0 & \text{otherwise} \end{cases}$ </td> </tr> <tr> <td>'Greater'</td> <td> $\text{IndStates}_i = \begin{cases} 1 & \text{if Level 0.}(\text{ID}) > \text{value} \\ 0 & \text{otherwise} \end{cases}$ </td> </tr> </tbody> </table> | type | Description | 'Level0' | No translation, use value in Level0 directly: $\text{IndStates}_i = \text{Level 0.}(\text{ID})$ | 'Equal' | $\text{IndStates}_i = \begin{cases} 1 & \text{if Level 0.}(\text{ID}) = \text{value} \\ 0 & \text{otherwise} \end{cases}$ | 'Between' | $\text{IndStates}_i = \begin{cases} 1 & \text{if value(1)} \leq \text{Level 0.}(\text{ID}) \leq \text{value(2)} \\ 0 & \text{otherwise} \end{cases}$ | 'Greater' | $\text{IndStates}_i = \begin{cases} 1 & \text{if Level 0.}(\text{ID}) > \text{value} \\ 0 & \text{otherwise} \end{cases}$ |
| type | Description | | | | | | | | | | | |
| 'Level0' | No translation, use value in Level0 directly: $\text{IndStates}_i = \text{Level 0.}(\text{ID})$ | | | | | | | | | | | |
| 'Equal' | $\text{IndStates}_i = \begin{cases} 1 & \text{if Level 0.}(\text{ID}) = \text{value} \\ 0 & \text{otherwise} \end{cases}$ | | | | | | | | | | | |
| 'Between' | $\text{IndStates}_i = \begin{cases} 1 & \text{if value(1)} \leq \text{Level 0.}(\text{ID}) \leq \text{value(2)} \\ 0 & \text{otherwise} \end{cases}$ | | | | | | | | | | | |
| 'Greater' | $\text{IndStates}_i = \begin{cases} 1 & \text{if Level 0.}(\text{ID}) > \text{value} \\ 0 & \text{otherwise} \end{cases}$ | | | | | | | | | | | |

| Name | Type | Description |
|---------------------|------------|---|
| | | 'Less' $\text{IndStates}_i = \begin{cases} 1 & \text{if Level 0.(ID) < value} \\ 0 & \text{otherwise} \end{cases}$ |
| value | vector | Value(s) for comparison, if type \neq 'Level0' |
| dInd _{ASM} | 3x3 matrix | Change in CCDB.Bus.Static.Ind _{ASM} matrix characterizing magnetically induced stray field vector at ASM sensor position when IndState changes from 0 to 1 |
| dInd _{VFM} | 3x3 matrix | Same as dInd _{ASM} for CCDB.Body.Ind _{VFM} and VFM sensor position |
| dAM _{ASM} | 3x3 matrix | Change in CCDB.AOCS.M _{ASM} matrix characterizing direct and induced stray field vector of AOCS magnetorquers at ASM sensor position when IndState changes from 0 to 1 |
| dAM _{VFM} | 3x3 matrix | Same as dAM _{ASM} for CCDB.AOCS.M _{VFM} and VFM sensor position |

Table 5-4 InducedInfo – Elements of CCDB.Bus.Induced Array

5.4.5 Calculation of Magnetorquer Currents

The actual currents in the magneto-torquers, Level1a.AOCS.**I_{mea_MTQ}**, are calculated as follows:

$$I_{mea_MTQ_{i+3v}} = I_i + D(I_i) \quad (5.4-10)$$

$$I_{mea_MTQ_{i+3(1-v)}} = 0 \quad (5.4-20)$$

where

$$v = L0.Bus.PCDU_A_RuALclStat \quad (5.4-30)$$

v = 0 is nominal, v = 1 is redundant.

$$I_i = \frac{CCDB.AOCS.G_MTQ \quad CCDB.AOCS.VZ_MTQ}{L0.AOCS.OBC_MTQ_ZENER+ - L0.AOCS.OBC_MTQ_ZENER- - (L0.AOCS.MTQi_Curr - L0.AOCS.OBC_MTQ_ZENER-)} \quad (5.4-40)$$

and

$$D(x) = \begin{cases} CCDB.AOCS.DH_MTQ & \text{if } x \geq 0 \\ CCDB.AOCS.DL_MTQ & \text{if } x < 0 \end{cases} \quad (5.4-50)$$

L0.AOCS corresponds to HK_xNOM_0_ (PID=4) SID=6, L0.Bus is SID=7.

5.4.6 Conversion of Cold Gas HK Data

The AOCS propulsion (cold gas tanks) house-keeping telemetry, Level1a.AOCS.Prop_HK, is computed from HK_xNOM_0_ (PID=4) SID=8 by

$$X = \text{Interpol}_{\text{Lin}}(\text{CCDB.TMC.SWARM_AuxSystemHkTm8TankTemp.TMC_ID}, \text{L0.ID}) \quad (5.4-55)$$

where X is a P_A, P_B, or V_i of Level1a.AOCS.Prop_HK or any of the thermistor voltages, V_Ci, which are converted to temperatures, T_Ci, as described in [AD01]. TMC_ID is CCDB look-up table identifier, and ID is the Level 0 channel identifier. The relation between X, TMC_ID, and ID is given in the following table:

| X | TMC_ID | ID | Description |
|------|---------------------|----------|-----------------------------|
| P_A | HPT_1_AN1__Signal | AHT00000 | Pressure transducer, Tank A |
| P_B | HPT_2_AN1__Signal | AHT00002 | Pressure transducer, Tank B |
| T_A1 | TCM_5_ANY_TankA1 | THT00083 | Temperature 1, Tank A |
| T_A2 | TCM_7_ANY_TankA2 | THT00113 | Temperature 2, Tank A |
| T_A3 | TCL_1_ANY_02A_TankA | THT00014 | Temperature 3, Tank A |
| T_A4 | TCL_3_ANY_02B_TankA | THT00042 | Temperature 4, Tank A |
| T_A5 | TCL_5_ANY_02C_TankA | THT00070 | Temperature 5, Tank A |
| T_B1 | TCM_5_ANY_TankB1 | THT00084 | Temperature 1, Tank B |
| T_B2 | TCM_7_ANY_TankB2 | THT00114 | Temperature 2, Tank B |
| T_B3 | TCL_1_ANY_03A_TankA | THT00015 | Temperature 3, Tank B |
| T_B4 | TCL_3_ANY_03B_TankA | THT00043 | Temperature 4, Tank B |
| T_B5 | TCL_5_ANY_03C_TankA | THT00071 | Temperature 5, Tank B |
| V_i | OBC__REF_3p3V_FGM_A | OHT00024 | Voltage reference |

Table 5-5 Prop_HK Conversion Identifiers

5.4.7 VFM Data Conversion

5.4.7.1 VFM Science Data

The VFM measurement data are transmitted in one of two ways: compressed (SID=11) or uncompressed (SID=14). If compressed data, 1st order differences are used, and

$$Ba_i = \begin{cases} \text{twos_complement}(Ba_1^{\text{raw}}) & \text{for } i = 1 \\ Ba_{(i-1)} + \text{twos_complement}(DBa_i^{\text{raw}}) & \text{for } i = 2, 3, \dots, 50 \end{cases} \quad (5.4-70)$$

where $Ba^{\text{raw}}/DBa^{\text{raw}}$ is the field component value from Level 0 from axis a , $a = X, Y, Z$. B^{raw} and DB^{raw} are 24-bit respectively 8-bit unsigned integers, twos_complements is the regular two's complement function: if x is an n -bit unsigned integer, then

$$\text{twos_complement}(x) = \begin{cases} x & \text{if } x < 2^{n-1} \\ x - 2^n & \text{otherwise} \end{cases} \quad (5.4-75)$$

If uncompressed data, BX, BY, BZ are stored directly in the ISP as 24-bit 2s-complement.

To convert Ba to engineering units, i.e. to Level 1a values, divide by $2^{6.5}$:

$$\text{Level1a.VFM.EU}_a = Ba / 2^{6.5} \quad (5.4-80)$$

5.4.7.2 VFM Temperatures

The VFM temperature readings are converted using 7th order polynomials:

$$\text{Level1a.VFM.T}_{XX} = \sum_{i=0}^7 C_{XX,i} \text{VET}_{XX}^i \quad (5.4-90)$$

where $XX = \text{CSC, CDC, EU}$; $C_{XX,i}$ are coefficients stored in the VFM ICDB; and

$$\text{VET}_{XX} = \text{RET}_{XX}/2^{16} \cdot 5V + 2.5V \quad (5.4-100)$$

where RET_{XX} being the 2's-complement signed values (16-bits) of the SCI_Temp field of the VFM ISP, with $XX = \text{CSC, CDC, EU}$ for $\text{L0.HK_Source} = 1, 2, 3$ respectively.

5.4.8 ASM Data Conversion

The ASM data conversions are as follows:

$$\text{Level1a.ASM.E} = 10^9 \cdot \text{Level0.ASM.B0} \cdot k_LSB \quad (5.4-110)$$

where k_LSB is stored in the ASM ICDB.

$$\text{Level1a.ASM.T}_{\text{Sensor}} = \left(A + B \cdot \ln(R) + C \cdot (\ln(R))^3 \right)^{-1} - 273.15 \quad (5.4-120)$$

where $A, B,$ and C are parameters in the Temp_Sens structure of the ASM ICDB, and

$$R = \frac{U \cdot (R_{\text{filter}} + R_{\text{ref}}) - 2.5 R_{\text{filter}}}{2.5 - U} \quad (5.4-130)$$

where R_{filter} and R_{ref} are parameters in the Temp_Sens structure, and

$$U = 2.5 (\text{L0.Temp} + 1/2) / (2^{12} - 1) \quad (5.4-140)$$

where L0.Temp is the raw temperature data of the ASM telemetry.

5.4.9 ACC Data Conversion

See Section 6.2 of [AD13].

5.4.10 STR Data Conversion – False Leap Second Correction

In the beginning of the Swarm Mission, the STR instruments suffered from a phenomenon named “false leap seconds” causing individual STR samples to be time-stamped (ca.) one second off. The following ad-hoc routine detects and corrects³ these. Let t_i^{raw} be the sequence of STR attitude timestamps of a given CHU, and t_i the corresponding sequence of corrected timestamps (in units of seconds). Then:

³ Consecutive samples suffering from false leap seconds are not corrected.

$$t_i = \begin{cases} t_i^{\text{raw}} - 0.992 & \text{iff } t_i^{\text{raw}} - t_{i-1}^{\text{raw}} > 1.5 \text{ and } t_{i+1}^{\text{raw}} - t_i^{\text{raw}} < 0.5 \\ t_i^{\text{raw}} + 1 & \text{iff } t_i^{\text{raw}} - t_{i-1}^{\text{raw}} < 0.5 \text{ and } t_{i+1}^{\text{raw}} - t_i^{\text{raw}} > 1.5 \\ t_i^{\text{raw}} & \text{otherwise} \end{cases} \quad (5.4-150)$$

5.5 Level 1a Data Description

The description of Level 1a data elements required for the Level 1b Processor is given in [AD14]. The data are grouped into blocks where each block contains a coherent set of observations. The relation between Level 1a Product Names and Data Sets and corresponding Level1a data structure is given in the table below.

| Product | Data Set | Level1a element |
|-------------|-------------------|-----------------|
| ASMxSCI_1a | MDR_ASM_SCI | ASM.Sci |
| VFMxSCI_1A | MDR_VFM_SCI | VFM.Sci |
| STRxSCI_1A | MDR_STR_SCI | STR.Sci |
| ACCxSCI_1A | MDR_ACC_SCI | ACC.Sci |
| EFIx_LP_1A | <i>See [AD08]</i> | |
| EFIxTII_1A | <i>See [AD08]</i> | |
| GPSxNOM_1A | <i>See [AD11]</i> | |
| HK_x_AOCS1A | MDR_MAG_HK | AOCS.Mag_HK |
| | MDR_THRU_HK | AOCS.Thru_HK |
| | MDR_PROP_HK | AOCS.Prop_HK |
| HK_xBUS_1A | MDR_STAT_HK | Bus.State |
| | MDR_CURR_HK | Bus.Curr |

6 Magnetic and Attitude Data Processing

This section describes the processing of magnetic and attitude data of Swarm. The primary Level 1b magnetic data product elements and ephemeris attitude element are listed Table 6-1.

| Product ⁴ | Element | Frame | Rate | Description |
|----------------------|---------------------------|------------|--------|---|
| Mag-H | \mathbf{B}_{VFM} | VFM | ~50 Hz | Magnetic vector data in the orthogonal VFM instrument frame at the basic VFM instrument sampling rate |
| Mag-L | \mathbf{B}_{VFM} | VFM | 1 Hz | As above but reduced to 1 Hz |
| Mag-H | \mathbf{B}_{NEC} | NEC | ~50 Hz | Magnetic vector data in the NEC (North-East-Center) terrestrial frame at the basic VFM instrument sampling rate |
| Mag-L | \mathbf{B}_{NEC} | NEC | 1 Hz | As Mag-L. \mathbf{B}_{VFM} above but in NEC frame |
| Mag-L | F | | 1 Hz | Magnetic field intensity (<i>scalar magnetic field</i>) – provided by the ASM instrument |
| Mag-H | \mathbf{q}_{CRF} | NEC ← CRF | ~50 Hz | Transformation: CRF (STR Common Reference Frame) to NEC frame |
| Mag-L | \mathbf{q}_{CRF} | NEC ← CRF | 1 Hz | Transformation: CRF (STR Common Reference Frame) to NEC frame |
| Eph | \mathbf{q} | ITRF ← S/C | 1 Hz | Transformation: S/C to ITRF frame |

Table 6-1 Main Level 1b Product Elements of Section 6

Generally, the processing of magnetic data consists of:

- Application of intrinsic instrument calibration parameters
- Subtraction of magnetic disturbances – magnetic stray fields from the spacecraft
- Resampling to desired sampling frequencies and/or time instants (not Mag-H. \mathbf{B} data)
- Translation of vector data into appropriate frame – using among other the attitude data of the STR

The processing of magnetic and attitude data is depicted in Figure 6-1 below with telemetry and some ephemeris inputs at the top and (main) Level 1b outputs at the bottom. The elements are further described in Table 6-2 below the figure. The details of the processing within the boxes are described in the Sections as indicated in the figure. The order of processing is largely dictated by the elements being passed between the individual processing boxes. To ease the description of the processings, the Sections focus on the single instruments, but the overall sequence of the processing is as follows:

⁴ Here, the short Level 1b Product names are used, see Table 4-2 for the “official” names.

1. Process GPSR and STR instrument level data, and perform MOD (Section 8 and 6.4)
2. Process VFM data until \mathbf{B}'_{VFM} and $t_{out,VFM}$ are reached.
3. Interpolate attitude data (from Step 1.)
4. Process ASM data generating F_{ASM} , t_{ASM} , and Level 1b.Mag-L.F (including related elements)
5. Finalize VFM processing: estimate and apply TCF.VFM parameters, compute Level 1b.Mag-H. \mathbf{B}_{VFM} and Level 1b.Mag-L. \mathbf{B}_{VFM} , and transform both to NEC frame (\mathbf{B}_{NEC}).

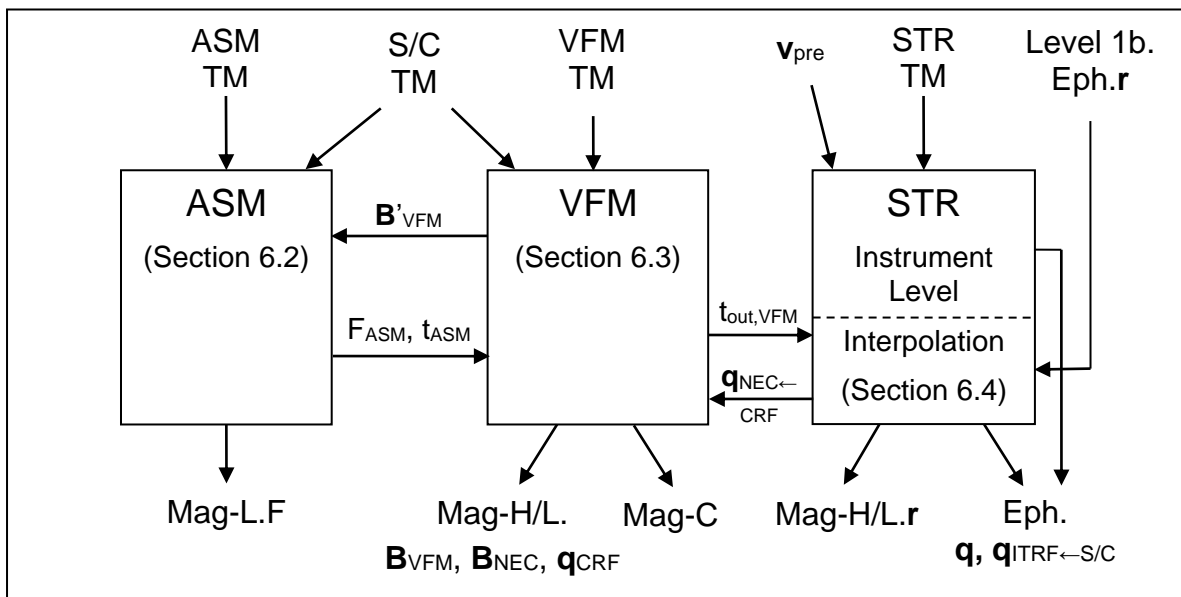


Figure 6-1 Overview of Magnetic Data Processing

| | Element | Description |
|---------------------------|---------------------|--|
| Level 1a inputs | ASM TM | ASM telemetry, measurements and HK |
| | S/C TM | S/C telemetry required to compute magnetic stray fields |
| | VFM TM | VFM telemetry, measurements and HK |
| | STR TM | STR telemetry, measurements and required HK |
| Intermediary input/output | v_{pre} | Preliminary S/C velocity, ITRF, required initially |
| | Level 1b.Eph.r | S/C position, ITRF, output from MOD – required for the final computation of \mathbf{r}_{VFM} |
| | \mathbf{B}'_{VFM} | Intermediary magnetic vector data (50 Hz) |
| | $t_{out,VFM}$ | Time-stamps of VFM measurements – 50 Hz |
| | F_{ASM} | Calibrated and corrected scalar magnetic data |

| | Element | Description |
|-----------------------|---|---|
| | t_{ASM} | Time instants of F_{ASM} measurements |
| | $\mathbf{q}_{NEC \leftarrow CRF}$ | Quaternion representation of $CRF \rightarrow NEC_{VFM}$ transformation, at UTC seconds (1 Hz) and at $t_{out,VFM}$ (50 Hz) |
| Final Level 1b output | Mag-L.F | Magnetic scalar data, 1 Hz |
| | Mag-H/L. \mathbf{B}_{XXX} | Magnetic vector data, 50 Hz and 1 Hz, VFM and NEC frame |
| | Mag-H/L. \mathbf{q}_{CRF} | Attitudes, same as $\mathbf{q}_{NEC \leftarrow CRF}$ above |
| | Mag-C | VFM calibration product, see Section 6.3 |
| | Eph. \mathbf{q} | Attitudes, STR Instrument Level 1b data |
| | Eph. $\mathbf{q}_{ITRF \leftarrow S/C}$ | Attitudes, 1 Hz, S/C \rightarrow ITRF transformation |
| | Mag-H/L. \mathbf{r} | Positions for magnetic products (VFM sensor position), ITRF |

Table 6-2 Elements of Figure 6-1

There are two additional, auxiliary magnetic products, ASMXAUX_1B and VFMXAUX_1B, containing detailed stray field information to be used for analysis of instrument and S/C performance and data analysis.

6.1 Magnetic Stray Fields

The magnetic stray fields are divided into three categories:

- State dependent (including static contribution)
- Electrically induced (by currents)
- Magnetically induced (through soft magnetic materials)

6.1.1 State Dependent Stray Fields

The static and state dependent stray fields are modelled by two vectors, *biases*, one for the VFM and one for the ASM sensor position. The total static stray field from the satellite body with all instruments and subsystems turned off are stored in the CCDB.Bus.Static.**Base**_{XXX} vectors, where XXX is ASM respectively VFM. All operational states of an instrument or subsystem – except thruster activation (see below) – causing a change in its steady magnetic field are registered in the Level 1a.Bus.State.**States** vector, and the corresponding change in the magnetic field vector is stored in **dB**_{XXX} of the corresponding entry in CCDB.Bus.State.Field. In case electrical heaters produce stray fields, these must be included in Level 1a.Bus.State.**States**. Stray fields caused by thruster activation are characterized by CCDB.AOCS.Thruster_{XXX}. I.e. the actual state dependent stray field at e.g. the VFM sensor position is given by:

$$\mathbf{dB}_{\text{State,VFM}} = \text{CCDB.Bus.Static.Base}_{\text{VFM}} + \mathbf{M}_{\text{State,VFM}} \times \text{Level 1a.Bus.State.States} + \text{CCDB.AOCS.Thruster}_{\text{VFM}} \times \quad (6.1-10)$$

$$\text{State}_{\text{Thruster}}(\text{Level 1a.AOCS.Thru_HK}, \text{L0.Bus.PCDU_A_RuALclStat}, \text{CCDB.AOCS.Thruster_Settling_Time}, t)$$

where

$$\mathbf{M}_{\text{State,XXX}}(:,i) = \text{CCDB.Bus.State.Field}(i).\mathbf{dB_XXX} \quad (6.1-15)$$

i.e. the i 'th column of $\mathbf{M}_{\text{State,XXX}}$ is $\text{CCDB.Bus.State.Field}(i).\mathbf{dB_XXX}$.

$\text{State}_{\text{Thruster}}$ maps the thruster activation telemetry into a 0/1 vector for given time instant t . $\text{Level1a.AOCS.Thru_HK}$ contains the three fields t , \mathbf{dt} and Valid (see Section 5.5) – \mathbf{dt} and Valid are vector/bitmask of length 12 corresponding to 8 attitude control and 4 orbit control thrusters. Only if $\text{Valid}_i = 1$, the contents of \mathbf{dt}_i is valid and contains the duration of the activation of thruster i – duration since the time-stamp, t , of $\text{Level1a.AOCS.Thru_HK}$. Note that \mathbf{dt}_i may be larger than 1 second, i.e. “extending” into the next $\text{Level1a.AOCS.Thru_HK}$ packet, and note that thruster duration may be overridden (e.g. terminated if $\mathbf{dt}_i = 0$) in subsequent packets. $\text{L0.Bus.PCDU_A_RuALclStat}$ (cf Section 5.4.5) indicates whether primary ($v=0$) or redundant ($v=1$) thrusters are activated. $\text{CCDB.AOCS.Thruster_Settling_Time}$ contains the estimated vibration settling time of the S/C following thruster activation I.e.

$$\text{State}_{\text{Thruster},i}(\text{Thru_HK}, v, \mathbf{st}, t) = \begin{cases} 1 & \text{if } t < \text{Thru_HK}(j).t + \text{Thru_HK}(j).\mathbf{dt} + \mathbf{st} \\ & \text{where } j \text{ is the largest } j \text{ for which} \\ & \text{Thru_HK}(j).\text{Valid}_{i-12v} = 1 \text{ and } t \geq \text{Thru_HK}(j).t \\ 0 & \text{otherwise} \end{cases} \quad (6.1-16)$$

6.1.2 Electrically Induced Stray Fields

The electrically induced stray fields originate from various bus currents, e.g. solar panel array currents, battery charge/discharge currents, and in particular currents in the magneto-torquer coils of the AOCS. The stray fields of the AOCS magnetotorquer coils are described temporally by their transfer function and magnetically by linear interpolation (table look-up) followed by matrix multiplication. These matrices ($\text{CCDB.AOCS.M}_{\text{XXX}}$) include the static and default state magnetically induced contributions from the S/C body. The electrically induced stray fields from other sources (Bus currents) are modelled by smoothing filters followed by look-up tables and matrix multiplication.

The parameters for electrically induced stray fields are stored in the CCDB.AOCS and CCDB.Bus.Current structures. The relevant fields are listed in Table 6-3.

| Field | Type | Description | |
|--|---|---|--|
| CCDB.AOCS parameters | | | |
| I_xfer | LUT1d | Current transfer look-up tables. Order: MTQ1_A, MTQ2_A, MTQ3_A, MTQ1_B, MTQ2_B, MTQ3_B | |
| M _{Xxx} | 3 x 6 matrix | Output multiplication matrix for sensor Xxx Xxx = VFM, ASM | |
| Transfer | D | real | |
| | wo | real | |
| | dt | real | |
| Temporal characterization parameters of AOCS coil transfer function. | | | |
| Transfer _{VFM} | <i>Characterization of AOCS coil and VFM instrument transfer functions.</i> | | |
| | dt | vector | Time offsets of transfer regions, 3 elements |
| | coeff1 | polynomial | Cubic polynomial for t in [t ₀ +dt ₁ ..t ₀ +dt ₂] |
| | coeff2 | polynomial | Cubic polynomial for t in]t ₀ +dt ₂ ..t ₀ +dt ₃] |
| Thruster _{Xxx} | 3 x 24 matrix | Thruster activation stray field matrix, for Xxx sensor position (see Section 6.1.1). Order: primary attitude 1-8, primary orbit 1-4, redundant attitude 1-8, redundant orbit 1-4. | |
| Max _{ASM} | vector | Maximum AOCS stray field vector at ASM sensor | |
| Max _{VFM} | vector | Maximum AOCS stray field vector at VFM sensor | |
| CCDB.Bus.Current parameters, 3 groups: Yyy = Bat, SP, other. | | | |
| Filter _{Yyy} | FIR_FP | Filter averaging parameter. See Appendix E Page 143 and [AD03]. | |
| Yyy(i).I_xfer | LUT1d | Current transfer look-up table | |
| Yyy(i).dB_Xxx | vector | Current dependent stray field vectors for Xxx sensor position, columns in M _{Current,Xxx} matrix. Xxx = ASM, VFM | |
| Max _{ASM} | vector | Maximum bus current stray field vector at ASM sensor | |
| Max _{VFM} | vector | Maximum bus current stray field vector at VFM sensor | |

Table 6-3 Structure(s) for Electrically Induced and State Dependent Stray Fields

For Bus currents, the stray field is computed as follows: Given an input vector of length k of telemetry currents, $Level1a.Bus.Curr.I_{group}$, each element is first converted using the corresponding $CCDB.Bus.Current.group.I_xfer$ look-up table (using $Interpol_{Lin}$), then they are filtered according to $CCDB.Bus.Current.Filt_{group}$ using the Filter function (see Appendix E Page 142f for these functions) yielding $I^{filt,group}$ – except for the battery current, which is a single current measured three times, $I^{filt,Bat}$ is hence a weighted average of the three measurements with weights $CCDB.Bus.Current.wt_{Batt}$:

$$I^{filt,Bat} = \sum_i wt_{Batt,i} Filter(Interpol_{Lin}(I_{Bat,i})) / \sum wt_{Batt} \quad (6.1-18)$$

In the event of large gaps (longer than $CCDB.Bus.Current.Filt_{group}.Max_Gap_Size$) there is no stray field correction for Bus currents, and data are flagged with missing Bus telemetry.

Now, the stray field at location Xxx (ASM, VFM, or Body) is calculated as:

$$\mathbf{dB}_{Bus,Xxx} = \sum_{group=SP,Bat,other} M_{Current,group,Xxx} \times \mathbf{I}^{filt,group} \quad (6.1-20)$$

where:

$$M_{Current,group,Xxx}(:,i) = CCDB.Bus.Current.group(i).\mathbf{dB_Xxx} \quad (6.1-25)$$

and *group* is SP, Bat, or other for the respective source groups.

The stray fields of the AOCS torquer coils are computed in much the same way as for the Bus currents. However the temporal characteristics of the AOCS fields are known in detail as these currents are carefully controlled; hence the filtering of the telemetry is replaced by temporal transfer characterisation functions. The basic transfer response is sketched in Figure 6-2, and the corresponding stray field is computed using the CCDB.AOCS parameters as specified in Eq. (6.1-27a). For the VFM, the transfer function of the VFM instrument needs to be considered, hence two different transfer functions for the currents are computed – one for the ASM and one for the VFM – see Eq. (6.1-27c) and Eq. (6.1-27d) respectively.

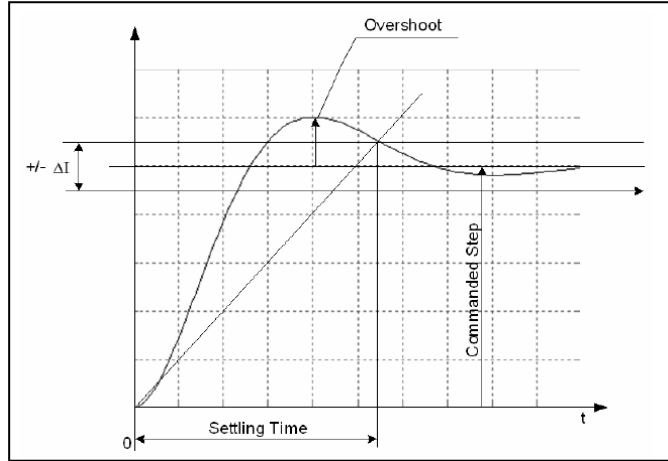


Figure 6-2 AOCS Magneto Torquer Transition

$$\mathbf{dB}_{\text{AOCS},\text{XXX}}(t) = \text{CCDB.AOCS.M}_{\text{XXX}} \times \mathbf{I}_{\text{AOCS},\text{XXX}}(t) \quad (6.1-27a)$$

where $\text{XXX} = \text{ASM or VFM}$. Given $\mathbf{I}_{\text{AOCS},i} = \text{Interpol}_{\text{Lin}}(\text{CCDB.AOCS.I_xfer}, \text{Level1a.AOCS.Mag_HK.Imea_MTQ}(i))$, the i^{th} torquer current sample measured and transformed at time $t_{\text{AOCS},i} = \text{Level1a.AOCS.Mag_HK.t}(i)$, then:

$$\mathbf{I}_{\text{AOCS},\text{XXX}}(t) = \mathbf{I}_{\text{AOCS},i} - y_{\text{XXX}}(t - t_{\text{AOCS},i}) \mathbf{dI}_{\text{AOCS},i},$$

$$\begin{cases} \text{for XXX = ASM and } t_{\text{AOCS},i} \leq t < t_{\text{AOCS},i+1} \\ \text{for XXX = VFM and } t_{\text{AOCS},i} \leq t - \text{CCDB.AOCS.Transfer}_{\text{VFM}} \cdot dt_1 < t_{\text{AOCS},i+1} \end{cases} \quad (6.1-27b)$$

where $\mathbf{dI}_{\text{AOCS},i} = \mathbf{I}_{\text{AOCS},i} - \mathbf{I}_{\text{AOCS},i-1}$. $y_{\text{ASM}}(dt)$ is given by:

$$y_{\text{ASM}}(dt) = \begin{cases} \frac{\sin(\text{acos}(D) + dt \text{ wo } \sqrt{1-D^2})}{e^{dt \text{ w } D} \sqrt{1-D^2}} & \text{for } dt < \text{CCDB.AOCS.Transfer} \cdot dt \\ 0 & \text{otherwise} \end{cases} \quad (6.1-27c)$$

where D and wo are the parameters of $\text{CCDB.AOCS.Transfer}$.

$y_{\text{VFM}}(dt)$ is given by:

$$y_{\text{VFM}}(dt) = \begin{cases} 1 & \text{for } dt < \text{CCDB} \dots dt_1 \\ 1 - \text{polyval}(\text{coeff1}, dt) & \text{for } \text{CCDB} \dots dt_1 \leq dt \leq \text{CCDB} \dots dt_2 \\ 1 - \text{polyval}(\text{coeff2}, dt) & \text{for } \text{CCDB} \dots dt_2 < dt \leq \text{CCDB} \dots dt_3 \\ 0 & \text{for } dt > \text{CCDB} \dots dt_3 \end{cases} \quad (6.1-27d)$$

where coeff1 and coeff2 are the parameters of $\text{CCDB.AOCS.Transfer}_{\text{VFM}}$, and $\text{CCDB} \dots dt = \text{CCDB.AOCS.Transfer}_{\text{VFM}} \cdot dt$ and $\text{polyval}(P,t)$ is the polynomial specified by P evaluated at t .

6.1.3 Magnetically Induced Stray Fields

Magnetically induced stray fields are modelled in two parts. One part corresponds to the induced field due to the ambient magnetic field; the other part corresponds to AOCS magnetorquer induced fields in state dependent equipment.

The soft-magnetic field induced by the ambient field is a combination of static+default-state and state-dependent contributions:

$$\mathbf{dB}_{\text{induced},X_{xx}} = (\text{CCDB.Bus.Static.Ind}_{X_{xx}} + \sum_i \text{Level1a.Bus.State.IndState}_i \text{CCDB.Bus.State.Induced}_i \cdot \text{dInd}_{X_{xx}}) \times \mathbf{B}'_{\text{Body}} \quad (6.1-30)$$

where X_{xx} is ASM or VFM. The sum of the matrices is done element-wise. $\mathbf{B}'_{\text{Body}}$ is the ambient magnetic field vector, $\mathbf{B}_{\text{ambient}} = \text{CCDB.Structure.VFM}_q^{-1} \times \mathbf{B}'_{\text{VFM}}$, in the S/C frame computed from the calibrated and corrected VFM measurements (see Section 6.3.4) plus the electrically induced field from bus currents, $\mathbf{dB}_{\text{Bus,Body}}$ (but not including AOCS currents):

$$\mathbf{B}'_{\text{Body}} = \mathbf{B}_{\text{ambient}} + \mathbf{dB}_{\text{Bus,Body}} \quad (6.1-41)$$

The state dependent, magnetically induced field of the AOCS magnetorquers is computed as follows:

$$\mathbf{dB}_{\text{AOCS-Ind},X_{xx}} = \left(\sum_i \text{Level1a.Bus.State.IndState}_i \text{CCDB.Bus.State.Induced}_i \cdot \text{dAM}_{X_{xx}} \right) \times \mathbf{I}_{\text{AOCS},X_{xx}} \quad (6.1-50)$$

where $\mathbf{I}_{\text{AOCS},X_{xx}}$ are the mapped AOCS torquer currents from Eq. (6.1-27b). The summed matrix of Eq. (6.1-50) may be added to $\text{CCDB.AOCS.M}_{X_{xx}}$ before multiplication with \mathbf{I}_{AOCS} :

$$\mathbf{dB}_{\text{AOCS},X_{xx}} = (\text{CCDB.AOCS.M}_{X_{xx}} + \sum_i \text{Level1a.Bus.State.IndState}_i \text{CCDB.Bus.State.Induced}_i \cdot \text{dAM}_{X_{xx}}) \times \mathbf{I}_{\text{AOCS},X_{xx}} \quad (6.1-60)$$

6.2 Absolute Scalar Magnetometer – ASM

6.2.1 Introduction

The Absolute Scalar Magnetometer (ASM) measures the magnetic field intensity at the tip of the boom. The ASM is an absolute instrument, i.e. it is not subject to changes of its intrinsic parameters over time. It uses the PPS as the absolute, external reference.

[AD05] contains descriptions of the ASM intrinsic processing algorithms for both the nominal scalar mode and the experimental vector mode. Both modes generate scalar (magnetic field intensity) data; the processing of these is described in this chapter, including the *system level* algorithms for stray field correction. Vector data from the ASM vector mode (as well as burst mode data) are only provided as Level 1a data⁵.

6.2.2 Input and Output Parameters

| Inputs | | | | | |
|----------|--------------------------|---|--|---------------------------|---------------------|
| Element | | Description | Unit | Range ⁶ | |
| Level 1a | ASM.Sci.E | Raw ASM measurement | eu | | |
| | ASM.Sci.N | ASM reference frequency count | | 29 – 30 * 10 ⁶ | |
| | AOCS.Mag_HK | Magneto-torquer coil currents | A | ±10 ² | |
| | AOCS.Thru_HK | Thruster activations | | 0/1 | |
| | Bus.State | States of instruments/subsystems with varying magnetic disturbance – incl. induced | | 0/1 | |
| | Bus.Curr | Bus currents e.g. solar panels, main power bus (one vector with all currents) | A | ± 2 * 10 ⁴ | |
| | B' _{VFM} | Calibrated and corrected magnetic field vector measurements from the VFM (using TCF.VFM ^{init} parameters) | nT | ± 66,000 | |
| CCDB | A S M | b_mod | Vector mode modulation | nT | 0 – 10 ³ |
| | | B_rem | Remanent magnetization (static stray field vector) | nT | 0 – 10 |
| | | B_rf | RF field amplitude | nT | 0 – 100 |
| | | Delay | Delay between actual measurement and timestamp | s | ±1 |
| | | Induced | Induced magnetization (matrix) | | ±10 ⁻⁴ |
| | | k_BS | Bloch-Siegert correction coefficient | nT ² | 0 – 10 ⁵ |

⁵ The ASMXAUX_1B Level 1b Product contain additional data suited for the Level 1a ASM vector data.

⁶ In case of a vector or matrix, **Range** indicates the range of the single elements.

| | | | | | |
|---|-------------|--|--|-------------|------------------|
| | Filter | Coeff | Matrix holding coefficients of ASM filter designed for 50 Hz sampling frequency | | ± 5 |
| | | Delay | Delay introduced by ASM filter (<i>group delay</i> , both scalar and vector mode) | s | 0 – 5 |
| L 1 B P . A S M | Dist_Max | | Total maximum magnetic disturbance intensity at ASM sensor position | nT | 1 – 30 |
| | Freq_Div | | NMR frequency divider | | $10^2 - 10^3$ |
| | Limits | | Structure holding limits for outlier detection and/or rejection, see Table 6-4 | | |
| | N_Avg | | ASM.Sci.N Filter parameters | | |
| | NMR | | He ⁴ gyromagnetic frequency | GHz/ T | ≈ 28.024 |
| | Spline_Pars | | B-spline parameters for ASM interpolation, see text and [AD03] | | |
| Structure. ASM_q_VFM | | Rotation of ASM frame to VFM frame, i. e. VFM→ASM transformation cf. Table 3-1 | | | ± 1 |
| AOCS | | Structure characterizing the magnetic stray field vector of the AOCS at ASM sensor position. Includes any non-linearities, time-characteristics of the AOCS coil system, static and default-state induced effects, and the maximum disturbance from the AOCS. See Table 6-3 in Section 6.1.2 | | | |
| Bus | | Structure characterizing the magnetic stray field (electrical and magnetical induced) vector of the S/C; static, state dependent, and bus currents dependent parts. Includes values for the maximum disturbances and uncertainty estimate of stray field calculation. See Table 6-3 | | | |
| L1BP.VFM.Max_ ASM_VFM_Diff | | Maximum ASM – VFM scalar discrepancy, for flagging | | nT | 0 – 100 |
| VFM.Ind_ASM | | Dipole field of VFM at ASM sensor position | | | $\pm 10^{-4}$ |
| Structure. VFM_q | | Rotation of VFM sensor frame to S/C frame | | | ± 1 |
| Outputs | | | | | |
| Element/Group | | Description | | Unit | Range |
| Level 1b _{Inst.} .ASM.F | | ASM Level 1b data at instrument level, i.e. converted ASM measurements, not corrected for any stray fields | | nT | 15,000 – 66,000 |
| Level 1b _{Inst.} .ASM.F _{err} | | | | nT | 0 – 100 |

| | | | | |
|-----------------------|---------------------|---|-----|-----------------|
| t_{ASM} | | Time instants of non-rejected ASM measurements | UTC | |
| F_{ASM} | | Fully converted and corrected magnetic field intensity at t_{ASM} time instants (i.e. not corrected for filter group delay) | nT | 15,000 – 66,000 |
| Level 1b. Mag-L | F | Fully converted and corrected magnetic field intensity at UTC seconds | nT | 15,000 – 66,000 |
| | F_{error} | Error estimate of F | nT | 0 – 100 |
| | dF_{AOCS} | AOCS stray field correction | nT | ± 50 |
| | dF_{other} | Stray field correction – all other sources | nT | ± 20 |
| | Flags _{SF} | Flags related to the ASM data | | |
| | ASM_Freq_Dev | Deviation of frequency calibration data | | |
| ASMXAUX_1B (Level 1b) | | Auxiliary Level 1b product containing magnetic stray fields at ASM sensor position | | |

6.2.3 ASM Algorithm Overview

The overall processing is sketched in Figure 6-3 below: First, the raw output (Level 1a.ASM.Sci.E, rate: 1 Hz, timestamps $t_{0,ASM}$) from the ASM is converted to physical units (nT), corrected for the Bloch-Siegert effect, and corrected for delays in timestamps (from $t_{0,ASM}$ to t_{ASM}). This constitutes the Level 1b_{Inst.}ASM data, the ASM *instrument Level 1b* scalar product containing the perturbed magnetic field intensity measurements at corrected time instants, t_{ASM} . Note: this includes stray fields from the ASM itself.

Then outlier detection and/or rejection is performed. Followed by corrections for magnetic disturbances (stray fields) of the ASM itself, of the VFM, and of the rest of the spacecraft. These disturbances need to be filtered according to the intrinsic filter of the ASM instrument (see Section 6.2.4 below). This constitutes the fully calibrated and corrected scalar magnetic measurements, F_{ASM} , at instrument time instants (t_{ASM})

These data are then adjusted for the group delay of the ASM intrinsic filter, i.e. the measurements are shifted in time from t_{ASM} to $t_{out,ASM}$.

Finally, these data are interpolated to yield the scalar elements of the Level 1b.Mag-L product at UTC seconds. The interpolation process also bridges small gaps (a few samples) in the ASM data stream typically caused by missing telemetry (missing ISP) or outlier rejection.

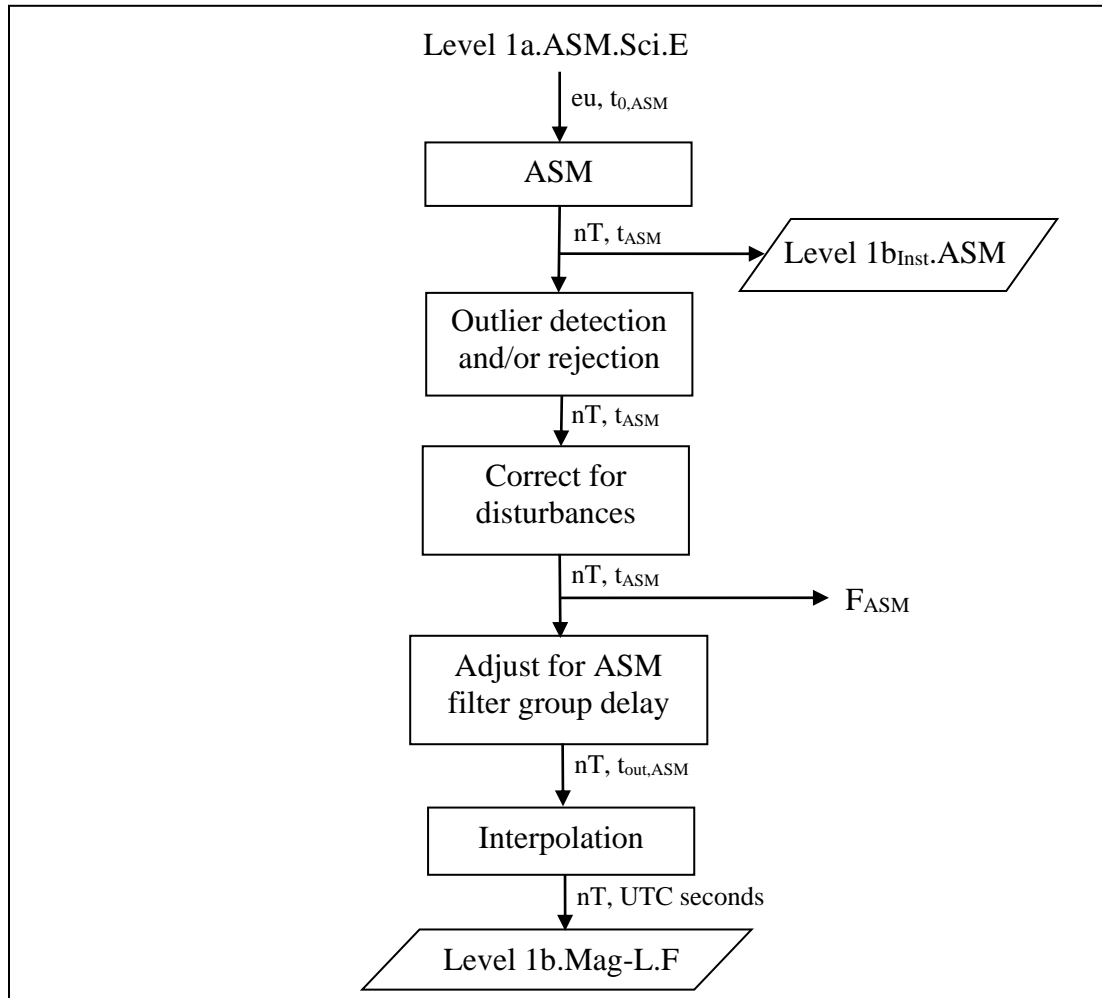


Figure 6-3 ASM Processing Overview

6.2.4 Detailed Description of ASM Processing

The processing of the ASM data is shown in detail in Figure 6-4 on the next page. The elements in the figure are as follows:

| | |
|--------------------|---|
| $F^{(i)}$ | The magnetic field intensity after processing step i. These are given at the corrected time instants of the ASM samples, t_{ASM} , except $F^{(4)}$ which are given at $t_{out,ASM}$ time instants. |
| $F^{(i)}_{err}$ | The uncertainty estimate of $F^{(i)}$. |
| ΔF_{Total} | The total magnetic disturbance from the S/C at the ASM sensor location, filtered according to the ASM intrinsic filter. |
| κ | Uncertainty of ΔF_{Total} due to lack of needed telemetry. |
| ε | Total uncertainty estimate of ΔF_{Total} . |

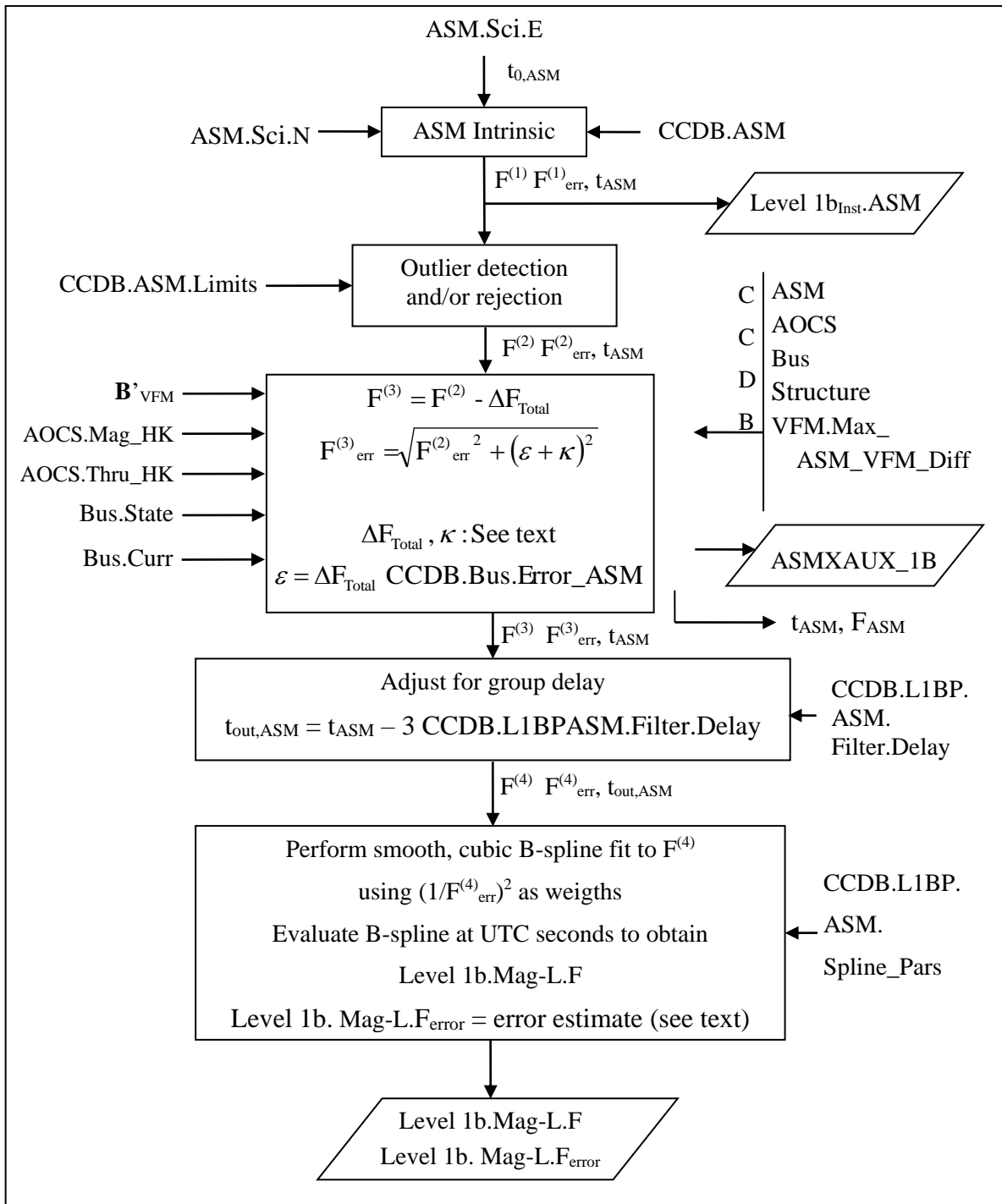


Figure 6-4 ASM Processing

6.2.4.1 ASM Intrinsic Processing

The ASM intrinsic processing consists of conversion of the raw measurements (Level 1a. ASM.Sci.E) into physical units (nT) using the actual frequency of the internal ASM reference oscillator given by the Level 1a.ASM.Sci.N telemetry (in the following, the “Level 1a” prefix is omitted). As ASM.Sci.N represents the oscillator count between two consecutive PPS (Pulse Per Second) this is first filtered to avoid spurious PPS’s to propagate to the ASM data. This is done with the Filter function, see page 143 (Appendix E) – gaps are handled as for the Bus currents, see Section 6.1.2. Now, with N_Avg, Freq_Div and NMR being elements of the CCDB.L1BP.ASM structure:

$$F^{(0)} = \text{ASM.Sci.E Filter}(N_Avg, \text{ASM.Sci.N}) \text{ Freq_Div} / \text{NMR} \quad (6.2-10)$$

$F^{(0)}$ is further corrected for the Bloch-Siegert effect and – in vector mode – for the aliasing effect, see [AD05]. I.e. (CCDB.ASM prefix omitted):

$$\begin{aligned} F^{(1)} &= F^{(0)} - \Delta F_{\text{Bloch-Siegert}} - \Delta F_{\text{aliasing}} \\ &= F^{(0)} + k_BS B_rf^2 / F^{(0)} - b_mod^2 / 2F^{(0)} \end{aligned} \quad (6.2-20)$$

Finally, the Level 0 timestamps are corrected for processing delays (group delays introduced by the ASM instrument filter are corrected later):

$$t_{\text{ASM}} = t_{0,\text{ASM}} - \text{CCDB.ASM.Delay} \quad (6.2-30)$$

The error estimate, $F^{(1)}_{\text{err}}$ is set to 10 pT.⁷

Falgs_F is set according to the availability of ASM.Sci.N data for the filter in Eq. (6.2-10), and according to the presence of ASM sampling start or a data gap within 8 seconds prior to the current sample.

The ASM_Freq_Dev quality indicator of the ASM instrument is the square root of the deviation of Level1a.ASM.Sci.N and the filtered value of same. Let $N = \text{Level1a.ASM.Sci.N}$ and $N^{\text{filt}} = \text{Filter}(\text{CCDB.L1BP.ASM.N_Avg}, N)$ (N^{filt} is used in Eq. (6.2-10)) then:

$$\text{ASM_Freq_Dev} = \begin{cases} \sqrt{N - N^{\text{filt}}} & \text{if } N \geq N^{\text{filt}} \\ -\sqrt{N^{\text{filt}} - N} & \text{if } N^{\text{filt}} > N \end{cases} \quad (6.2-35)$$

6.2.4.2 Outlier Detection

Outliers are detected by pure out-of-range check plus a range check of 2nd order time derivatives of $F^{(1)}$.

The CCDB.L1BP.ASM.Limits structure contains the following fields:

| Field | Type | Unit | Comment |
|-----------|--------|-------------------|--------------------------------------|
| Range | vector | nT | Allowed range, e.g. [10,000..66,000] |
| Max_Accel | real | nT/s ² | Maximum allowed acceleration |

⁷ $F^{(1)}_{\text{err}}$ is no longer raised after sampling start or a data gap – these data are only flagged.

| Field | Type | Unit | Comment |
|--------------|------|-------------------|---|
| Pass_Accel | real | nT/s ² | Accelerations below this are accepted Between Pass_Accel and Max_Accel samples are flagged as <i>suspicious</i> and associated with raised uncertainty estimates |
| Max_Gap_Size | real | s | Definition of size of data gaps |

Table 6-4 CCDB.L1BP.ASM.Limits Structure

First, all $F^{(1)}$ samples outside Range are discarded. Then, the 1st and 2nd order time derivatives, F' respectively F'' , of the remaining field measurements are computed:

$$F'_i = (F_i - F_{i-1}) / (t_i - t_{i-1}) \tag{6.2-40}$$

$$F''_i = 2(F'_{i+1} - F'_i) / (t_{i+1} - t_{i-1}) \tag{6.2-50}$$

where in Eq. (6.2-50) $i = 2, 3, \dots, n-1$.

For all blocks of consecutive outliers, i.e. blocks for which $|F''_i| > \text{Max_Accel}$ for all $i = i_1, \dots, i_2$, remove samples depending on the length of the block as follows:

1. If block has one sample, remove sample F_{i_1}
2. If block has two samples, remove sample with highest $|F''|$
3. If block has three or more samples, remove samples i_1+1, \dots, i_2-1 (all but first and last)

Additionally, if the block begins or ends at a gap in data or at the ends of the data:

4. If $(t_{i_1} - t_{i_1-1}) > \text{CCDB.L1BP.ASM.Spline_Pars.Max_Gap_Size}$ remove also sample F_{i_1}
5. If $(t_{i_1-1} - t_{i_1-2}) > \text{CCDB.L1BP.ASM.Spline_Pars.Max_Gap_Size}$ or $i_1 = 2$ (at beginning of data) remove also samples F_{i_1-1} and F_{i_1}
6. If $(t_{i_2+1} - t_{i_2}) > \text{CCDB.L1BP.ASM.Spline_Pars.Max_Gap_Size}$ remove also sample F_{i_2}
7. If $(t_{i_2+2} - t_{i_2+1}) > \text{CCDB.L1BP.ASM.Spline_Pars.Max_Gap_Size}$ or $i_2 = n-1$ (at end of data) remove also samples F_{i_2} and F_{i_2+1}

When completed, recomputed F'' using non-rejected samples and re-perform the checks above for blocks of $|F''_i| > \text{Pass_Accel}$ this time marking samples as suspicious (flag value 4 in Table 6-5) and raised error estimates of all samples j marked as suspicious:

$$F^{(2)}_{j,\text{err}} = \sqrt{(F^{(1)}_{j,\text{err}})^2 + \Delta F_j^2} \tag{6.2-60}$$

$$\Delta F_j = F_j - (F_{j-1} + (F_{j+1} - F_{j-1}) (t_j - t_{j-1}) / (t_{j+1} - t_{j-1})) \tag{6.2-70}$$

ΔF_j is the difference between F_j and the linearly interpolated value of F_{j-1} and F_{j+1} . F_{j-1} and F_{j+1} are non-outliers but possibly suspicious. If at end of data ($j = 1$ or n) use extrapolation in Eq. (6.2-70).

6.2.4.3 Stray Fields

The calculation of stray fields is done at 50 Hz data rate at $t_{out,VFM}$ time instants in order to obtain sufficient accuracy in the later filter processing; $t_{out,VFM}$ is chosen for convenience since VFM measurements are used for ambient field information. The stray field vectors are then converted to their scalar equivalents using \mathbf{B}'_{VFM} , and filtered according to the ASM instrument filter (designed for 50 Hz data rate). Finally, these data are interpolated to the t_{ASM} time instants and subtracted from the $F^{(2)}$ measurements.

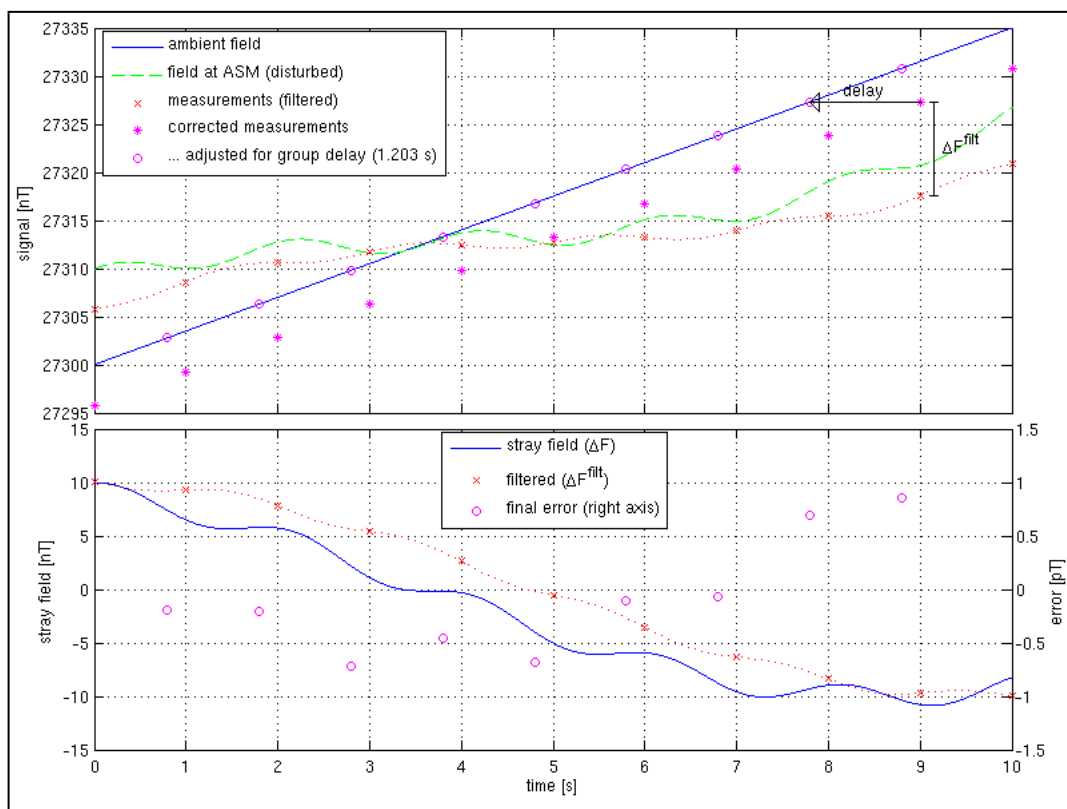


Figure 6-5 Example of ASM Measurements and Stray Fields

Figure 6-5 above illustrates an example of the stray field effect on ASM measurements showing, in the upper plot, both undisturbed (“ambient field” in blue) and disturbed (green) field intensities as well as the corresponding ASM measurements (filtered internally in the ASM at 1 kHz, shown in red). The lower plot shows the stray field intensity (blue) and its filtered value (red). The application of this is indicated in the upper plot by the vertical ΔF^{filt} bar and shown by the magenta stars, which are then corrected for the filter group delay to yield the undisturbed field measurements (magenta circles). The final errors between the measurements and the true field are shown to be virtually zero (< 1 pT) by magenta circles in the lower plot.

The processing required for the stray field computation is shown in Figure 6-6 below. First, any gaps in the \mathbf{B}'_{VFM} data less than 60 seconds in length are filled with linearly interpolated

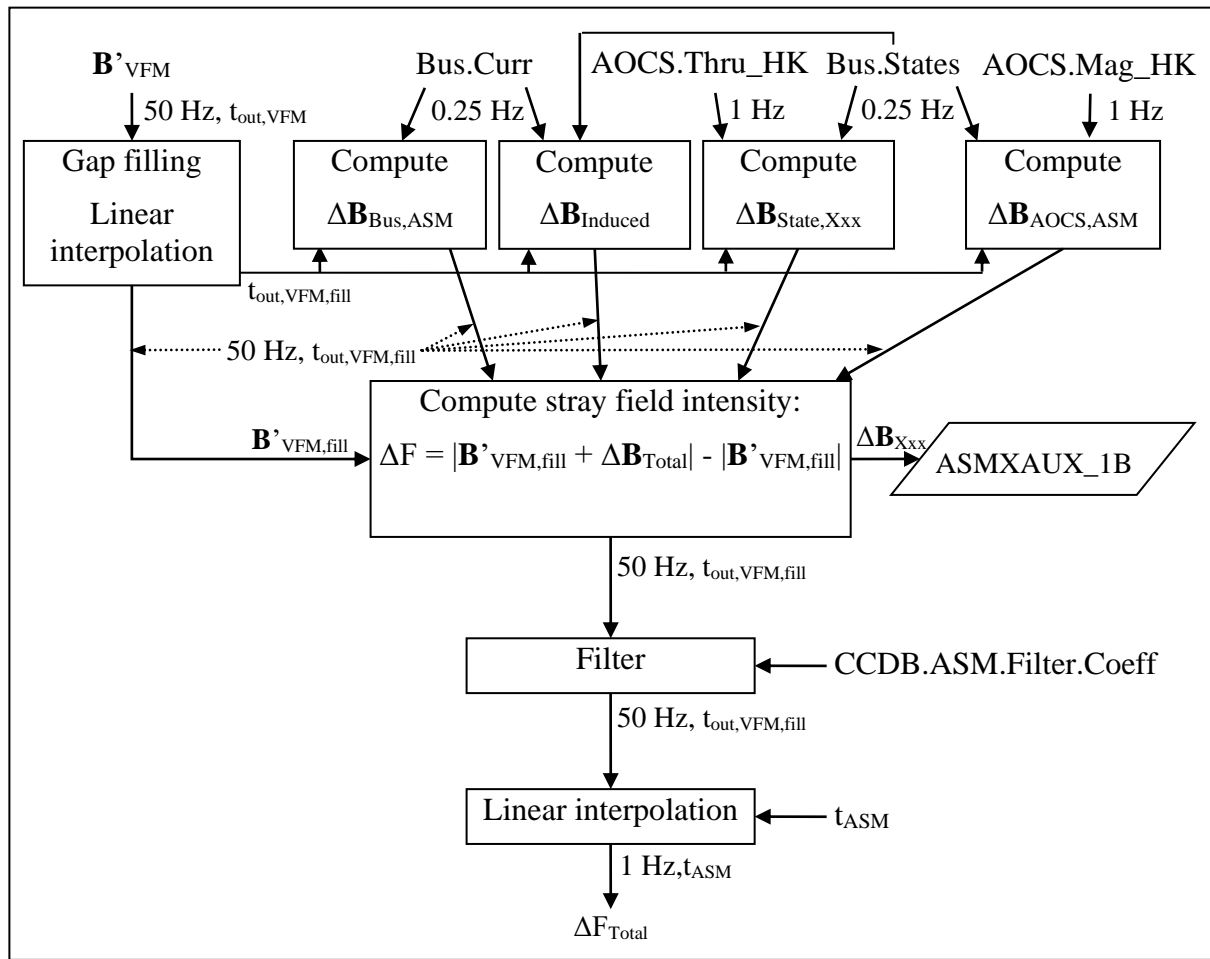


Figure 6-6 ASM Stray Field Processing

values. This also provides the $t_{out,VFM,fill}$ time-instants. Then, the Bus.Curr. \mathbf{I}_{group} telemetry currents are filtered, linearly interpolated to the $t_{out,VFM,fill}$ time-instants, and converted to stray field vectors ($\Delta \mathbf{B}_{Bus,XXX}$) using the CCDB.Bus specification (see Section 6.1.2). This must be done for the ASM sensor ($XXX = ASM$) as well as S/C body ($XXX = Body$) which is used in the calculation of the magnetically induced field. The AOCS.Mag_HK.**Imea_MTQ** currents are transformed according to the CCDB.AOCS (which includes the temporal properties of the transfer function of the AOCS) and CCDB.Bus.State.Induced.dAM_{ASM} specifications to yield $\Delta \mathbf{B}_{AOCS,ASM}$ at the $t_{out,VFM,fill}$ time-instants, cf Section 6.1.2. Note: the $\Delta \mathbf{B}_{AOCS,ASM}$ only contains the stray fields of the magneto-torquer coils, it does not include stray fields from latch valves and thrusters – these are contained in $\Delta \mathbf{B}_{Bus,ASM}$.

$\Delta \mathbf{B}_{State,ASM}$ is computed (cf. Section 6.1.1):

$$\Delta \mathbf{B}_{State,ASM} = \text{CCDB.Bus.Static.Base}_{ASM} + \text{M}_{State,ASM} \times \text{Interpolate}_{Step}(\text{Level1a.Bus.State.States}, t_{out,VFM,fill}) + \text{CCDB.AOCS.Thruster}_{XXX} \times \text{State}_{Thruster}(\text{Level1a.AOCS.Thru_HK}, t_{out,VFM,fill}) \quad (6.2-80)$$

$\text{Interpolate}_{Step}$ simply repeats the last state at the provided input time instants ($t_{out,VFM,fill}$). $\text{State}_{Thruster}$ returns the thrusters states at the provided input time instants ($t_{out,VFM,fill}$).

The magnetically induced stray field contribution is computed (cf. Section 6.1.3):

$$\Delta \mathbf{B}_{\text{Induced}} = (\text{CCDB.Bus.Static.Ind}_{\text{ASM}} + \sum_i \text{Level1a.Bus.State.IndState}_i \cdot \text{CCDB.Bus.State.Induced}_i \cdot \text{dInd}_{\text{ASM}}) \times (\mathbf{VFM_q}^{-1} \times \mathbf{B}'_{\text{VFM,fill}} + \Delta \mathbf{B}_{\text{Bus,Body}}) \quad (6.2-85)$$

The CCDB.Structure prefix of $\mathbf{VFM_q}$ (and $\mathbf{ASM_q_VFM}$ below) has been omitted.

The next step computes the magnetic stray field from the VFM and ASM, $\Delta \mathbf{B}_{\text{VFM}}$ respectively $\Delta \mathbf{B}_{\text{ASM}}$, and adds all the stray field parts into $\Delta \mathbf{B}_{\text{Total}}$. Note: $\Delta \mathbf{B}_{\text{VFM}}$, $\Delta \mathbf{B}_{\text{ASM}}$ and $\Delta \mathbf{B}_{\text{Total}}$ are in the VFM frame, all the other $\Delta \mathbf{B}_{\text{xxx}}$ are in the S/C frame.

$$\Delta \mathbf{B}_{\text{VFM}} = \text{CCDB.VFM.Ind_ASM} \times \mathbf{B}'_{\text{VFM,fill}} \quad (6.2-90)$$

$$\Delta \mathbf{B}_{\text{ASM}} = \mathbf{ASM_q_VFM}^{-1} \times (\text{CCDB.ASM.B_rem} + \text{CCDB.ASM.Induced} \times \mathbf{ASM_q_VFM} \times \mathbf{B}'_{\text{VFM,fill}}) \quad (6.2-100)$$

$$\Delta \mathbf{B}_{\text{Total}} = \Delta \mathbf{B}_{\text{VFM}} + \Delta \mathbf{B}_{\text{ASM}} + \mathbf{VFM_q} \times (\Delta \mathbf{B}_{\text{State,ASM}} + \Delta \mathbf{B}_{\text{Bus,ASM}} + \Delta \mathbf{B}_{\text{AOCS,ASM}} + \Delta \mathbf{B}_{\text{Induced}}) \quad (6.2-110)$$

The various $\Delta \mathbf{B}_{\text{xxx,ASM}}$ elements – $\Delta \mathbf{B}_{\text{Bus,ASM}}$ and $\Delta \mathbf{B}_{\text{State,ASM}}$ split into distinct parts – are transformed into the ASM sensor frame by $(\text{CCDB.Structure,})\mathbf{ASM_q_VFM}$ ($\Delta \mathbf{B}_{\text{VFM}}$) or $\mathbf{VFM_q} \otimes \mathbf{ASM_q_VFM}$ (all other $\Delta \mathbf{B}_{\text{xxx,ASM}}$) and stored in the ASMXAUX_1B Level 1b Product according to the following table, where $\mathbf{q} = \mathbf{VFM_q} \times \mathbf{ASM_q_VFM}$, and $\Delta \mathbf{B}_{\text{Src,ASM}|_{\text{xxx}}}$ indicates the contribution from XXX to $\Delta \mathbf{B}_{\text{Src,ASM}}$.

| ASMXAUX_1B element | Value |
|-----------------------|---|
| t | t _{out,VFM,fill} |
| dB _{AOCS} | $\mathbf{q} \times \Delta \mathbf{B}_{\text{AOCS,ASM}}$ |
| dB _{Thrust} | $\mathbf{q} \times \Delta \mathbf{B}_{\text{State,ASM} _{\text{Thruster}}}$ |
| dB _{Battery} | $\mathbf{q} \times \Delta \mathbf{B}_{\text{Bus,ASM} _{\text{Battery}}}$ |
| dB _{SP} | $\mathbf{q} \times \Delta \mathbf{B}_{\text{Bus,ASM} _{\text{Solar Panels}}}$ |
| dB _{Bus} | $\mathbf{q} \times \Delta \mathbf{B}_{\text{Bus,ASM} _{\text{other}}}$ |
| dB _{VFM} | $\mathbf{ASM_q_VFM} \times \Delta \mathbf{B}_{\text{VFM,ASM}}$ |
| dB _{Static} | $\mathbf{q} \times \text{CCDB.Bus.Static.Base}_{\text{ASM}}$ |
| dB _{Ind} | $\mathbf{q} \times \Delta \mathbf{B}_{\text{Induced}(,ASM)}$ |
| dB _{State} | $\mathbf{q} \times \Delta \mathbf{B}_{\text{State,ASM} }$ (excl. thrusters and static part) |

Now, ΔF is calculated:

$$\Delta F = |\mathbf{B}'_{\text{VFM,fill}} + \Delta \mathbf{B}_{\text{Total}}| - |\mathbf{B}'_{\text{VFM,fill}}| \quad (6.2-120)$$

The next step is the filtering of ΔF . Let \mathbf{a} and \mathbf{b} be the rows of `CCDB.ASM.Filter.Coeff`:

$$b_i = \text{CCDB.ASM.Filter.Coeff}_{1,i}$$

$$a_i = \text{CCDB.ASM.Filter.Coeff}_{2,i}$$

Let j be the sample number ($j = 1, 2, \dots$), i the filter *depth* ($i = 0, 1, 2, 3$), and $\Delta F^{(0)} = \Delta F$, then the filter calculation is as follows:

$$\Delta F_j^{(i+1)} = b_1 \Delta F_j^{(i)} + b_2 \Delta F_{j-1}^{(i)} + b_3 \Delta F_{j-2}^{(i)} - a_2 \Delta F_{j-1}^{(i+1)} - a_3 \Delta F_{j-2}^{(i+1)} \quad (6.2-130)$$

($a_1 = 1$, per definition, and is not used.)

The starting condition of the filter is:

$$\begin{aligned} \Delta F_0^{(i)} &= \Delta F_1^{(i)} - \delta^{(i)} & \Delta F_{-1}^{(i)} &= \Delta F_0^{(i)} - \delta^{(i)} \\ \Delta F_0^{(i+1)} &= \Delta F_0^{(i)} - d \cdot \delta^{(i)} & \Delta F_{-1}^{(i+1)} &= \Delta F_0^{(i+1)} - \delta^{(i)} \\ \delta^{(i)} &= \Delta F_2^{(i)} - \Delta F_1^{(i)} & d &= \text{CCDB.L1BP.ASM.Filter.Delay} / (t_2 - t_1) \end{aligned} \quad (6.2-140)$$

t_1 and t_2 are the times of ΔF_1 and ΔF_2 .

Whenever there is a gap in $t_{\text{out,VFM,fill}}$, the filter is “re-started”.

The ASM uses three invocations of the filter, hence $\Delta F^{(3)}$ are the appropriate filtered stray fields. They are linearly interpolated to the t_{ASM} time instants to yield the ΔF_{Total} .

The computation of the recordings of the AOCS stray field corrections in the Level 1b.Mag-C and Mag-L products, dF_{AOCS} , is done by performing Eq. (6.2-120), the filtering and the interpolation in time using $\Delta \mathbf{B}_{\text{AOCS}}$ in place of $\Delta \mathbf{B}_{\text{Total}}$. The interpolation in time is done to time instants t_{ASM} for Mag-C, and to $t_{\text{UTC}} + 3 \text{CCDB.ASM.Filter.Delay}$ for Mag-L (for the record at time t_{UTC}). dF_{other} is then computed by:

$$dF_{\text{other}} = \Delta F_{\text{Total}} - dF_{\text{AOCS}} \quad (6.2-145)$$

The factor κ , the uncertainty of ΔF_{Total} due to lack of telemetry, is computed as the average of the maximum amplitudes of unknown stray fields over the last $dt = 8 \text{CCDB.ASM.Filter.Delay}$ period. I.e. at time $t \in t_{\text{ASM}}$:

$$\kappa = \begin{cases} \text{CCDB.L1BP.ASM.Dist_Max} & \text{if there are gaps in } \mathbf{B}'_{\text{VFM,fill}} \\ & \text{in the time interval } [t-dt\dots t] \\ \sum_k v_k / n & \text{otherwise. The sum is for all } v_k \\ & \text{in the time interval } [t-dt\dots t], \\ & n \text{ is the number of such } v_k \text{'s} \end{cases} \quad (6.2-150)$$

where v_k is defined for the time instants of $\mathbf{B}'_{\text{VFM,fill}}$, $t'_{\text{VFM,fill}}$ as:

$$v_k = v_{\text{AOCS},k} + v_{\text{State},k} + v_{\text{Curr},k} \quad (6.2-152)$$

with

$$v_{\text{AOCS},k} = \begin{cases} 0 & \text{if } t_{\text{AOCS},r} \leq t'_{\text{VFM,fill},k} \leq t_{\text{AOCS},r} + 1\text{s for some } r \\ \text{CCDB.AOCS.Max}_{\text{ASM}} & \text{otherwise} \end{cases} \quad (6.2-154)$$

$$v_{\text{State},k} = \begin{cases} 0 & \text{if } t_{\text{State},r} \leq t'_{\text{VFM,fill},k} \leq t_{\text{State},r} + 4\text{s for some } r \\ \text{CCDB.Bus.State.Max}_{\text{ASM}} & \text{otherwise} \end{cases} \quad (6.2-156)$$

$$V_{\text{Curr},k} = \begin{cases} 0 & \text{if } t_{\text{Curr},r} - 2s \leq t'_{\text{VFM,fill},k} \leq t_{\text{Curr},r} + 2s \text{ for some } r \\ \text{CCDB.Bus.Current.Max}_{\text{ASM}} & \text{otherwise} \end{cases} \quad (6.2-158)$$

where t_{xxx} are the time instants of the available Xxx telemetry.

The F_{ASM} output is the set of $F^{(3)}$ ($= F^{(2)} - \Delta F_{\text{Total}}$), these correspond to the t_{ASM} time instants.

6.2.4.4 Filter Group Delay Correction

The filter group delay correction is performed through a static time shift – cf. the vertical “delay” arrow in Figure 6-5:

$$t_{\text{out,ASM}} = t_{\text{ASM}} - 3 \text{CCDB.ASM.Filter.Delay} \quad (6.2-170)$$

The error estimate is propagated as-is: $F^{(4)}_{\text{err}} = F^{(3)}_{\text{err}}$.

6.2.4.5 Cubic B-Spline Interpolation

The final interpolation to obtain Level 1b.Mag-L.F at UTC seconds is an iteratively reweighted least squares cubic B-spline approximation to $F^{(4)}$. Observe the introduction of leap seconds, cf. Section 4.6. First, the $F^{(4)}$ data sequence is divided into data segments with data gaps not exceeding the maximum gap size as specified in `CCDB.L1BP.ASM.Spline_Pars.Max_Gap_Size`. Within each segment, a cubic B-spline f is estimated by an iteratively, reweighted least-squares fit that minimizes:

$$\chi^2 = \mathbf{d}^T \mathbf{C} \mathbf{d} + \lambda \mathbf{m}^T \Lambda \mathbf{m} \quad (6.2-180)$$

where:

\mathbf{m} is the *model* vector, i.e. the parameters (spline coefficients) describing f

$\mathbf{d} = F^{(4)} - f$ is the data residual vector of the current model

C : $C_{ij} = w_i G_{ij}$, where G is the design matrix (collocation matrix) for cubic B-splines for the given knots (internal spacing `CCDB.L1BP.ASM.Spline_Pars.Knot_Space`, with additional knots in the ends), see Appendix D, and \mathbf{w} are data weights computed as a combination of Huber weights $[RD6]$, $\mathbf{w}^{\text{Huber}}$, and the data uncertainties, $F^{(4)}_{\text{err}}$. Let $\alpha = \text{Spline_Pars.Weight_Huber}$, $\beta = \text{CCDB.L1BP.ASM.Spline_Pars.Weight_ErrEst}$, and $\sigma_{F_{\text{err}}} = \text{rms}(F^{(4)}_{\text{err}})$ (summed over data within the current segment), then:

$$\mathbf{w} = \alpha \mathbf{w}^{\text{Huber}} + \beta \mathbf{w}^{\text{data}} + \min(\mathbf{1} - \alpha - \beta, \mathbf{0}) \quad (6.2-190)$$

$\mathbf{w}^{\text{Huber}}$ are the Huber weights, they down-weight outliers and are determined iteratively, starting with $w_i^{\text{Huber}} = 1$ in the first iteration. $\mathbf{w}^{\text{Huber}}$ of the next iteration is computed by:

$$w_i^{\text{Huber}} = \min\left(1, \frac{1.5}{|d_i/\sigma|}\right) \quad (6.2-200)$$

where σ is the root-mean-squared (rms) misfit of \mathbf{d} weighted by the weights \mathbf{w} of the preceding iteration:

$$\sigma = \sqrt{\frac{\sum (w_i d_i)^2}{\sum w_i}} \quad (6.2-210)$$

\mathbf{w}^{data} are the data uncertainty weights; $\mathbf{w}^{\text{data}} = \mathbf{w}^{\text{d}} / \text{mean}(\mathbf{w}^{\text{d}})$ where $w^{\text{d}} = 1/(F_{\text{err}}^{(4)} + 0.003)$.

λ is the damping factor of the second time-derivative, i.e. the damping of the acceleration of f , λ is given in CCDB.L1BP.ASM.Spline_Pars.Acc_Damping.

Λ is the block diagonal acceleration (second time-derivative) damping matrix, see Appendix D.

χ^2 of Eq. (6.2-180) is minimized by iteratively computing $\mathbf{m} = (\mathbf{G}^T \mathbf{C} + \lambda \Lambda)^{-1} \mathbf{C}^T \mathbf{F}^{(4)}$ and $\mathbf{w}^{\text{Huber}}$ until the relative change in \mathbf{m} is infinitesimal (though maximum 30 iterations):

$$\sqrt{\sum (m_i - m_i^{\text{prev}})^2} / \sqrt{\sum m_i^2} < 10^{-5} \quad (6.2-220)$$

For all UTC seconds within the selected data segment, f is evaluated to yield Level 1b.Mag-L.F.

The error estimate of Level 1b.Mag-L.F, Level 1b.Mag-L.F_{error}, is the weighted sum of the error estimate of the four nearest samples (indices j):

$$\mathbf{F}_{\text{error}} = \beta \frac{\sum \mathbf{F}_{j,\text{err}}^{(5)} \text{wt}_j}{\sum \text{wt}_j} \quad (6.2-230)$$

where

$$\mathbf{F}_{\text{err}}^{(5)} = \sqrt{(\mathbf{F}_{\text{err}}^{(4)})^2 + (\mathbf{F}^{(4)} - f)^2} \quad (6.2-240)$$

f is the B-splines evaluated at $t_{\text{out,VFM}}$ time instants, and

$$\text{wt}_j = 1 / (|t - t_j| + 10^{-3}) \quad (6.2-250)$$

with t = time of $\mathbf{F}_{\text{error}}$ and t_j = time of $\mathbf{F}_{j,\text{err}}^{(5)}$.

β is the uncertainty increase factor due to missing ASM samples – 5 is approximately the minimum, nominal value of $\sum \text{wt}_j$:

$$\beta = \max(1, 5 / \sum \text{wt}_j) \quad (6.2-260)$$

6.2.4.6 Flags

The flags of the ASM measurements, Level 1b.Mag-L.Flags_F, are computed as the sum of the values specified in Table 6-5 below for which the associated conditions are true.

| Value | Condition |
|-------|---|
| 1 | ASM is running in vector mode |
| 2 | ASM frequency calibration data trouble: outlier detected, gap, or not enough samples for filtering (by Filter(CCDB.L1BP.ASM.N_Avg, Level 1a.ASM.Sci.N)) |
| 4 | One or more of the 4 nearest ASM samples is detected as suspicious |

| Value | Condition |
|-------|---|
| 8 | Within 8 seconds after: <ul style="list-style-type: none"> • ASM restart • Loss of magnetic field lock, or • Telemetry gap |
| 16 | One or more of the 4 nearest ASM samples differs from the VFM measurement, i.e. $ F^{(4)} - \text{InterpolateLin}(\mathbf{B}'_{\text{VFM,fill}}) > \text{CCDB.Max_ASM_VFM_Diff}$ for at least one of the four nearest $F^{(4)}$. |
| 32 | One or more of the 4 nearest ASM samples are missing or rejected |
| 64 | VFM instrument is turned off (i.e. no $\mathbf{B}'_{\text{VFM,fill}}$ data available) |
| 255 | Not enough ASM samples available for generating Mag-L.F value |

Table 6-5 Values and Conditions of Flags_{SF}

6.3 Vector Field Magnetometer – VFM

6.3.1 Introduction

The Vector Field Magnetometer (VFM) measures the magnetic field vector at the tip of the optical bench on the boom. The sensor is a 3-axis Compact Spherical Coil (CSC) with a 3-axis Compact Detector Coil (CDC) inside. The instrument operates as a closed-loop system adjusting the compensating CSC currents to maintain a null field at the detector coils within the sphere. The currents in the CSC coils are measured and digitized (by an ADC) and this constitutes the raw measurements of the instrument. See [AD06] for a detailed description of the instrument, and for the Level 1b algorithm described by the instrument supplier.

The VFM is an analogue instrument and as such subject to temporal changes due to radiation and aging effects of the electronics. The effects are only significant in the bias and linear scale parameters of the characterization; hence these parameters are estimated daily through a comparison of the VFM output with the ASM scalar magnetometer output. Additionally, the non-orthogonality angles of the VFM sensor may also be estimated in this process. The allowed change from day to day in the parameters is controlled group-wise by weight parameters specified in the CCDB. The parameters estimated daily are stored in a *Temporal Calibration File* (TCF) as an auxiliary data product.

6.3.2 Input and Output Parameters

| Inputs | | | | |
|----------|--------------------------------------|--|------|---------------------|
| Element | | Description | Unit | Range |
| Level 1a | VFM.Sci.EU | Raw VFM measurement | eu | $\pm 92,682$ |
| | VFM.Sci.T _X | VFM temperature, multiplexed CDC, CSC, and EU | °C | -40 – +50 |
| | VFM.Sci.Src _{T_X} | Temperature source | | 0 – 3 |
| | VFM.Sci.DPU_id | Active unit identifier | | 2, 3 |
| | AOCS.Mag_HK | Magneto-torquer coil currents | A | ± 0.2 |
| | AOCS.Thru_HK | Thruster activations | | 0/1 |
| | Bus.State | States of instruments/subsystems with varying magnetic disturbance | | 0/1 |
| | Bus.Curr | Bus currents e.g. solar panels, main power bus | A | ± 20 |
| Level 1b | t _{ASM} | Time-instants of screened ASM measurements, not corrected for ASM filter delay | UTC | |
| | F _{ASM} | Calibrated and corrected ASM measurements at t _{ASM} time-instants | nT | 15,000 – 66,000 |
| | q _{NEC←CRF} | Rotation of NEC _{VFM} to CRF frame | | ± 1 |
| | q _{error} | Error estimate of q _{NEC←CRF} | " | 0 – 10 ³ |

| | | | | | | |
|----------------------|---|--|--|---|-----------------------|-------------------|
| C C D B | V F M | C a l | b₀ | Bias vector, at 0 °C and t = t ₀ | eu | ±100 |
| | | | b_t | Bias vector change with time | eu/yr | ±10 |
| | | | b_{EU} | Bias vector change with electronics (EU) temperature | eu/°C | ±1 |
| | | | b_{CDC} | Bias vector change with sensor detector temperature | eu/°C | ±1 |
| | | | deltab _{CDC} | Bias vector look-up table (LutId) for sensor detector temperature | eu | ±1 |
| | | | Filt _{T,CDC} | Filter parameter for T _{CDC} | | |
| | | | Filt _{T,CSC} | Filter parameters for T _{CSC} | | |
| | | | Filt _{T,EU} | Filter parameters for T _{EU} | | |
| | | | s₀ | Sensitivity vector, at 0 °C and t = t ₀ | eu/nT | ±2 |
| | | | s_t | Sensitivity vector change with time | eu/ (nT yr) | ±10 ⁻³ |
| | | | s_{CSC} | Sensitivity vector change with sensor sphere temperature | eu/ (nT °C) | ±10 ⁻⁴ |
| | | | s_{CDC} | Sensitivity vector change with detector temperature | eu/ (nT °C) | ±10 ⁻⁴ |
| | | | s_{EU} | Sensitivity vector change with EU temperature | eu/ (nT °C) | ±10 ⁻⁴ |
| | | | t ₀ | Base time for time changes | UTC | |
| | | | t_d | Timestamp, instrument processing and filter group delays for each component | s | ±10 |
| | | | t _{T,CSC} | Latency of T _{CSC} measurements | s | ±10 ³ |
| | | | t _{T,CDC} | Latency of T _{CDC} measurements | s | ±10 ³ |
| | | | t _{T,CDC_s} | Latency of T _{CDC} for scaling (s _{CDC}) | s | ±10 ³ |
| | | | t _{T,EU} | Latency of T _{EU} measurements | s | ±10 ³ |
| | | | u ₁ , u ₂ , u ₃ | Sensor non-orthogonality angles | " | ±10 ³ |
| k₂ | 2 nd order linearization factors | 1/eu | ±10 ⁻⁴ | | | |
| k₃ | 3 rd order linearization factors | 1/eu ² | ±10 ⁻⁹ | | | |
| L 1 | Dist_Max | Total maximum magnetic disturbance vector at VFM sensor | nT | ±50 | | |
| B P · | EstW eights | <i>Specification of apriori weights for TCF.VFM parameter estimation</i> | | | | |
| | | Min_ Samples | Minimum number of samples for doing TVF.VFM estimation | | 100 – 10 ⁵ | |

| | | | | |
|-----------------------------|---|---|----|-------------|
| V F M | Bias | Bias weighth | | $0 - 10^6$ |
| | Scale | Scale weighth | | $0 - 10^6$ |
| | n_orth | Non-orthogonality weighth | | $0 - 10^6$ |
| | A | Component variance amplification | | $0 - 100$ |
| | Limit | Limit of component variance effect | | $0.1 - 100$ |
| | Huber_factor | Huber weight factor | | $1 - 100$ |
| | Recalc_Limit | Limit for parameter change triggering re-calculation | | $0 - 10^4$ |
| | Limits | Structure holding limits for outlier detection and/or rejection | | |
| | Max_ASM_VFM_Diff | Maximum ASM – VFM scalar discrepancy, for flagging | nT | $0 - 100$ |
| | Reduce_Pars | Parameters used in the sampling reduction algorithm | | |
| TCF_Aux | Structure holding auxiliary TCF.VFM records, see [AD03] | | | |
| AOCS | | Structure characterizing the magnetic stray field vectors of the AOCS torquer coils at the VFM sensor and various other positions. Includes non-linearities, AOCS-coil and VFM transfer functions, and maximum disturbance vector, see Table 6-3 in Section 6.1.2 | | |
| ASM.Filter | Coeff | ASM instrument filter coefficients | | ± 5 |
| | Delay | ASM filter group delay | s | $0 - 5$ |
| Bus | | Structure characterizing the magnetic field of S/C platform: bus currents, induced, states, and static fields at VFM sensor (and other) positions. See Table 6-3 in Section 6.1 | | |
| STR.VFM | | Stray magnetic field of STR at VFM sensor position | nT | ± 10 |
| Structure. STR_q_VFM | | Rotation of CRF frame to VFM sensor i.e. VFM→CRF transformation cf. Table 3-1 | | |
| Structure. STR_q_VFM_Err | | Error estimate of STR_q_VFM | " | $0 - 60$ |

| | | | | |
|--|--|---|-----|---------------------|
| | Structure. VFM_q | Rotation of VFM sensor frame to S/C frame | | |
| T C F · V F M i n p u t | <i>TCF.VFM record from previous Level 1b Product</i> | | | |
| | bias | Temporal biases | nT | ±100 |
| | scale | Temporal scales | | ±2 |
| | n_orth | Temporal non-orthogonality angles | " | ±50 |
| | rms | Rms misfit (after estimation) | nT | 0 – 10 |
| | cov | Parameter covariance matrix (9x9) | | 0 – 1 |
| | samples | Number of samples used in estimation | | 0 – 10 ⁵ |
| | trange | Time range of data used in estimation | UTC | |
| | W_scale | Scaling weights used | | |
| | DPU_id | VFM unit identifier | | 2, 3 |

| Outputs | | | | |
|----------------------------------|----------------------------|---|------|----------|
| Element | | Description | Unit | Range |
| Level 1b _{Inst.} .VFM | | VFM measurements converted using CCDB.VFM.Cal parameters, not corrected for stray fields | nT | ± 66,000 |
| B' _{VFM} | | Fully converted and corrected magnetic field, computed using TCF.VFM ^{init} parameters | nT | ± 66,000 |
| t _{out,VFM} | | Output time-instants of VFM measurements, 50 Hz | UTC | |
| TCF.VFM ^{output} | | Structure as on input with updated fields | | |
| Level 1b. Mag-H (50 Hz) | B _{VFM} | Fully converted and corrected magnetic field vectors in orthogonal VFM sensor frame at t _{out,VFM} time instants | nT | ± 66,000 |
| | B _{NEC} | Fully converted and corrected magnetic field vector in NEC _{VFM} frame, t _{out,VFM} time instants | nT | ± 66,000 |
| | B _{error} | Vector error estimate of B _{VFM} | nT | 0 – 100 |
| | dB _{Sun} | Sun induced stray field correction | nT | ±10 |
| | dB _{AOCS} | AOCS stray field correction | nT | ±50 |
| | dB _{other} | Stray field correction – all other sources | nT | ±20 |
| | Flags _B | Flags related to the VFM measurements | | |
| | Flags _{Platform} | Flags related to the S/C platform | | |

| | | | | |
|------------------------------|--|--|----|--------------|
| Level 1b. Mag-L (1 Hz) | \mathbf{B}_{VFM} | Fully converted and corrected magnetic field vectors in orthogonal VFM sensor frame at UTC seconds | nT | $\pm 66,000$ |
| | \mathbf{B}_{NEC} | Fully converted and corrected magnetic field vector in NEC_{VFM} frame, UTC seconds | nT | $\pm 66,000$ |
| | \mathbf{B}_{error} | Vector error estimate of \mathbf{B}_{VFM} | nT | 0 – 100 |
| | $d\mathbf{B}_{Sun}$ | Sun induced stray field correction | nT | ± 10 |
| | $d\mathbf{B}_{AOCS}$ | AOCS stray field correction | nT | ± 50 |
| | $d\mathbf{B}_{other}$ | Stray field correction – all other sources | nT | ± 20 |
| | Flags _{SB} | Flags related to the VFM measurements | | |
| Flags _{Platform} | Flags related to the S/C platform | | | |
| Level 1b.Mag-C | Level 1b calibration and verification data | | | |
| VFMX_AUX_1B (Level 1b) | Auxiliary Level 1b product containing magnetic stray fields at VFM sensor position | | | |

6.3.3 Algorithm Overview

The overall VFM processing is sketched in Figure 6-7 below. Only data with a common DPU_id is to be processed, minority data (DPU_id wise) are rejected. Data with VFM_{time} less than 20,000,000 (data from first ~2.5 second after VFM switch-on) are also rejected. Next, the raw output (Level 1a.VFM.Sci.EU, rate: 50 Hz, timestamps $t_{0,VFM}$) of the VFM is corrected for time-stamp, processing, and filter delays. Then, it is corrected and converted to physical units (nT) using the CCDB.VFM.Cal parameters and the Level 1a.VFM.Sci.T_X temperatures. This is the Level 1b_{Inst} VFM vector product. The rate is 50 Hz and the time-instants t_{VFM} .

Then, the preliminary vector field measurements, \mathbf{B}'_{VFM} , are computed using the TCF.VFM^{init} parameters. TCF.VFM^{init} is the most recent (w.r.t. data being processed) TCF.VFM record among the TCF.VFM^{input} (from the previous Level 1b Product) and the CCDB.L1BP.VFM.TCF_Aux array – with DPU_id corresponding to Level 1a.VFM.Sci.DPU_id. Formally, let $t_0 = \text{Level 1a.VFM.Sci.t}_0$, then:

$$TCF.VFM^{init} = \begin{cases} TCF.VFM^{input} & \text{unless ...} \\ TCF_Aux_i & \text{if } TCF.VFM^{input}.DPU_id \neq \text{Level 1a.VFM.Sci.DPU_id} \\ & \text{or } t_0 \geq TCF_Aux_i.trange_{min} > TCF.VFM^{input}.trange_{min} \\ & \text{with } TCF_Aux_i.DPU_id = \text{Level 1a.VFM.Sci.DPU_id;} \\ & TCF_Aux_i \text{ is the latest TCF_Aux record (trange}_{min} \text{ wise)} \\ & \text{for which the above holds.} \end{cases} \quad (6.3-5)$$

Next, outliers are detected and accordingly rejected or flagged as suspicious samples.

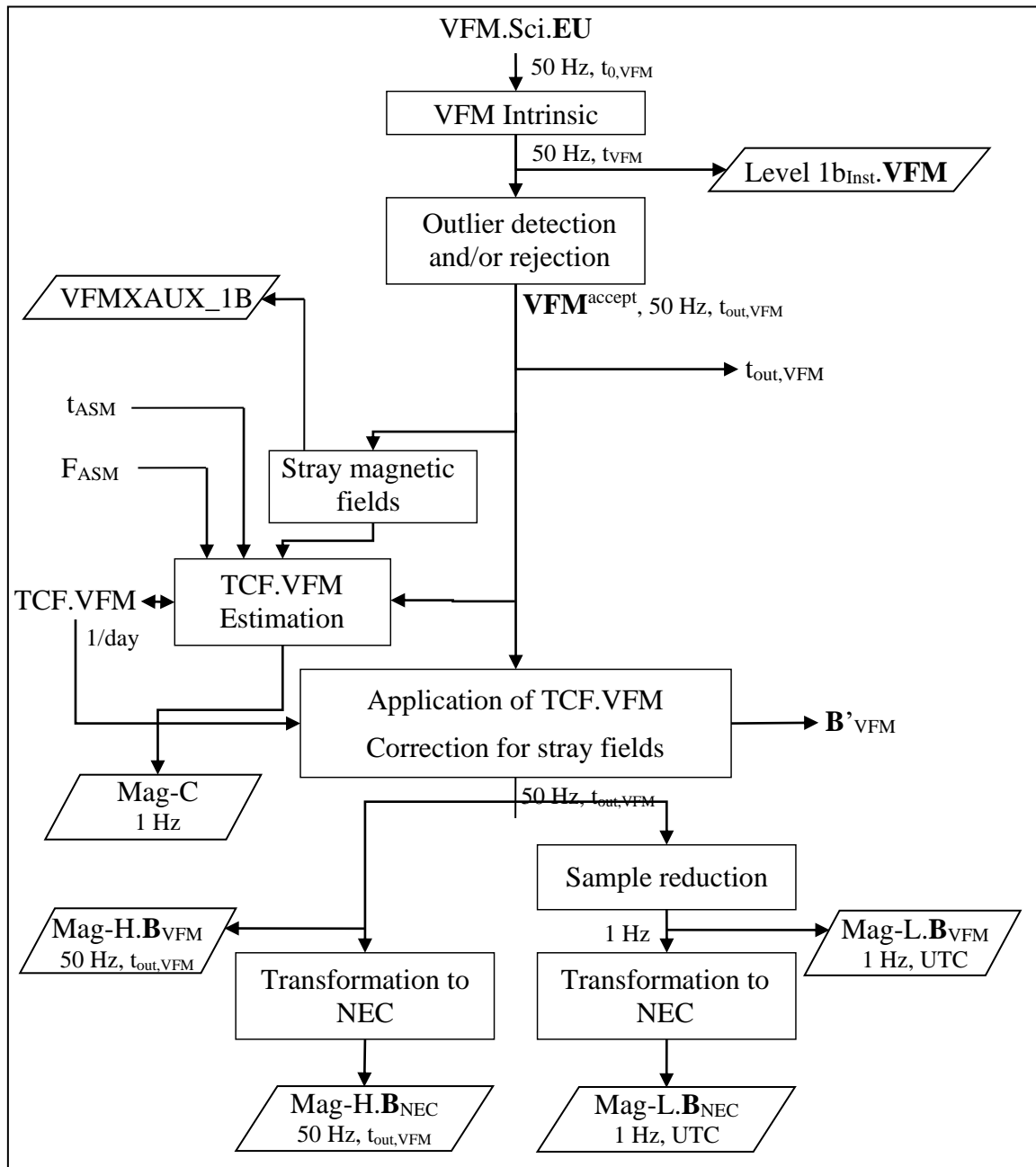


Figure 6-7 VFM Processing Overview

Now, the magnetic stray fields from the rest of the S/C at the VFM sensor position – at the time instants of the VFM measurements, $t_{out,VFM} (= t_{VFM})$ – are computed. The phase linearity and fast response of the VFM Bessel filter makes it unnecessary to apply a filter to the stray fields as was the case for the ASM. However, the characterization of the AOCS torquer coil disturbances possibly needs to take the VFM filter into account.

Next, the internal temporal changes of the VFM electronics⁸ and possibly any change in the non-orthogonalities of the CSC are modeled by the TCF.VFM parameters which are estimated by comparison of VFM data with the fully corrected ASM scalar data (F_{ASM}).

⁸ Due to radiation and age, not modeled by the CCDB.VFM.Cal parameters.

The new estimates of the TCF.VFM parameters, $\text{TCF.VFM}^{\text{output}}$, are applied to all the VFM data of the actual day. Together with the correction for stray magnetic fields the Level 1b.Mag-H. \mathbf{B}_{VFM} data are obtained. I.e. fully converted and corrected magnetic vector data in the orthogonal VFM sensor frame. The rate is 50 Hz and the time instants $t_{\text{out,VFM}}$.

Then Level 1b.Mag-L. \mathbf{B}_{VFM} , the 1 Hz magnetic vector product in the VFM frame at UTC seconds, is extracted.

Finally, the magnetic field vectors \mathbf{B}_{VFM} at 50 Hz and 1 Hz are transformed via the Common Reference Frame (CRF) into the NEC frame. This completes the generation of the Level 1b.Mag-H. \mathbf{B}_{NEC} and Level 1b.Mag-L. \mathbf{B}_{NEC} products.

Note: the rotation from the VFM to the CRF frame is estimated pre-flight and refined in-flight. Hence periodic updates of `CCDB.Structure.STR_q_VFM` are foreseen and consequently reprocessing of the final step above is required regularly. See also Section 4.2.

6.3.4 Detailed Description of VFM Processing

6.3.4.1 Intrinsic VFM Processing

First, the timestamps are corrected for any processing and filter delays:

$$t_{\text{VFM}} = t_{0,\text{VFM}} - \text{median}(\text{CCDB.VFM.Cal.t}_d) \quad (6.3-10)$$

Then the instrument calibration parameters of `CCDB.VFM` are applied to convert the measurements into physical units (nT) and into an orthogonal frame defined as the VFM frame. This follows closely the description in [AD06]. Initially, the linearization terms are applied and the components are linearly interpolated to the unified time-instants, t_{VFM} (in the following, the `CCDB.VFM.Cal` structure prefix has been omitted for clarity – all parameters are elements of this structure):

$$E_i = \text{Interpolate}(t_{0,\text{VFM}} - t_{d,i}, 1 + ((k_{2,i} + k_{3,i} \text{EU}_i) \text{EU}_i) \text{EU}_i, t_{\text{VFM}}) \quad (6.3-20)$$

where EU_i are the components of `Level 1a.VFM.Sci.EU`.

The rest of the conversion is conveniently described in matrix form:

$$\text{Level 1b}_{\text{Inst.}} \mathbf{VFM} = \mathbf{P}^{-1} \times \mathbf{S}^{-1} \times (\mathbf{E} - \mathbf{b}) \quad (6.3-30)$$

The bias vector, \mathbf{b} , is given by:

$$\mathbf{b} = \mathbf{b}_0 + \frac{\mathbf{b}_t(t - t_0)}{365 \cdot 86400 \text{ s/yr}} + \mathbf{b}_{\text{EU}} T_{\text{EU}} + \mathbf{b}_{\text{CDC}} T_{\text{CDC}} + \text{Interpol}_{\text{Lin}}(\text{deltab}_{\text{CDC}}, T_{\text{CDC}}) \quad (6.3-40)$$

where t is the time of the measurement to convert, T_{XXX} are de-multiplexed, filtered, time-shifted, linearly interpolated values of `Level 1a.VFM.Sci.TX`, i.e. T_{XXX} are values of linear interpolation in time to the t_{VFM} time-instants of T'_{XXX} :

$$T_{\text{XXX}} = \text{Interpol}_{\text{Lin}}(T'_{\text{XXX}}, t_{\text{VFM}} + \text{CCDB.VFM.Cal.t}_{T,\text{XXX}}) \quad (6.3-43)$$

where

$$T'_{\text{XXX}} = \text{Filter}(\text{CCDB.L1BP.VFM.Cal.Filt}_{\text{XXX}}, \text{de-multi}(\text{Level 1a.VFM.Sci.T}_{\text{XXX}})) \quad (6.3-45)$$

The $\text{Interpol}_{\text{Lin}}$ and Filter functions of Eq. (6.3-40) and (6.3-45) are defined in Appendix E.

The diagonal scaling matrix, \mathbf{S}^{-1} , is:

$$\mathbf{S}^{-1} = \begin{pmatrix} s_1 & 0 & 0 \\ 0 & s_2 & 0 \\ 0 & 0 & s_3 \end{pmatrix}^{-1} = \begin{pmatrix} 1/s_1 & 0 & 0 \\ 0 & 1/s_2 & 0 \\ 0 & 0 & 1/s_3 \end{pmatrix} \quad (6.3-50)$$

where $\mathbf{s} = (s_1, s_2, s_3)$ is given by:

$$\mathbf{s} = \mathbf{s}_0 + \frac{\mathbf{s}_i(t - t_0)}{365 \cdot 86400 \text{ s/yr}} + \mathbf{s}_{\text{CSC}} \mathbf{T}_{\text{CSC}} + \mathbf{s}_{\text{CDC}} \mathbf{T}_{\text{CDC},s} + \mathbf{s}_{\text{EU}} \mathbf{T}_{\text{EU}} \quad (6.3-60)$$

\mathbf{T}_{CSC} and $\mathbf{T}_{\text{CDC},s}$ are computed according to Eq. (6.3-43) (with $\text{XXX} = \text{CSC}$ and CDC,s respectively).

Finally, the matrix converting to the orthogonal VFM frame, \mathbf{P}^{-1} , is:

$$\mathbf{P}^{-1} = \begin{pmatrix} 1 & 0 & 0 \\ -\sin u_1 & \cos u_1 & 0 \\ \sin u_2 & \sin u_3 & \sqrt{1 - \sin^2 u_2 - \sin^2 u_3} \end{pmatrix}^{-1} = \begin{pmatrix} 1 & 0 & 0 \\ \sin u_1 / \cos u_1 & 1 / \cos u_1 & 0 \\ -\frac{\sin u_1 \sin u_3 + \cos u_1 \sin u_2}{w \cos u_1} & -\frac{\sin u_3}{w \cos u_1} & \frac{1}{w} \end{pmatrix} \quad (6.3-70)$$

where $w = \sqrt{1 - \sin^2 u_2 - \sin^2 u_3}$. Note: u_i is given in arc-seconds (") and shall be converted, e.g. $\sin u_1 = \sin_{\text{rad}}(u_1 / 3600 * \pi/180)$.

Define the uncertainty: $\mathbf{VFM}_{\text{err}} = (0.03, 0.03, 0.03) \text{ nT}$.

6.3.4.2 Outlier Detection

The VFM outlier detection is similar to the ASM procedure. First, the Level 1b_{Inst}.VFM (VFM for short) are converted to scalar values, $F^{\text{VFM}} = |\mathbf{VFM}|$ upon which a simple range check is performed. Then, the acceleration of both vector components as well as of the scalar response are checked.

The CCDB.L1BP.VFM.Limits structure contains the following fields:

| Field | Type | Unit | Comment |
|-------------|------------|-------------------|---|
| Range | 2-d vector | nT | Allowed range, e.g. [14000, 66000] |
| Max_Accel | real | nT/s ² | Maximum allowed acceleration of vector components |
| Max_F_Accel | real | nT/s ² | Maximum allowed acceleration of scalar response |
| Pass_Accel | real | nT/s ² | Vector component accelerations below this are accepted Between Pass_Accel and Max_Accel samples are flagged and associated with raised uncertainty estimates |

| Field | Type | Unit | Comment |
|--------------|------|-------------------|--|
| Pass_F_Accel | real | nT/s ² | Scalar field accelerations below this are accepted Between Pass_F_Accel and Max_F_Accel: flag and raise uncertainty estimates |
| Max_Gap_Size | real | s | Definition of size of data gaps |

Table 6-6 CCDB.L1BP.VFM.Limits Structure

First, all F^{VFM} samples outside Range are discarded. Then, the 1st and 2nd order time derivatives of the vector components and of the scalar response (F^{VFM}) of the remaining samples, A' respectively A'' , are computed:

$$A'_i = (A_i - A_{i-1}) / (t_i - t_{i-1}) \quad (6.3-80)$$

$$A''_i = 2(A'_{i+1} - A'_i) / (t_{i+1} - t_{i-1}) \quad (6.3-90)$$

Eq. (6.3-80) and (6.3-90) are computed for $A = VFM_x, VFM_y, VFM_z$, and F^{VFM} .

$VFM_{x/y/z}''$ are checked versus Max_Accel and Pass_Accel, $F^{VFM}''_i$ versus Max_F_Accel and Pass_Accel similar as for the ASM outlier detection.

For samples flagged as suspicious, the associated error estimates are raised:

$$VFM_{k,err}^{new} = \sqrt{VFM_{k,err}^2 + \Delta VFM_k^2}, k = 1,2,3 \quad (6.3-100)$$

$$\Delta VFM = VFM_j - (VFM_{j-1} + (VFM_{j+1} - VFM_{j-1}) (t_j - t_{j-1}) / (t_{j+1} - t_{j-1})) \quad (6.3-110)$$

ΔVFM is the vector difference between VFM_j and the linearly interpolated value of VFM_{j-1} and VFM_{j+1} (using only accepted VFM samples).

Let VFM^{accept} denote the Level 1b_{Inst.} VFM samples that are not rejected.

6.3.4.3 Filter Group Delay Correction

The correction for the VFM instrument filter group delay is included in CCDB.VFM.Cal.t_d, cf. Eq. (6.3-10), hence for VFM^{accept} samples:

$$t_{out,VFM} = t_{VFM} \quad (6.3-120)$$

6.3.4.4 Stray Magnetic Fields

The calculation of the magnetic disturbances, ΔB , of the VFM measurements is given by Eq. (6.3-130) below. Note: this computation needs to be done at all time instants of VFM^{accept} , $t_{out,VFM}$, i.e. at 50 Hz. As the filter of the VFM instrument is very fast and very phase linear, this has only to be taken into account for the AOCS torquer coil disturbances. This is handled by using the transfer characteristic of the combined torquer coil and VFM transfer functions stored in the CCDB.AOCS.Transfer_{VFM} structure, see Section 6.1.2.

Note: the $\Delta B_{AOCS,VFM}$ only contains the stray fields of the magneto-torquer coils, it does not include stray fields from latch valves and thrusters – these are contained in $\Delta B_{State,VFM}$.

The stray fields from the S/C body and the bus currents are computed as for the ASM (see pp. 53-55 plus Section 6.1). For clarity, the parameters are written without the Level 1a prefix, and $\mathbf{VFM_q}$ without the CCDB.Structure prefix:

$$\Delta \mathbf{B} = \text{CCDB.STR.VFM} + \text{Interpol}_{\text{Lin}}(\Delta \mathbf{B}_{\text{Sun}}) + \mathbf{VFM_q} \times \left(\begin{array}{l} \Delta \mathbf{B}_{\text{AOCS,VFM}}(\text{AOCS.Mag_HK.Imea_MTQ}) + \\ \text{CCDB.Bus.Static.Base}_{\text{VFM}} + \\ \mathbf{M}_{\text{State,VFM}} \times \text{Interpolate}_{\text{Step}}(\text{Bus.State.States}) + \\ \Delta \mathbf{B}_{\text{Induced,VFM}} + \\ \text{CCDB.AOCS.Thruster}_{\text{VFM}} \times \text{State}_{\text{Thruster}}(\text{AOCS.Thru_HK}) + \\ \Delta \mathbf{B}_{\text{Bus,VFM}} \end{array} \right) \quad (6.3-130)$$

where $\Delta \mathbf{B}_{\text{Sun}}$ is computed for every UTC second (and interpolated linearly in time to $t_{\text{out,VFM}}$ time instants) as follows: first, the Sun incident angles on the spacecraft, denoted α and β , are computed as described below where \mathbf{r} is the S/C position and $\mathbf{r}_{\text{Sun}} = \text{xl_sun}(t)$ the Sun position (both in ITRF). $\Delta \mathbf{B}_{\text{Sun}}$ is then computed as a 2-D linearly interpolation in $\text{CCDB.L1BP.VFM.dB_Sun}$, cf. Eq. (6.3-134).

$$\mathbf{q}_{\text{S/C} \leftarrow \text{ITRF}} = \mathbf{q}_{\text{ITRF} \leftarrow \text{ICRF}}^{-1} \times \mathbf{q}_{\text{CRF} \leftarrow \text{ICRF}} \times \text{CCDB.Structure.STR_q}^{-1} \quad (6.3-131)$$

$$\mathbf{s} = \mathbf{q}_{\text{S/C} \leftarrow \text{ITRF}} \times (\mathbf{r}_{\text{Sun}} - \mathbf{r}) \quad (6.3-132)$$

$$\alpha = \text{atan2}(s_z, s_x), \quad \beta = \text{atan2}(-s_y, \sqrt{s_x^2 + s_z^2}) \quad (6.3-133)$$

$$\Delta \mathbf{B}_{\text{Sun}} = \text{Interpol}_{\text{Lin}}(\alpha, \beta, \text{CCDB.L1BP.VFM.dB_Sun}) \quad (6.3-134)$$

Gaps in positions and/or quaternions are filled with cubic inter-/extrapolation, up to ± 1 minute for quaternions and ± 10 minutes for position; outside these limits, α , β , and $\Delta \mathbf{B}_{\text{Sun}}$ are all set to zero.

$\Delta \mathbf{B}_{\text{Bus,VFM}}$ (in Eq. (6.3-130)) is computed as described in Section 6.1.2 using filtered, linearly interpolated Level 1a.Bus.Curr. $\mathbf{I}_{\text{group}}$ currents (at $t_{\text{out,VFM}}$ time instants), and $\Delta \mathbf{B}_{\text{Induced,VFM}}$ is computed as:

$$\Delta \mathbf{B}_{\text{Induced,VFM}} = (\text{CCDB.Bus.Static.Ind}_{\text{VFM}} + \sum_i \text{Level1a.Bus.State.IndState}_i \cdot \text{CCDB.Bus.State.Induced}_i \cdot \text{dInd}_{\text{VFM}}) \times (\mathbf{VFM_q}^{-1} \times \mathbf{B}'_{\text{VFM}} + \Delta \mathbf{B}_{\text{Bus,Body}}) \quad (6.3-135)$$

\mathbf{B}'_{VFM} is calculated by Eq. (6.3-180) below and $\Delta \mathbf{B}_{\text{Bus,Body}}$ as described in Section 6.1.2. The recursion in the calculation of $\Delta \mathbf{B}$ is avoided by setting $\Delta \mathbf{B}_{\text{Induced,VFM}} = 0$ in the \mathbf{B}'_{VFM} term in Eq. (6.3-135).

$\Delta \mathbf{B}$ is used in the following subsections. The various elements of $\Delta \mathbf{B}$ are transformed to the VFM sensor frame by $\text{CCDB.Structure.VFM_q}$ (except CCDB.STR.VFM and $\Delta \mathbf{B}_{\text{Sun}}$) and stored in the VFMX AUX_1B Level 1b Product.

The uncertainty of $\Delta \mathbf{B}$, $\Delta \mathbf{B}_{\text{err}}$, reflects any missing telemetry required to compute $\Delta \mathbf{B}$. Basically, $\Delta \mathbf{B}_{\text{err}}$ grows from $\mathbf{0}$ (where all telemetry is available) – piecewise – linearly up to the maximum $\Delta \mathbf{B}$ possible. Specifically, $\Delta \mathbf{B}_{\text{err}}$ is computed for all $t_{\text{out,VFM}}$ time-instants as:

$$\Delta \mathbf{B}_{\text{err}} = \alpha_{\text{Sun}} \Delta \mathbf{B}_{\text{Sun}}^{\text{Max}} + \alpha_{\text{AOCS}} \Delta \mathbf{B}_{\text{AOCS}}^{\text{Max}} + \alpha_{\text{Curr}} \Delta \mathbf{B}_{\text{Bus,Current}}^{\text{Max}} + \alpha_{\text{State}} \Delta \mathbf{B}_{\text{Bus,State}}^{\text{Max}} \quad (6.3-140)$$

where $\Delta \mathbf{B}_{\text{XXX}}^{\text{Max}} = \text{CCDB.XXX.Max}_{\text{VFM}}$ or $\text{CCDB.L1BP.VFM.dB_Sun_Max}$ for $\text{XXX} = \text{Sun}$. The formulas for α_{XXX} are given next.

Given a time $t \in t_{\text{out,VFM}}$, let dt_{Pos} and dt_{Att} be the respective differences in time between t and the time-instants of the nearest position respectively attitude information, then

$$\alpha_{\text{Sun}} = \begin{cases} 0 & \text{if } |dt_{\text{Pos}}| < 60s \\ & \text{and } |dt_{\text{Att}}| < 10s \\ \min \left(1, \frac{\max(0, |dt_{\text{Pos}}| - 60s) / 600s + \max(0, |dt_{\text{Att}}| - 10s) / 60s}{\max(0, |dt_{\text{Pos}}| - 60s) / 600s + \max(0, |dt_{\text{Att}}| - 10s) / 60s} \right) & \text{otherwise} \end{cases} \quad (6.3-145)$$

Let $t_i \leq t \leq t_{i+1}$, where t_i are the time-instants of Level 1a.AOCS. **Mag_HK.Imea_MTQ** telemetry, then

$$\alpha_{\text{AOCS}} = \begin{cases} 0 & \text{if } t - t_i \leq 1s \\ 1 & \text{otherwise} \end{cases} \quad (6.3-150)$$

Let $t_i \leq t \leq t_{i+1}$, where t_i are the time-instants of Level 1a.Bus.Curr, then

$$\alpha_{\text{Curr}} = \begin{cases} 0 & \text{if } t - t_i \leq 3s \text{ or } t_{i+1} - t \leq 3s \\ \frac{t - t_i - 3s}{6s} & \text{if } t_i + 3 < t < \min(t_i + 9s, t_{i+1} - 9s) \\ \frac{t_{i+1} - t - 3s}{6s} & \text{if } \max(t_i + 9s, t_{i+1} - 9s) < t < t_{i+1} - 3s \\ 1 & \text{if } t_i + 9s \leq t \leq t_{i+1} - 9s \end{cases} \quad (6.3-170)$$

Let $t_i \leq t \leq t_{i+1}$, where t_i are the time-instants of Level 1a.Bus.State, then

$$\alpha_{\text{State}} = \begin{cases} 0 & \text{if } t - t_i \leq 4s \\ 1 & \text{otherwise} \end{cases} \quad (6.3-175)$$

6.3.4.5 Computation of \mathbf{B}'_{VFM}

The computation of the fully converted – using the $\text{TCF.VFM}^{\text{init}}$ parameters – and stray field corrected magnetic field vector measurements, \mathbf{B}'_{VFM} , is:

$$\mathbf{B}'_{\text{VFM}} = \mathbf{P}'^{-1} \times \mathbf{S}'^{-1} \times (\mathbf{VFM}^{\text{accept}} - \mathbf{b}') - \Delta \mathbf{B} \quad (6.3-180)$$

where $\mathbf{b}' = \text{TCF.VFM}^{\text{init}}.\text{bias}$ and the \mathbf{P}' and \mathbf{S}' matrices are as for the intrinsic VFM processing (Eq. (6.3-50) and (6.3-70)) with $\mathbf{s}' = \text{TCF.VFM}^{\text{init}}.\text{scale} + \mathbf{s}_\beta \cdot \beta + \mathbf{s}_{\text{exp}} \cdot \exp(-(t-t_0)/\tau)$ and $(u'_1, u'_2, u'_3) = \text{TCF.VFM}^{\text{init}}.\mathbf{n}_{\text{orth}}$. \mathbf{s}_β , \mathbf{s}_{exp} , t_0 and τ are elements of the VFM section of the L1BP part of the CCDB, and β is the Sun incident angles on the spacecraft described in Eq. (6.3-133).

At this point, the ASM processing needs to be performed to obtain the ASM measurements, \mathbf{F}_{ASM} at t_{ASM} time instants.

6.3.4.6 Estimation of TCF.VFM Parameters

The estimation of the TCF.VFM parameters uses the method described in [RD1]. This is an iteratively, reweighted least-squares fit method that minimizes the difference between the ASM-filtered and interpolated scalar values of the corrected VFM measurements, $|\mathbf{B}_{VFM}|$, and the calibrated and corrected ASM measurements, F_{ASM} .

First, the set of VFM, ASM measurement pairs, to be used for the estimation process, is selected as depicted in Figure 6-8 below and is as follows: For all ASM samples (time t_{ASM}) select the \mathbf{VFM}^{accept} data points less than 0.01 s from t_{ASM} . Now, the following conditions are checked:

- There shall be no gaps in the \mathbf{VFM}^{accept} data in the preceding 8 seconds and following 30 ms.
- The S/C telemetry required to compute magnetic stray fields shall be available to allow proper stray field computations, i.e. $\Delta\mathbf{B}_{err} = \mathbf{0}$ for the preceding 8 seconds

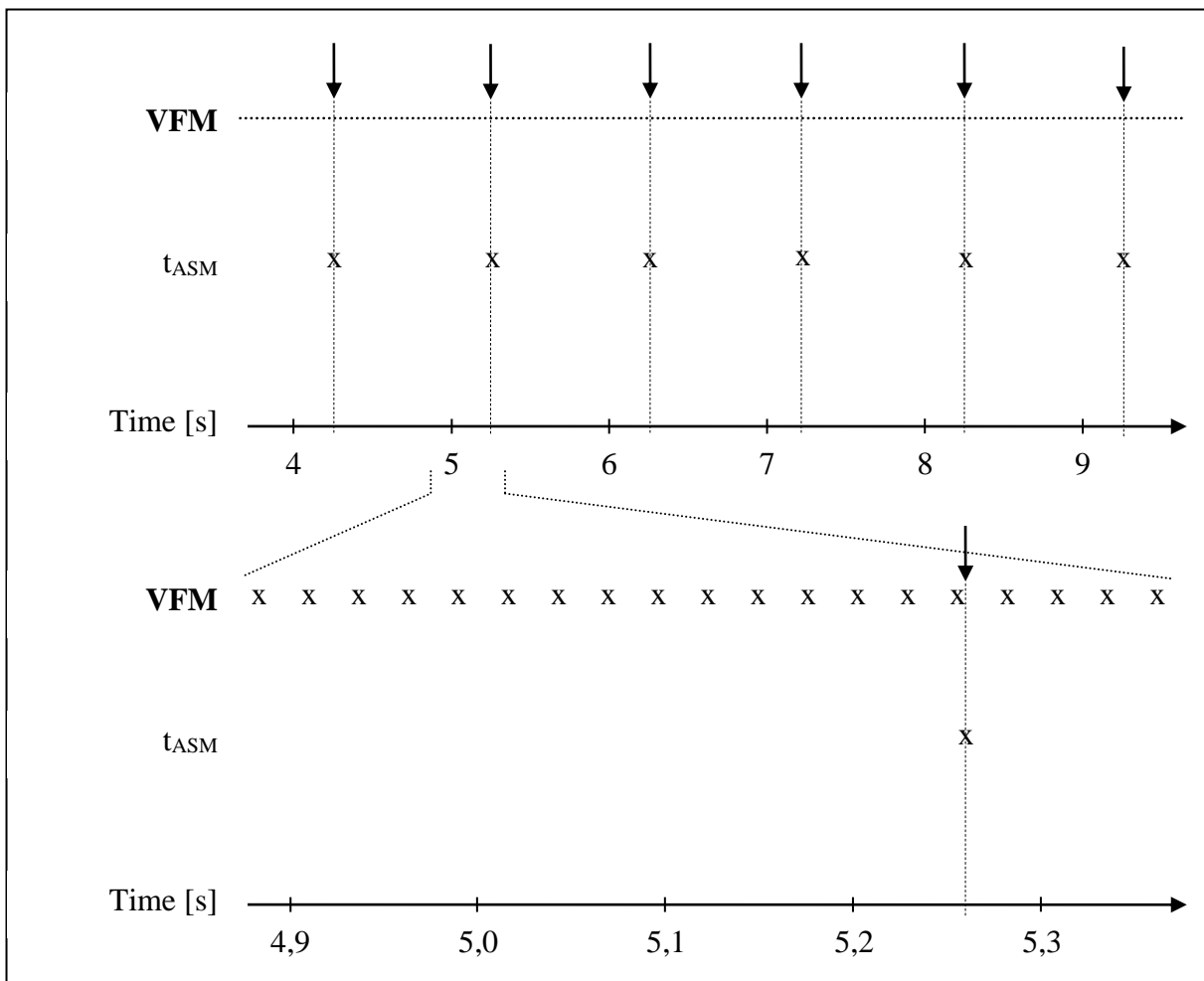


Figure 6-8 Selection of VFM-ASM Data for TCF.VFM Estimation

Only VFM, ASM pairs for which both conditions are fulfilled are to be used in TCF.VFM estimation process.

When all applicable ASM samples within the current day have been found and the number of samples is greater than CCDB.L1BP.VFM.EstWeights.Min_Samples, the parameters TCF.VFM.bias, TCF.VFM.scale and TCF.VFM.n_orth are estimated through an iterative, reweighted least-squares-fit algorithm. The TCF.VFM^{init} parameters are used as a-priori information in the algorithm such that the estimated parameters only have limited deviations from the previous set of parameters – depending on the (CCDB.L1BP.VFM.)EstWeights parameters. However, if the a-priori information is based on data much older than the current data, the deviations are allowed to be larger. The weights of the VFM axes bias and scale parameters, in particular the VFM y axis, are also made dependent on the variance of the selected VFM^{accept} unit vector components, as periodical spacecraft maneuvers are planned to enhance the otherwise poor estimation of the y axis parameters. These maneuvers are hence automatically detected by the Level 1b processor through this variance dependent weighting.

Basically, the fit minimizes:

$$\chi^2 = \mathbf{d}^T \mathbf{w}^T \mathbf{G} \mathbf{d} + (\mathbf{m} - \mathbf{m}_p)^T \Lambda (\mathbf{m} - \mathbf{m}_p) \quad (6.3-190)$$

where

\mathbf{m} is the model vector of biases, scales and non-orthogonalities (length 9), $\mathbf{m} = (\mathbf{bias} \ \mathbf{scale} \ as2r \cdot \mathbf{n_orth})$ with $as2r = \pi/180/3600$ (arc-seconds to radians).

\mathbf{m}_p is the a-priori model information, i.e. $\mathbf{m}_p = (\text{TCF.VFM}^{init}.bias \ \text{TCF.VFM}^{init}.scale \ as2r \cdot \text{TCF.VFM}^{init}.n_orth)$.

\mathbf{d} is the data residual vector (same length as selected F_{ASM}):

$$d_i = F_{ASM,i} - \text{Interpol}_{Lin}(\text{filter}(|\mathbf{B}(\mathbf{m})|), t_{asm,i}) \quad (6.3-200)$$

where filter is the ASM filter applied to the $|\mathbf{B}(\mathbf{m})|$ 50 Hz time-series, linearly interpolated to the $t_{ASM,i}$ time instant. See Eq. (6.2-130) and Eq. (6.2-140) on page 56 how to computer filter. $\mathbf{B}(\mathbf{m})$ are the converted and corrected VFM samples – at the full, 50 Hz data rate – using model vector \mathbf{m} :

$$\mathbf{B}(\mathbf{m}) = \mathbf{P}(\mathbf{m})^{-1} \mathbf{S}(\mathbf{m})^{-1} (\mathbf{VFM}^{accept} - \mathbf{b}(\mathbf{m})) - \Delta \mathbf{B} \quad (6.3-210)$$

where

$$\mathbf{b}(\mathbf{m}) = (m_1, m_2, m_3) \quad (6.3-220)$$

with $w = \sqrt{1 - \sin^2 m_8 - \sin^2 m_9}$ (Note: m_7 through m_9 are in radians.)

$$\mathbf{S}^{-1}(\mathbf{m}) = \begin{pmatrix} \frac{1}{(m_4 + s_{\beta,1} \cdot \beta + s_{exp,1} \cdot e^{-(t-t_0)/\tau})} & 0 & 0 \\ 0 & \frac{1}{(m_5 + s_{\beta,2} \cdot \beta + s_{exp,2} \cdot e^{-(t-t_0)/\tau})} & 0 \\ 0 & 0 & \frac{1}{(m_6 + s_{\beta,3} \cdot \beta + s_{exp,3} \cdot e^{-(t-t_0)/\tau})} \end{pmatrix} \quad (6.3-230)$$

where s_β , s_{exp} , t_0 and τ are elements of the VFM section of the L1BP part of the CCDB, and β is the Sun incident angles on the spacecraft described in Eq. (6.3-133)

and

$$\mathbf{P}^{-1}(\mathbf{m}) = \begin{pmatrix} 1 & 0 & 0 \\ \sin m_7 / \cos m_7 & 1 / \cos m_7 & 0 \\ -\frac{\sin m_7 \sin m_9 + \cos m_7 \sin m_8}{w \cos m_7} & -\frac{\sin m_9}{w \cos m_7} & \frac{1}{w} \end{pmatrix} \quad (6.3-240)$$

G is the design matrix evaluated at \mathbf{m} :

$$\mathbf{G} = \frac{\partial \mathbf{d}(\mathbf{m})}{\partial \mathbf{m}} \quad (6.3-250)$$

Since $\mathbf{d}(\mathbf{m})$ is linear in $|\mathbf{B}(\mathbf{m})|$ and F_{ASM} is constant w.r.t. the partial derivatives:

$$\begin{aligned} G_{ij} &= \text{Interpol}_{\text{Lin}} \left(\text{filter} \left(\frac{-\partial |\mathbf{B}(\mathbf{m})|}{\partial m_j}, t_{ASM,i} \right) \right) \\ &\equiv \text{Interpol}_{\text{Lin}} \left(\text{filter}(g_j), t_{ASM,i} \right) \end{aligned} \quad (6.3-260)$$

Since $|\mathbf{B}(\mathbf{m})| = \sqrt{\mathbf{B}(\mathbf{m})^T \mathbf{B}(\mathbf{m})}$ and

$\mathbf{B}(\mathbf{m})^T = (\mathbf{VFM}^{\text{accept}} - \mathbf{b}(\mathbf{m}))^T \mathbf{S}(\mathbf{m})^{-1} (\mathbf{P}(\mathbf{m})^{-1})^T - \Delta \mathbf{B}^T$, we get:

$$(g_1, g_2, g_3) = -\mathbf{S}(\mathbf{m})^{-1} (\mathbf{P}(\mathbf{m})^{-1})^T \mathbf{B}(\mathbf{m}) / |\mathbf{B}(\mathbf{m})| \quad (6.3-270)$$

$$g_j = \frac{(\mathbf{VFM}_{j-3} - m_{j-3})}{(m_j + s_{\beta,j-3} \cdot \beta + s_{exp,j-3} \cdot e^{-(t-t_0)/\tau})} g_{j-3} \quad \text{for } j = 4,5,6 \quad (6.3-280)$$

$$g_j = \frac{\left(\mathbf{B}(\mathbf{m})^T \frac{\partial \mathbf{P}(\mathbf{m})^{-1}}{\partial m_j} \mathbf{S}(\mathbf{m})^{-1} (\mathbf{VFM}_{j-6} - m_{j-6}) + (\mathbf{VFM}_{j-6} - m_{j-6})^T \mathbf{S}(\mathbf{m})^{-1} \left(\frac{\partial \mathbf{P}(\mathbf{m})^{-1}}{\partial m_j} \right)^T \mathbf{B}(\mathbf{m}) \right)}{2|\mathbf{B}(\mathbf{m})|} \quad \text{for } j = 7,8,9 \quad (6.3-290)$$

$$\frac{\partial \mathbf{P}(\mathbf{m})^{-1}}{\partial m_7} = \begin{pmatrix} 0 & 0 & 0 \\ 1/\cos^2 m_7 & \sin m_7 / \cos^2 m_7 & 0 \\ -\frac{\sin m_9}{w \cos^2 m_7} & -\frac{\sin m_7 \sin m_9}{w \cos^2 m_7} & 0 \end{pmatrix} \quad (6.3-300)$$

$$\frac{\partial P(\mathbf{m})^{-1}}{\partial m_8} = \begin{pmatrix} 0 & 0 & 0 \\ 0 & 0 & 0 \\ -\cos m_8 \frac{\cos m_7 \cos^2 m_9 + \sin m_7 \sin m_8 \sin m_9}{w^3 \cos m_7} & -\frac{\sin m_8 \cos m_8 \sin m_9}{w^3 \cos m_7} & \frac{\sin m_8 \cos m_8}{w^3} \end{pmatrix} \quad (6.3-305)$$

$$\frac{\partial P(\mathbf{m})^{-1}}{\partial m_9} = \begin{pmatrix} 0 & 0 & 0 \\ 0 & 0 & 0 \\ -\cos m_9 \frac{\sin m_7 \cos^2 m_8 + \cos m_7 \sin m_8 \sin m_9}{w^3 \cos m_7} & -\frac{\cos^2 m_8 \cos m_9}{w^3 \cos m_7} & \frac{\sin m_9 \cos m_9}{w^3} \end{pmatrix} \quad (6.3-310)$$

\mathbf{w} are data weights after Huber (with sigma-factor from CCDB.L1BP.VFM.EstWeights), i.e. initially $\mathbf{w} = \mathbf{1}$ (all ones), for the $k+1$ 'th iteration given \mathbf{d}^k and \mathbf{w}^k of the k 'th iteration:

$$w_i^{k+1} = \min\left(1, \text{EstWeights.Huber_factor} / \left|d_i^k / \sigma^k\right|\right) \quad (6.3-320)$$

with

$$\sigma^k = \sqrt{\sum (w_i^k d_i^k)^2 / \sum w_i^k} \quad (6.3-330)$$

Λ is the a-priori model diagonal weight matrix. It is designed to use uniformly scaled CCDB.L1BP.VFM.EstWeights parameters; to adopt a logarithmic decay in the age of the TCF.VFM^{init} parameters with a half-time of 5 days, and to adapt to the variance of the VFM normalized components (to automatically detected S/C maneuvers). Let n be the number of selected samples of F_{ASM} , $\gamma = (1, 3 \cdot 10^4, 3 \cdot 10^4)$, and t_0 the time of the first VFM^{accept} sample. Then:

$$\Lambda_{ii} = n\lambda \begin{cases} \gamma_1 \eta_i \text{EstWeights.Bias} & \text{for } i=1,2,3 \\ \gamma_2 \eta_{i-3} \text{EstWeights.Scale} & \text{for } i=4,5,6 \\ \gamma_3 \text{EstWeights.n_orth} & \text{for } i=7,8,9 \end{cases} \quad (6.3-340)$$

$$1/\lambda = 1 + \ln \left(\frac{|\text{TCF.VFM}^{\text{init}} \cdot \text{trange}_2 - t_0| + c}{c} \right) \quad (6.3-350)$$

$$c = \frac{5 \cdot 86400 \text{ s}}{e - 1} \quad (6.3-360)$$

The component variance weight factor, η , is computed for all three components:

$$\eta_i = \min \left(\text{EstWeights.Limit}_i, \frac{2n \text{ EstWeights.A}}{\sum \left(\frac{\text{VFM}_i}{|\text{VFM}|} \right)^2} \right) \quad (6.3-365)$$

where the sum is taken over the n VFM samples selected for the estimation.

Now, \mathbf{m} is estimated by iteration: $\mathbf{m}^0 = \mathbf{m}_p$ and

$$\mathbf{m}^{k+1} = \mathbf{m}^k + 0.8 \left((\mathbf{G}^k)^T \mathbf{w}^k \mathbf{G}^k + \Lambda \right)^{-1} \left((\mathbf{G}^k)^T \mathbf{w}^k \mathbf{d}(\mathbf{m}^k) + \Lambda (\mathbf{m}_p - \mathbf{m}^k) \right) \quad (6.3-370)$$

where

$$\mathbf{G}^k = \left. \frac{\partial \mathbf{d}(\mathbf{m})}{\partial \mathbf{m}} \right|_{\mathbf{m}=\mathbf{m}^k} \quad (6.3-380)$$

The algorithm is iterated until the weighted (with γ), change in \mathbf{m} is infinitesimal (though no more than 30 iterations), i.e. until:

$$\sqrt{\sum \gamma_{[i/3]}^2 (\mathbf{m}_i^{k+1} - \mathbf{m}_i^k)^2} < 10^{-4} \quad (6.3-390)$$

This completes the estimation of TCF.VFM. Set the fields of TCF.VFM^{output} as follows with \mathbf{m} and σ the final model vector and weighted sigma:

bias = (m₁, m₂, m₃)

scale = (m₄, m₅, m₆)

n_orth = (m₇, m₈, m₉) / as2r

rms = σ

cov = $(\mathbf{G}^T \mathbf{G} + \Lambda)^{-1}$

W_scale = log₁₀(diagonal of Λ), with log₁₀(0) \equiv -999

trange = the range of selected t_{ASM}

samples = the number of selected F_{ASM}

DPU_id = the DPU_id of the VFM data

In case the final model-vector, \mathbf{m} , deviates significantly from the initial vector, $\mathbf{m}_p = \mathbf{m}^0$, i.e. if $\sqrt{\sum \gamma_{[i/3]}^2 (\mathbf{m}_i - \mathbf{m}_i^0)^2} > \text{CCDB.L1BP.VFM.EstWeights.Recalc_Limit}$, the processing of ASM and VFM data need to be redone starting at the stray field computation and correction using the TCF.VFM^{output} as TCF.VFM^{init}.

6.3.4.7 Generation of Mag-C Data

The Mag-C data product is the VFM calibration evaluation, verification and re-estimation data product. It contains the following elements – in case no TCF.VFM estimation is performed, replace $\mathbf{B}(\mathbf{m})$ by \mathbf{B}'_{VFM} in the table below: In case there are no ASM data available for the entire day, Mag-C data are generated using $t_{\text{ASM}} = \text{UTC}$ seconds for the day, the F , dF_{AOCS} , dF_{other} , and F_{error} values are all set to zero.

| Element | Description |
|------------------------------|--|
| t | Time from t_{ASM} |
| \mathbf{r} | Position, ITRF, spherical coordinates at time t |
| F | ASM reference field from F_{ASM} (at time t) |
| dF_{AOCS} | Magneto-torquer stray field correction applied to F |
| dF_{other} | Rest of stray field correction applied to F |
| F_{error} | Error estimate $F^{(3)}_{\text{err}}$, from Figure 6-4 |
| F_{VFM} | Fully corrected, ASM-filtered, interpolated VFM field intensity response: $\text{Interpol}_{\text{Lin}}(\text{filter}(\mathbf{B}(\mathbf{m})))$ where \mathbf{m} is the final model vector |
| dt_{VFM} | Time offset of the VFM sample nearest to $t_{\text{out,ASM}} = t - 3 * \text{CCDB.ASM.Filter.Delay}$: $dt_{\text{VFM}} = t_{\text{out,VFM}} - t_{\text{out,ASM}}$ |
| \mathbf{B} | $\mathbf{B}(\mathbf{m})$ at time $t_{\text{out,VFM}}$ of dt_{VFM} above |
| $d\mathbf{B}_{\text{Sun}}$ | $\Delta\mathbf{B}$ at time $t_{\text{out,VFM}}$ of dt_{VFM} above, Sun induced part |
| $d\mathbf{B}_{\text{AOCS}}$ | $\Delta\mathbf{B}$ at time $t_{\text{out,VFM}}$ of dt_{VFM} above, magneto-torquer part |
| $d\mathbf{B}_{\text{other}}$ | $\Delta\mathbf{B}$ at time $t_{\text{out,VFM}}$ of dt_{VFM} above, non magneto-torquer part |
| \mathbf{B}_{pre} | Pre-calibrated VFM magnetic field vector, $\mathbf{VFM}^{\text{accept}}$, at time $t_{\text{out,VFM}}$ of dt_{VFM} above |
| \mathbf{EU}_{VFM} | Level 1a.VFM.Sci.EU used to generate \mathbf{B} |
| T_{CDC} | CDC temperature linearly interpolated to time $t_{\text{out,VFM}}$ of dt_{VFM} above |
| T_{CSC} | CSC temperature linearly interpolated to time $t_{\text{out,VFM}}$ of dt_{VFM} above |
| T_{EU} | EU temperature linearly interpolated to time $t_{\text{out,VFM}}$ of dt_{VFM} above |
| alpha | Solar inclination angle, rotation about $-y$ axis, S/C frame, linearly interpolated to time $t_{\text{out,VFM}}$ of dt_{VFM} above |
| beta | Solar inclination angle, angle to $-y$ axis, S/C frame, linearly interpolated to time $t_{\text{out,VFM}}$ of dt_{VFM} above |

Table 6-7 Mag-C Product Elements

6.3.4.8 Application of TCF and Correction for Stray Fields

The TCF.VFM parameters obtained above are applied to all $\mathbf{VFM}^{\text{accept}}$ samples of the current day and the correction for stray magnetic fields is performed yielding the Level 1b.Mag-H. \mathbf{B}'_{VFM} data. This is done as the computation of \mathbf{B}'_{VFM} , see Eq. (6.3-180)

In case the TCF.VFM parameters are not estimated (due to insufficient number of samples), Level 1b.Mag-H. $\mathbf{B}_{VFM} = \mathbf{B}'_{VFM}$, and TCF.VFM^{init} rather than TCF.VFM^{output} is stored in the TCF.VFM Data Set of the Level 1b Products.

The Level 1b.Mag-H. \mathbf{B}_{error} (VFM frame) is computed component-wise as the root-sum-squares of the uncertainties:

$$\mathbf{B}_{VFM, err} \Big|_i = \sqrt{\frac{\text{VFM}_{err} \Big|_i^2 + (\Delta B_i \text{ CCDB.Bus.Error}_{VFM})^2 + \Delta B_{err} \Big|_i^2 + \text{TCF.VFM}^{\text{output or init}} \text{.rms}^2}{2}} \quad (6.3-400)$$

6.3.4.9 Sample Reduction

The Level 1b.Mag-H. \mathbf{B}_{VFM} vector data are reduced to 1 Hz sample rate at UTC seconds using the following method – observing the introduction of leap seconds, cf. Section 4.6. Elements of the reduction method described in [RD2] are used. The basic procedure is to filter the \mathbf{B}_{VFM} vectors component-wise using the Filter function of Appendix E on Page 143 with the CCDB.L1BP.VFM.Reduce_Pars.Filter coefficients followed by a fit of Chebychev polynomials to 0.1 – 10 second intervals of data using robustly reweighted iterative least squares. The value of the fitted polynomial at the desired sampling point is reported as the reduced-rate sample. The uncertainty is estimated by a bootstrap variability of the fitted values under repeatedly resampling of the residuals and re-fitting.

After filtering, the detailed processing for each target time t (UTC second) is:

- Select segment of $\leq n$ filtered VFM samples, $n = \text{CCDB.L1BP.VFM.Reduce_Pars}$. Window, preferably centered at t , but with some skewness allowed: there shall be at least $\sqrt{3n}$ samples before and after t . Up to two or three gaps of 1 – 3 samples are allowed – they are filled with linearly interpolated values to get exactly n equally spaced samples (drop samples at end). Note: some (filtered) VFM samples may be skipped or used twice.
- Fit Chebychev polynomials of degree $\text{CCDB.L1BP.VFM.Reduce_Pars.Degree}$ to each vector component of the segment using iteratively reweighted least squares with robust Tukey’s biweights. These weights are parameterized by the $\text{CCDB.L1BP.VFM.Reduce_Pars.Weight_Param}$ parameter.
- Estimate the scale for the weight function using a two-step procedure, starting with the median absolute deviation of the data in a window from their median to get the first scale estimate, then updating the scale estimate once using the median absolute deviation from the first polynomial fitted using weights calibrated to the first scale estimate. In all cases, the scale is only applied if above 10^{-3} . The fit tends to converge in 7-20 iterations, depending in part on details of the weight function.
- Report the value of the fitted polynomial at the target time t as the sample at the reduced rate, i.e. the Level 1b.Mag-L. \mathbf{B}_{VFM} data point. Estimate the standard error of the fitted polynomial at this point using $\text{CCDB.L1BP.VFM.Reduce_Pars.Bootstraps}$ bootstraps, by pretending that the fitted function is correct and drawing with replacement from the residuals to the fitted function to produce sets of “pseudo-data”,

fitting those pseudo-data by the same iterative procedure, and reporting the standard deviation of the fitted values.

The error estimate of the 1 Hz product is computed by root-sum-square adding the standard error estimates, se , to the average, possibly weighted, $\mathbf{B}_{VFM, err}$ of the n (real) samples in the segment:

$$\text{Level 1b.Mag - L.}\mathbf{B}_{error}|_i = \sqrt{\left(\frac{\sum \mathbf{B}_{VFM, err}|_i}{n}\right)^2 + se_i^2} \quad (6.3-410)$$

$d\mathbf{B}_{AOCS}$ and $d\mathbf{B}_{other}$ of the Level1b.MagL product is filled with linear interpolated values of the corresponding elements of the Level1b.MagH product.

6.3.4.10 Transformation to NEC Frame

The \mathbf{B}_{VFM} of the Level 1b Mag-H and Mag-L products are transformed to \mathbf{B}_{NEC} , the NEC_{VFM} frame of the VFM using $\mathbf{q}_{NEC \leftarrow CRF}$ and $CCDB.Structure.STR_q_CRF$:

$$\mathbf{B}_{NEC} = \mathbf{q} \times \mathbf{B}_{VFM} \quad (6.3-420)$$

$$\mathbf{q} = CCDB.Structure.STR_q_VFM \otimes \mathbf{q}_{NEC \leftarrow CRF} \quad (6.3-430)$$

The attitude error estimates, Att_{error} , is the root-sum-square of the input q_{error} error estimate and $CCDB.Structure.STR_q_VFM_err$:

$$\text{Level 1b.Mag} \begin{Bmatrix} \mathbf{H} \\ \mathbf{L} \end{Bmatrix} . Att_{error} = \sqrt{q_{error}^2 + CCDB.STR_q_VFM_err^2} \quad (6.3-440)$$

6.3.4.11 Flags

The flags of the 50 Hz VFM measurements, Level 1b.Mag-H.Flags_B, are computed as the sum of the values specified in Table 6-8 below for which the associated conditions are true.

| Value | Description |
|-------|--|
| 1 | ASM instrument turned off |
| 2 | VFM temperature trouble (any temperature): outlier detected, gap, or not enough samples for filtering |
| 4 | Suspicious VFM sample |
| 8 | Discrepancy between ASM and VFM measurements, i.e. $ \text{Level 1b.Mag-H.}\mathbf{B}_{VFM} - \text{Interpolate}_{Cubic}(F_{ASM}) > CCDB.Max_ASM_VFM_Diff$ |

Table 6-8 Level 1b Mag-H Flags_B values

The flags of the 1 Hz VFM measurements, Level 1b.Mag-L.Flags_B, are slightly different. They are computed as the sum of the values (except 255) specified in Table 6-9 below for which the associated conditions are true. For values 2, 4, and 16 the CCDB.L1BP.VFM.Reduce_Pars.Window VFM samples used in the sample reduction (previous page) are considered

| Value | Description |
|-------|--|
| 1 | ASM instrument turned off |
| 2 | VFM temperature trouble (any temperature): outlier detected, gap, or not enough samples for filtering |
| 4 | More than 5 suspicious VFM samples (in sample reduction window) |
| 8 | Discrepancy between ASM and VFM measurements: $ \text{Level 1b.Mag-L.B}_{\text{VFM}} - \text{Level 1b.Mag-L.F} > \text{CCDB.L1BP.VFM.Max_ASM_VFM_Diff}$ |
| 16 | Gap in VFM samples (by rejection or missing data) |
| 255 | Insufficient VFM data available for generating Level 1b.Mag-L.B _{xxx} (not combined with any of the above) |

Table 6-9 Level 1b Mag-L Flags_B values

The computation of Flag_{SPlatform} of either Mag-H or Mag-L are computed as the sum of the values specified in Table 6-10 below for which the associated conditions are true – for Mag-L considering VFM samples in the sampling reduction window as for Flags_B above.

| Value | Description |
|-------|---|
| 1 | Thruster latch valves open, thrusters not activated |
| 2 | Thrusters activated |
| 4 | Gap in Bus telemetry, 1 or 2 samples missing ⁹ |
| 8 | Outlier detected in any Bus currents (from Filter function) |
| 16 | Not enough data for filtering Bus currents (due to large gap or jump in data) |
| 32 | Change in any of the states listed in CCDB.Bus.State.Field and CCDB.Bus.State.Induced according to Bus telemetry, i.e. State _{before} ≠ State _{after} |
| 64 | No Bus telemetry available (for extended period) |
| 128 | Gap in AOCS telemetry ⁹ |
| 256 | Position information based on on-board (GPSR) navigational solution |

Table 6-10 Level 1b Mag-H/L Flag_{SPlatform} values

⁹ 1% slack compared to the nominal sampling rate is allowed.

6.4 Star Tracker – STR

¹⁰The Star Tracker is comprised of three Camera Head Units (CHUs) mounted on the inner-most end of the optical bench. Nominally, the attitudes of all three heads are provided simultaneously at 1 Hz rate, however one head is regularly blinded by the Sun leaving the attitudes of just two heads. The attitudes of the 2-3 CHU are combined into one attitude, the attitude of the STR Common Reference Frame (CRF). The combination uses the method described in [RD3]. The attitudes of CRF are then interpolated to obtain the CRF and S/C attitudes at required time instants: 50 Hz VFM measurements, 2 Hz EFI measurements and UTC seconds.

6.4.1 Input and Output Parameters

| Inputs | | | | | | |
|---|--------------------------------------|-----------------|---|---|------------------|------------------|
| Element | | | Description | Unit | Range | |
| L e v e l 1 a | S T R · S c i | Att1 | q | Orientation of CHU1 in ICRF frame, i.e. q is the transformation CHU1 ← ICRF | | ±1 |
| | | | Info | Structure with additional information, see Table 6-11 | | |
| | | Att2 | | Same as Att1 but for CHU2 | | |
| | | Att3 | | Same as Att1 but for CHU3 | | |
| | AOCS.Prop_HK | | | Propellant telemetry | | |
| | AOCS.Thru_HK. | | | AOCS thruster activation | | |
| | v_{pre} | | | Preliminary S/C velocity, ITRF | m/s | ±10 ⁴ |
| t_{out,EFI} | | | Output time-instants of EFI data, 2 Hz | UTC | | |
| t_{out,VFM} | | | Output time-instants of VFM data, 50 Hz | UTC | | |
| Level 1b.Eph.r | | | S/C position, ITRF | m | ±10 ⁷ | |
| C C D R B L I B P : S T R | S T R | AberrationalCor | | Application of aberrational correction | | 0 – 4 |
| | | Delay | | Delay of time-stamp | s | ±0.2 |
| | | Kappa | | Accuracy of rotation about boresight expressed in units of pointing accuracy | | 1 – 10 |
| | L I B P : S T R | MinConform | | Level of conformity required between pairs of CHU attitudes after rotation to CRF with STR_q_CRF | | 0.9 – 1 |
| | | Spline_Pars | | B-spline parameters for CRF interpolation | | |

¹⁰ The STR processing description is placed in this Section for historical reasons. The instrument level processing is actually performed in the GPSR and MOD processing context.

| Inputs | | | | |
|--|--|---|-----------------|------------|
| Element | | Description | Unit | Range |
| S t r u c t u r e | STR_q | Rotation of CRF to S/C frame | | ± 1 |
| | STR_q_CHU | Mean rotation of CRF to CHUs frame | | ± 1 |
| | SC_CoG | Structure with parameters for calculating the position of CoG in S/C coordinates as a function of propellant levels | | |
| | VFM_r | Position of VFM sensor, S/C coordinates | m | ± 10 |
| | Constants | c | Speed of light | m/s |
| | Sun | Structure containing constants for computing Earth velocity about the Sun | | |
| Outputs | | | | |
| Element | | Description | Unit | Range |
| $\mathbf{q}_{\text{NEC} \leftarrow \text{CRF}}$ | | Rotation of NEC_{VFM} to CRF frame at UTC seconds and at $t_{\text{out,VFM}}$ time-instants | | ± 1 |
| q_{error} | | Uncertainty estimates of $\mathbf{q}_{\text{NEC} \leftarrow \text{CRF}}$ | " | 0 – 30 |
| $\mathbf{q}_{\text{NEC} \leftarrow \text{S/C}}$ | | Rotation of NEC_{VFM} to S/C frame at $t_{\text{out,EFI}}$ time-instants | | ± 1 |
| $\dot{\mathbf{q}}_{\text{ITRF} \leftarrow \text{S/C}}$ | | Time-derivative of S/C \rightarrow ITRF rotation | s^{-1} | ± 2 |
| L e v e l 1 b | Eph. $\mathbf{q}_{\text{CRF} \leftarrow \text{ICRF}}$ | Rotation of CRF to ICRF frame at STR time instants (Instrument Level 1b data) | | ± 1 |
| | Eph. $\mathbf{q}_{\text{ITRF} \leftarrow \text{S/C}}$ | Rotation of ITRF to S/C frame at UTC seconds (“S/C Attitude”) | | ± 1 |
| | Eph. q_{error} | Uncertainty estimate of Level 1b.Eph. $\mathbf{q}_{\text{ITRF} \leftarrow \text{S/C}}$ | " | 0 – 30 |
| | Mag-L/H. \mathbf{r}_{VFM} | VFM sensor position, ITRF, 1 and 50 Hz | m | $\pm 10^7$ |
| | Mag-L/H. $\mathbf{q}_{\text{NEC} \leftarrow \text{CRF}}$ | STR CRF to NEC_{VFM} transformation | | ± 1 |
| | XXX.Flags q | Attitude flags of products XXX = Eph, Mag-L, Mag-H | | |

The Level 1a.Sci.Att_i.Info structure contains the following fields:

| Field | Description | Unit | Range |
|-------|--|------|--------|
| Seq | Sequence: If 1 only fine-tuning of attitude is performed, otherwise initial attitude determination is also performed. | | 0, 1 |
| Cor | Correction: If 1, aberrational and/or precession/nutation correction is performed. | | 0, 1 |
| HR | HighRate: If 1, considerable smearing of the image is observed – only half the integration time and half the number of pixels are used | | 0, 1 |
| BBO | Big Bright Objetc: If 1, a considerable part of the image is obscured | | 0, 1 |
| t_ref | Time Ref: If 1, the internal STR time is not synchronized to GPS. | | 0, 1 |
| Valid | Valid: If 1, the provided attitude is valid. | | 0, 1 |
| Res | Uncertainty estimate in pointing of Att _i .q | " | 0 – 30 |

Table 6-11 Info Flags of STR Telemetry

6.4.2 Algorithm

6.4.2.1 Overview

First, the time-stamps are corrected for any delays: $t_{out,STR} = t_{0,STR} - CCDB.STR.Delay$. Then the aberrational correction is verified and if necessary applied. The valid attitudes of the STR are combined into common attitude solutions, $\mathbf{q}_{CRF \leftarrow ICRF}$, providing the CRF \rightarrow ICRF transformations. This is the Level 1b_{Inst}.STR product. Then these are interpolated to the time-instants to be used (UTC seconds, $t_{out,VFM}$, etc.) using a smoothing, cubic B-spline method. Finally, the various, required output transformations are generated by combining series of transformations.

6.4.2.2 Aberrational Correction

The *aberrational* effect is a shift of the observed position of a light source proportional to the relative¹¹ velocity of the observer (the S/C) perpendicular to the line of sight (of the CHU_i). The velocity of the S/C in ICRF frame causes *orbital aberration*, whereas the Earths velocity around the Sun causes *annual aberration*. The S/C velocity is given by \mathbf{v}_{pre} (and \mathbf{r}_{pre}) converted to ICRF: $\mathbf{v}_{pre}^{ICRF} = \mathbf{Q} \mathbf{R} \mathbf{W} \mathbf{v}_{pre}^{ITRF} + \mathbf{Q} \mathbf{R} d\mathbf{R}/dt \times \mathbf{W} \mathbf{r}_{pre}^{ITRF}$ (see Section 8.4, Eq. 8.4-10 for the matrices Q, R, and W) followed by cubic Lagrange interpolation to $t_{out,STR}$ time-instants. The Earth velocity, \mathbf{v}_{Earth} is computed using time, $t_{out,STR}$, and the CCDB.Constants.Sun parameters (prefix omitted):

$$\mathbf{v}_{Earth} = \frac{-c1 \sin(a_{ecc})\mathbf{SA} + c2 \cos(a_{ecc})\mathbf{SB}}{1 - Eccentricity \cos(a_{ecc})} \quad (6.4-95)$$

where

$$a_{ecc} = a_{mean} + Eccentricity \sin(a_{mean}) \quad (6.4-96)$$

¹¹ Relative with respect to the speed of light, $c = 299,792,458$ m/s.

$$a_{\text{mean}} = (t_{\text{out,STR}} - t_{\text{Perigee}}) \text{Mean_Motion} \quad (6.4-97)$$

The computation of the actual aberrational correction is given in Appendix E.4.

The aberrational correction to apply – the velocity to use in Appendix E.4, \mathbf{v}_{obs} – is determined by CCDB.STR.AbrerrationalCor and Att_i.Info.Cor according to the table below. The “On-ground aberrational correction” flag is only set, when Att_i.Info.Cor = 0 and AberrationalCor = 1, 2, or 3.

| AberrationalCor | \mathbf{v}_{obs} | | Flag |
|-----------------|---|---|--------------------------------|
| | Att _i .Info.Cor = 0 | Att _i .Info.Cor = 1 | |
| 0 | $\mathbf{0}$ | $\mathbf{0}$ | 0 |
| 1 | $\mathbf{v}_{\text{Earth}} + \mathbf{v}_{\text{pre}}^{\text{ICRF}}$ | $\mathbf{0}$ | 1 - Att _i .Info.Cor |
| 2 | $\mathbf{v}_{\text{Earth}} + \mathbf{v}_{\text{pre}}^{\text{ICRF}}$ | $\mathbf{v}_{\text{pre}}^{\text{ICRF}}$ | 1 - Att _i .Info.Cor |
| 3 | $\mathbf{v}_{\text{Earth}} + \mathbf{v}_{\text{pre}}^{\text{ICRF}}$ | $\mathbf{v}_{\text{Earth}}$ | 1 - Att _i .Info.Cor |
| 4 | $\mathbf{v}_{\text{Earth}} + \mathbf{v}_{\text{pre}}^{\text{ICRF}}$ | $\mathbf{v}_{\text{Earth}} + \mathbf{v}_{\text{pre}}^{\text{ICRF}}$ | 0 |

6.4.2.3 Attitude Combination

The combined transformation from ICRF to CRF, Level 1b_{Inst}.STR. $\mathbf{q}_{\text{CRF} \leftarrow \text{ICRF}}$, is computed using a least squares fit with weights corresponding to the actual uncertainty of the STR attitude data including the anisotropic uncertainty of the estimation of the rotation about the camera boresight axis.

In the following, the Level 1a.STR.Sci, CCDB.STR and CCDB.Structure prefixes for the data and parameters have been omitted for clarity.

Only valid, consistent and high quality attitudes are used, i.e. the following conditions must be met:

- Att_i.Info.Valid must be 1
- Att_i.Info.HR must be 0
- Att_i. \mathbf{q} must have unity length, i.e. $\sum_{j=1}^4 q_j^2 = 1$ – to within given precision, i.e. check

$$\left| \sum_{j=1}^4 q_j^2 - 1 \right| < 2 \cdot 10^{-9}$$

Additionally, for samples with Att_i.Info.BBO = 1, the inter-boresight angle(s) (IBA) between the individual CHU’s is checked against the nominal IBA designated by CCDB.Structure.STR_q_CHU. For optimization purposes, the cosines of the angles are used, since for the inter-boresight angle, iba, between two CHU quaternions $\mathbf{q1}$ and $\mathbf{q2}$:

$$\cos(\text{iba}) = (\mathbf{q1}^{-1} \times \mathbf{ez}) \cdot (\mathbf{q2}^{-1} \times \mathbf{ez}) \equiv \text{ib} \quad (6.4-99a)$$

where $\mathbf{ez} = (0 \ 0 \ 1)^T$ is the unit vector of the z-axis. The nominal “ib” for CHU i and j, $\text{ib}_{i,j,\text{nom}}$, is

$$ib_{i,jnom} = (\text{STR_q_CHU}_i \times \mathbf{ez}) \cdot (\text{STR_q_CHU}_j \times \mathbf{ez}) \quad (6.4-99b)$$

A CHU sample with $\text{Att}_i.\text{Info.BBO} = 1$ is rejected if for any Att_j where the three bullets above are met (valid, not HR, and unit length) and $\text{Att}_j.\text{Info.BBO} = 0$:

$$|ib_{i,j} - ib_{i,jnom}| > \sqrt{2(1 - \text{MinConform})} / \text{Kappa} \quad (6.4-99c)$$

otherwise Att_i is included.

Additionally, the attitudes from the 3 CHU must be consistent, this is checked below.

Let

$$\tilde{\Lambda}_i = (\mathbf{R}_{\text{CHU}_i \leftarrow \text{CRF}})^T \begin{pmatrix} \sigma_i^2 & 0 & 0 \\ 0 & \sigma_i^2 & 0 \\ 0 & 0 & \kappa^2 \sigma_i^2 \end{pmatrix}^{-1} \mathbf{R}_{\text{CHU}_i \leftarrow \text{CRF}} \quad (6.4-100)$$

where $\sigma_i = \max(\text{Att}_i.\text{Res}, 0.3)$, $\kappa = \text{Kappa}$ and $\mathbf{R}_{\text{CHU}_i \leftarrow \text{CRF}}$ is the rotation matrix corresponding to the STR_q_CHU_i^{-1} (the i^{th} row of $\text{CCDB.Structure.STR_q_CHU}$) parameter. Let

$$\mathbf{q}^i = \text{q4positive}(\text{STR_q_CHU}_i^{-1} \otimes \text{Att1}.\mathbf{q}^{-1} \otimes \text{Att}_i.\mathbf{q} \otimes \text{STR_q_CHU}_i) \quad (6.4-110)$$

where q4positive returns the quaternion with positive 4th component, i.e:

$$\text{q4positive}(\mathbf{q}) = \begin{cases} \mathbf{q} & \text{iff } q_4 \geq 0 \\ -\mathbf{q} & \text{iff } q_4 < 0 \end{cases} \quad (6.4-115)$$

Then $\mathbf{q}^i \approx (0 \ 0 \ 0 \ 1)$, i.e. close to unity, provided the attitudes from CHU1 and CHU $_i$ are consistent. If $|q_4^i| < \text{CCDB.L1BP.STR.MinConform}$ the attitudes are considered inconsistent and only the pair (j,k) of attitudes with highest $|q^{j,k}_4| \geq \text{MinConform}$ are used ($\mathbf{q}^{j,k} \equiv \mathbf{q}^k$). If no such pair exist – use the attitude with the lowest σ_i . Let

$$\Delta_i = 2 (q_1^i, q_2^i, q_3^i)^T \quad (6.4-120)$$

then

$$\text{Level 1b}_{\text{Inst}}.\text{STR}.\mathbf{q}_{\text{CRF} \leftarrow \text{ICRF}} = \text{Att1}.\mathbf{q} \otimes \text{STR_q_CHU}_1 \otimes (\boldsymbol{\varepsilon}, \sqrt{1 - \boldsymbol{\varepsilon}^2}) \quad (6.4-130)$$

where

$$\boldsymbol{\varepsilon} = \frac{1}{2} (\tilde{\Lambda}_1 + \tilde{\Lambda}_2 + \tilde{\Lambda}_3)^{-1} (\tilde{\Lambda}_2 \Delta_2 + \tilde{\Lambda}_3 \Delta_3) \quad (6.4-140)$$

The description above assumes all three attitudes qualify for use. If Att2 or Att3 is invalid or does not qualify, the products of the disregarded attitude are ignored in Eq. (6.4-140). If Att1 is disregarded, $\text{Level 1b}_{\text{Inst}}.\text{STR}.\mathbf{q}_{\text{CRF} \leftarrow \text{ICRF}}$ is computed as follows:

$$\mathbf{q}^{2,3} = \text{STR_q_CHU}_2^{-1} \otimes \text{Att2}.\mathbf{q}^{-1} \otimes \text{Att3}.\mathbf{q} \otimes \text{STR_q_CHU}_3 \quad (6.4-150)$$

$$\Delta_{2,3} = 2 (q^{2,3}_1, q^{2,3}_2, q^{2,3}_3)^T \quad (6.4-160)$$

$$\boldsymbol{\varepsilon}' = \frac{1}{2} (\tilde{\Lambda}_2 + \tilde{\Lambda}_3)^{-1} (\tilde{\Lambda}_3 \Delta_{2,3}) \quad (6.4-170)$$

$$\text{Level 1b}_{\text{Inst}}.\text{STR}.\mathbf{q}_{\text{CRF} \leftarrow \text{ICRF}} = \text{Att2}.\mathbf{q} \otimes \text{STR_q_CHU}_2 \otimes (\boldsymbol{\varepsilon}', \sqrt{1 - \boldsymbol{\varepsilon}'^2}) \quad (6.4-180)$$

If only one attitude is applicable, Att_i , Level 1b_{Inst}.STR.q_{CRF←ICRF} = $Att_i.q \otimes STR.q_CHU_i$.

This also applies in case none of the attitude pairs complies to the conformity requirement ($|q^i_4| \geq CCDB.L1BP.STR.MinConform$) in which case the attitude with the lowest σ ($Att_i.Res$) and BBO = 0 is used – if all considered attitudes have BBO = 1, the one with the lowest σ is used.

The uncertainty estimate of the combined quaternion is computed as follows:

$$\text{Level 1b}_{Inst}.STR.q_{error} = \sqrt{3/2} \frac{1}{\sum 1/\sigma_i} \quad (6.4-190)$$

where the sum is taken over the attitudes used in the calculation of Level 1b_{Inst}.STR.q_{CRF←ICRF}. If only one attitude, Att_i , is used:

$$\text{Level 1b}_{Inst}.STR.q_{error} = \kappa \sigma_i = \text{Kappa } Att_i.Res \quad (6.4-200)$$

6.4.2.4 Interpolation of Attitudes

The Level 1b_{Inst}.STR.q_{CRF←ICRF} data (also stored in Level 1b.Eph) are interpolated to achieve the attitude at the required time-instants. As the time-instants are different for different processing chains, this process is repeated in the operational processors. The method for attitude interpolation is identical to the method used for ASM data, cf. Page 57, i.e. it is an iteratively reweighted least squares cubic B-spline approximation. Observe the introduction of leap seconds, cf. Section 4.6

First, the q_{CRF←ICRF} data sequence is divided into segments with gaps not exceeding the maximum gap size as specified in (CCDB.L1BP.STR.)Spline_Pars.Max_Gap_Size. Then jumps in q_{CRF←ICRF} caused by the sign ambiguity of quaternions are removed by changing signs on all four quaternion components on all q_{CRF←ICRF} following a jump in one component of more than 0.9. Within each segment, a cubic B-spline f is estimated for each of the four quaternion components. The fit minimizes:

$$\chi^2 = \mathbf{d}^T \mathbf{C} \mathbf{d} + \lambda \mathbf{m}^T \Lambda \mathbf{m} \quad (6.4-210)$$

where:

\mathbf{m} is the *model* vector, i.e. the parameters (spline coefficients) describing f

$\mathbf{d} = q_{CRF←ICRF,i} - f(\mathbf{m})$, is the data residual vector of the current model – of component i .

C : $C_{ij} = w_i G_{ij}$, where G is the design matrix (collocation matrix) for cubic B-splines for the given knots (internal spacing CCDB.L1BP.STR.Spline_Pars.Knot_Space, with additional knots in the ends), see Appendix D. \mathbf{w} are data weights computed as a combination of Huber weights [RD6], \mathbf{w}^{Huber} , and the data uncertainties, (Level 1b_{Inst}.STR.)q_{error}. Let $\alpha = \text{Spline_Pars.Weight_Huber}$, $\beta = \text{Spline_Pars.Weight_ErrEst}$, and $\sigma_{q_error} = \text{rms}(\mathbf{q}_{error})$, then:

$$\mathbf{w} = \alpha \mathbf{w}^{Huber} + \beta 1.5 \sigma_{q_error} / (|\mathbf{q}_{error}| + 0.1) + \max(\mathbf{1} - \alpha - \beta, \mathbf{0}) \quad (6.4-220)$$

\mathbf{w}^{Huber} are determined iteratively. Initially, $\mathbf{w}^{Huber} = \mathbf{1}$. \mathbf{w}^{Huber} of the next iteration is computed by (i is the vector index):

$$w_i^{\text{Huber}} = \min\left(1, \frac{1.5}{|d_i/\sigma|}\right) \quad (6.4-230)$$

where σ is the root-mean-squared (rms) misfit of \mathbf{d} weighted by the weights \mathbf{w} of the preceding iteration:

$$\sigma = \sqrt{\frac{\sum (w_i d_i)^2}{\sum w_i}} \quad (6.4-240)$$

$\lambda = \text{Spline_Pars.Acc_Damping}$ is the damping factor of the second order time-derivatives.

Λ is the block diagonal acceleration damping matrix, see Appendix D.

Equation (6.4-210) is solved by computing $\mathbf{m} = (\mathbf{G}^T \mathbf{C} + \lambda \Lambda)^{-1} \mathbf{C}^T \mathbf{q}_{\text{CRF} \leftarrow \text{ICRF},i}$, and the whole procedure is iterated by recomputing \mathbf{w} , \mathbf{C} (\mathbf{G} is constant), \mathbf{d} and \mathbf{m} until (though max 30 iterations):

$$\sqrt{\sum (m_i - m_i^{\text{prev}})^2} / \sqrt{\sum m_i^2} < 10^{-5} \quad (6.4-245)$$

The estimated B-splines are evaluated at UTC seconds and at the time-instants $t_{\text{out,VFM}}$ and $t_{\text{out,EFI}}$ – within the time-frames of the $\mathbf{q}_{\text{CRF} \leftarrow \text{ICRF}}$ data segments. After evaluation of the four B-splines the quaternions are normalized:

$$\mathbf{q}^{\text{norm}} = \mathbf{q} / \sqrt{\sum q_i^2} \quad (6.4-250)$$

This completes the $\mathbf{q}_{\text{CRF} \leftarrow \text{ICRF}}$ at all required time-instants.

The calculation of $\dot{\mathbf{q}}_{\text{ITRF} \leftarrow \text{S/C}}$ is done using the time-derivative of $\mathbf{q}_{\text{CRF} \leftarrow \text{ICRF}}$ – the derivative of $\mathbf{q}_{\text{ITRF} \leftarrow \text{ICRF}}$ is very small in comparison and is ignored; the other transformations are constant. The derivative of $\mathbf{q}_{\text{CRF} \leftarrow \text{ICRF}}$ is computed using the derivatives of the B-splines estimated above. The calculation of B-spline derivatives is given in Appendix D.

The error estimates of the combined quaternions (Level 1b_{Inst}.STR. $\mathbf{q}_{\text{CRF} \leftarrow \text{ICRF}}$) are modified to form an intermediate error estimate, $\mathbf{q}_{\text{error}}^{\text{new}}$. This is the rms value of the original error estimate and the deviations from the four cubic B-splines, f_i evaluated at the $t_{\text{out,STR}}$ time-instants (within the current segment):

$$\mathbf{q}_{\text{error}}^{\text{new}} = \sqrt{(\text{Level 1b}_{\text{Inst}} \cdot \mathbf{q}_{\text{error}}^2 + \eta \sum (q_i - f_i)^2 / 4) / 2} \quad (6.4-260)$$

where $\eta = 3600 \cdot 180 / \pi$ converts to arc-seconds, the unit of $\mathbf{q}_{\text{error}}$.

The error estimates of the interpolated attitudes are computed as the weighted average of the four nearest attitudes (sample numbers i):

$$\mathbf{q}_{\text{error}}^{\text{out}} = \beta \frac{\sum \mathbf{q}_{\text{error},i}^{\text{new}} \text{wt}_i}{\sum \text{wt}_i} \quad (6.4-270)$$

where

$$wt_i = 1/(|t - t_i| + 10^{-3}) \quad (6.4-280)$$

with t = time of the interpolated output quaternion and t_i = time of $q_{\text{error},i}^{\text{new}}$ – the time instants of the four nearest Level 1b_{Inst} quaternions. (“+ 10⁻³” just to avoid division by zero)

$$\beta = \max(1, 21/\sum wt_i) \quad (6.4-290)$$

β increases the error estimate in case there are gaps in the Level 1b_{Inst} data (sum over four nearest samples).

6.4.2.5 Flags

The values of Flag_q are given in Table 6-12 below. The higher flag values (“more serious”) take precedence over lower values, except for the “On-ground aberrational correction” condition (value 8) which is combined (added) to all other values, if applicable.

| Value | Description |
|----------|--|
| 1,2,3 | Lack of 1 or 2 attitudes of CHU_i in 4 nearest STR samples, $i = \text{Value} (1,2,3)$ |
| 4,5,6 | Lack of 3 or 4 attitudes of CHU_i in 4 nearest STR samples, $i = \text{Value}-3$ |
| 8 | On-ground aberrational correction of any attitude sample among 4 nearest STR samples. This value may be added to the value of all other applicable conditions. |
| 16,17,18 | BBO flag set for CHU_i of least one of 4 nearest STR samples, $i = \text{Value}-15$, other CHU’s ok (i.e. these values override values 1-6 in case BBO is set) |
| 19 | 2-4 attitudes based on CHU3 and {CHU1 or CHU2} in 4 nearest STR samples, i.e. CHU3 active in all 4 STR samples whereas CHU1 and CHU2 fail intermittently |
| 20 | 2-4 attitudes based on CHU2 and {CHU1 or CHU3} in 4 nearest STR samples, i.e. CHU2 active in all 4 STR samples whereas CHU1 and CHU3 fail intermittently |
| 21 | 2-4 attitudes based on CHU1 and {CHU2 or CHU3} in 4 nearest STR samples, i.e. CHU1 active in all 4 STR samples whereas CHU2 and CHU3 fail intermittently |
| 22 | 3-4 attitudes based on two heads, and all three heads failing intermittently |
| 32,33,34 | 1 or 2 attitudes based on CHU_i alone (other CHU’s missing) in 4 nearest STR samples, $i = \text{Value}-31$ |
| 35 | 2 attitudes based on one, intermittent CHU alone in 4 nearest STR samples, |
| 48 | 1 attitude sample missing among 4 nearest STR samples (data gap) |
| 49 | 2 attitude samples missing among 4 nearest STR samples |
| 50 | 3 or more attitude samples missing among 4 nearest STR samples |
| 51,52,53 | 3 or 4 attitudes based on CHU_i alone in 4 nearest STR samples, $i = \text{Value}-50$ |
| 54 | 3 or 4 attitudes based on one, intermittent CHU alone in 4 nearest STR samples |
| 255 | No STR data available for generating attitude information (large data gap) |

Table 6-12 Flag_q Values

6.4.2.6 Generation of Other Transformations and of \mathbf{r}_{VFM}

Level 1b.Eph. $\mathbf{q}_{\text{ITRF}\leftarrow\text{S/C}}$ at UTC seconds (1 Hz):

$$\text{Level 1b.Eph.}\mathbf{q}_{\text{ITRF}\leftarrow\text{S/C}} = \mathbf{STR_q} \otimes \mathbf{q}_{\text{CRF}\leftarrow\text{ICRF}}^{-1} \otimes \mathbf{q}_{\text{ITRF}\leftarrow\text{ICRF}} \quad (6.4-300)$$

where $\mathbf{q}_{\text{ITRF}\leftarrow\text{ICRF}}$ is the quaternion representation of $\mathbf{R}_{\text{ITRF}\leftarrow\text{ICRF}}$, the ICRF \rightarrow ITRF transformation, see Section 8.4. Here and in the following, the CCDB.Structure prefix has been omitted.

\mathbf{r}_{VFM} – position of the VFM sensor in ITRF frame – is computed at UTC seconds:

$$\text{Level 1b.Mag-L.}\mathbf{r}_{\text{VFM}} = \text{Level 1b.Eph.}\mathbf{r} + \mathbf{q}_{\text{ITRF}\leftarrow\text{S/C}} \times (\mathbf{VFM_r} - \mathbf{r}_{\text{CoG}}) \quad (6.4-310)$$

with \mathbf{r}_{CoG} computed once per day – at noon – as specified in Appendix E page 145f..

Level 1b.Mag-H. \mathbf{r}_{VFM} (at $t_{\text{out,VFM}}$ time-instants) is computed by a cubic Lagrange interpolation of Level 1b.Mag-L. \mathbf{r}_{VFM} .

$\mathbf{q}_{\text{NEC}\leftarrow\text{CRF}}$ at UTC seconds (Level 1b.Mag-L. $\mathbf{q}_{\text{NEC}\leftarrow\text{CRF}}$) and $t_{\text{out,VFM}}$ time-instants (Level 1b.Mag-H. $\mathbf{q}_{\text{NEC}\leftarrow\text{CRF}}$):

$$\mathbf{q}_{\text{NEC}\leftarrow\text{CRF}} = \mathbf{q}^{-1}_{\text{CRF}\leftarrow\text{ICRF}} \otimes \mathbf{q}_{\text{ITRF}\leftarrow\text{ICRF}} \otimes \mathbf{q}_{\text{NEC}\leftarrow\text{ITRF}} \quad (6.4-330)$$

$\mathbf{q}_{\text{ITRF}\leftarrow\text{ICRF}}$ at $t_{\text{out,VFM}}$ (50 Hz) may be computed by cubic Lagrange interpolation and re-normalization of $\mathbf{q}_{\text{ITRF}\leftarrow\text{ICRF}}$ at 1 Hz.

$\mathbf{q}_{\text{NEC}\leftarrow\text{ITRF}}$ is the quaternion representation of the $\mathbf{R}_{\text{NEC}\leftarrow\text{ITRF}}$ ITRF \rightarrow NEC(\mathbf{r}_{VFM}) transformation matrix, cf. Appendix C.

Computation of $\mathbf{q}_{\text{NEC}\leftarrow\text{S/C}}$ at $t_{\text{out,EFI}}$ time-instants is similar:

$$\mathbf{q}_{\text{NEC}\leftarrow\text{S/C}} = \mathbf{STR_q} \otimes \mathbf{q}^{-1}_{\text{CRF}\leftarrow\text{ICRF}} \otimes \mathbf{q}_{\text{ITRF}\leftarrow\text{ICRF}} \otimes \mathbf{q}_{\text{NEC}\leftarrow\text{ITRF}} \quad (6.4-340)$$

Here, $\mathbf{q}_{\text{NEC}\leftarrow\text{ITRF}}$ is also computed for the VFM sensor position – the tilt with respect to the NEC_{EFI} is insignificant w.r.t. EFI data.

7 Electric Field Instrument - EFI

7.1 Introduction

The Electric Field Instrument determines the ion density, the ion drift velocity, and the electric field at the S/C front panel (in-flight). The instrument consists of two components: the Langmuir Probe (LP) and the Thermal Ion Imager (TII).

7.2 Input and Output Parameters

| Inputs | | | | | |
|---------------------------------|--------------------------|------------------------------|---|-------|-----|
| Elements | | Description | Unit | Range | |
| L e v e l l a | L P | I₁ | Current of ion-saturation, linear e- region, and retarded e- region in probe 1 | eu | TBD |
| | | I₂ | Current of ion-saturation, linear e- region, and retarded e- region in probe 2 | eu | TBD |
| | | D₁ | Derivative of ion-saturation, linear e- region, and retarded e- region in probe 1 | eu | TBD |
| | | D₂ | Derivative of ion-saturation, linear e- region, and retarded e- region in probe 2 | eu | TBD |
| | | I_{FP} | 16 values of currents from the face plate | eu | TBD |
| | | Bias₁ | Bias voltage from tracking current on probe 1 | eu | TBD |
| | | Bias₂ | Bias voltage from tracking current on probe 2 | eu | TBD |
| | | U_{1,ret} | Voltage bias retarded e- region probe1 | eu | TBD |
| | | U_{2,ret} | Voltage bias retarded e- region probe2 | eu | TBD |
| | | Status | Possible overflows detected in processing | | TBD |
| | LP_Conf | LP configuration data | | | |
| L P - O f f | L P | FP_{Bias,Off} | Face plate, bias offsets | eu | TBD |
| | | FP_{Curr,Off} | Face plate, current offsets | eu | TBD |
| | - O f f | P1_{Bias,Off} | Probe 1, bias offsets | eu | TBD |
| | | P1_{Curr,Off} | Probe 1, current offsets | eu | TBD |
| | | P1_{Ref,ADC2} | Probe 1, reference ADC2 | eu | TBD |
| | | P1_{Ground} | Probe 1, ground | eu | TBD |
| | | P1_k | Probe 1 slope, current offset | eu | TBD |
| | | P1_m | Probe 1 constant, current offset | eu | TBD |
| | | P2_{Bias,Off} | Probe 2, bias offsets | eu | TBD |
| P2_{Curr,Off} | Probe 2, current offsets | eu | TBD | | |

| Inputs | | | | |
|-----------------|------------------|---|-------------|--------------|
| Elements | | Description | Unit | Range |
| | $P2_{Ref,ADC1}$ | Probe 2, reference ADC1 | eu | TBD |
| | $P2_{Ground}$ | Probe 2, ground | eu | TBD |
| | $P2_k$ | Probe 2 slope, current offset | eu | TBD |
| | $P2_m$ | Probe 2 constant, current offset | eu | TBD |
| | T | LP electronics board temperature | °C | -30 – 40 |
| L | $I_{sw,1}$ | Sweep mode currents, probe 1 | eu | TBD |
| P | $I_{sw,2}$ | Sweep mode currents, probe 2 | eu | TBD |
| – | dt | Step duration | s | 0 – 0.1 |
| S | dU | Step height | V | ±0.1 |
| w | U_0 | Starting bias | V | ±10 |
| e | n_{Inv} | Step at which sign of step height is inverted | | 0 – 255 |
| e | n | Number of sweep samples between steps | | 0 – 255 |
| P | DownCIC | Downsampling in FPGA CIC filter | | 0 – 255 |
| | DownCPU | Downsampling in CPU | | 0 – 255 |
| | CtrlMode | Control bits, mode | | 0 – 255 |
| | CtrlHW | Control bits, hardware | | 0 – 255 |
| T | $x_{1st,16Hz,H}$ | First x-moments over brightest columns, H sensor | | TBD |
| I | $y_{1st,16Hz,H}$ | First y-moments over brightest columns, H sensor | | TBD |
| I | $y_{2nd,16Hz,H}$ | Sum of the 2 nd y-moments over brightest columns, H sensor | | TBD |
| | $x_{1st,2Hz,H}$ | First x-moment, normalized, H sensor | | TBD |
| | $y_{1st,2Hz,H}$ | First y-moment, normalized, H sensor | | TBD |
| | $N_{i,H}$ | Profile of column totals, H sensor | | TBD |
| | $x_{1st,16Hz,V}$ | First x-moments over brightest columns, V sensor | | TBD |
| | $y_{1st,16Hz,V}$ | First y-moments over brightest columns, V sensor | | TBD |
| | $y_{2nd,16Hz,V}$ | Sum of the 2 nd y-moments over brightest columns, V sensor | | TBD |
| | $x_{1st,2Hz,V}$ | First x-moment, normalized, V sensor | | TBD |
| | $y_{1st,2Hz,V}$ | First y-moment, normalized, V sensor | | TBD |
| | $N_{i,V}$ | Profile of column totals, V sensor | | TBD |

| Inputs | | | | | | |
|---|----------------------|---|---|--|----------------------------|----------------------------|
| Elements | | | Description | Unit | Range | |
| | T | U_{FP} | Faceplate voltage | eu | 0 – 5 | |
| | I | tw | Shutter pulse width | s | 0 – 0.5 | |
| | I | tp | Shutter period | s | 0 – 0.5 | |
| | – | T_{CCD} | Temperature of CCDs | °C | -40 – 40 | |
| | H | U_{grid} | Bias grid voltages (2 sensors) | eu | TBD | |
| | K | U_{MCP} | MCP voltages (2 sensors) | eu | TBD | |
| | | U_{phos} | Phosphor voltages (2 sensors) | eu | TBD | |
| | | AOCS.Mag_HK | Magneto-torquer coil currents | A | $\pm 10^2$ | |
| | | AOCS.Thru_HK | Thruster activations | | 0/1 | |
| | TCF.LP | | | Structure holding LP offset calibration parameters | | [AD02] |
| Level 1b.Mag-H. B_{NEC} | | | Magnetic field vector in NEC frame | nT | $\pm 66,000$ | |
| Level 1b.Eph. $q_{ITRF \leftarrow S/C}$ | | | Transformation from S/C to ITRF frame | | ± 1 | |
| Level 1b.Mag-L. r | | | VFM position, ITRF | m | $\pm 10^7$ | |
| Level 1b.Eph. v | | | S/C velocity, ITRF | m/s | $\pm 10^4$ | |
| C C D B | L P | ... | Please refer to [AD09] for extensive list of instrument level processing parameters | | | |
| | | Sun | Structure with look-up tables for visibility of probes, see [AD03] | | | |
| | T I I | ... | Please refer to [AD08] for extensive list of instrument level processing parameters | | | |
| | | C o n s t a n t s | e | Electron charge | C | $\sim 1.60 \cdot 10^{-19}$ |
| | | | m_e | Electron mass | kg | $\sim 9.11 \cdot 10^{-31}$ |
| | m_H | | Proton (Hydrogen) mass | kg | $\sim 1.67 \cdot 10^{-27}$ | |
| | u | | Atomic mass unit | kg | $\sim 1.66 \cdot 10^{-27}$ | |
| | eps0 | | Permittivity | F/m | $\sim 8.85 \cdot 10^{-12}$ | |
| | Kb1 | | Boltzmann constant | J/K | $\sim 1.38 \cdot 10^{-23}$ | |
| | Kb2 | | Boltzmann constant | eV/K | $\sim 8.61 \cdot 10^{-5}$ | |
| r_E | Mean radius of Earth | m | $\sim 6.372 \cdot 10^6$ | | | |

| Outputs | | | |
|---------------------------|--------------------------------------|---|-----------------|
| Elements | | Description | Unit |
| Level 1b Plasma | $\mathbf{v}_{H,Ion}$ | Ion velocity, H-sensor | m/s |
| | $\mathbf{v}_{V,Ion}$ | Ion velocity, V-sensor | m/s |
| | \mathbf{v}_{Ion} | Ion velocity, NEC frame | m/s |
| | $\mathbf{v}_{S/C}$ | S/C velocity, NEC frame | m/s |
| | \mathbf{E} | Electric field vector, NEC frame | V/m |
| | ne | Plasma density | m ⁻³ |
| | T_{elec} | Electron temperature | K |
| | $\Phi_{S/C}$ | Spacecraft potential | V |
| | par_{error} | Error estimates of all the above parameters except $\mathbf{v}_{S/C}$ | |
| | rms _{fit,H} | RMS fit error from TII x-profile fit, H sensor | |
| | rms _{fit,V} | RMS fit error from TII x-profile fit, V sensor | |
| | var _{x,H} | Variance in 16 Hz x moment, H sensor | |
| | var _{y,H} | Variance in 16 Hz y moment, H sensor | |
| | var _{x,V} | Variance in 16 Hz x moment, V sensor | |
| | var _{y,V} | Variance in 16 Hz y moment, V sensor | |
| | $d\mathbf{v}_{mtq,H}$ | Velocity deflection due to magnetotorquer, H sensor | m/s |
| | $d\mathbf{v}_{mtq,V}$ | Velocity deflection due to magnetotorquer, V sensor | m/s |
| | SAA | South Atlantic Anomaly proximity indicator | |
| | Flags _{SLP} | Source and method of LP data | |
| | Flags _{SLP,ne} | Flags related to ne (plasma density) | |
| | Flags _{SLP,Telec} | Flags related to T_{elec} | |
| | Flags _{SLP,Us/c} | Flags related to $\Phi_{S/C}$ (spacecraft potential) | |
| | Flags _{TII} | Flags related to tii measurements | |
| Flags _{Platform} | Flags related to the S/C platform | | |
| LP _{LastConfig} | Time since last configuration packet | s | |
| LP _{LastSweep} | Time since last sweep packet | s | |
| TCF.LP | LP offset calibration parameters | | |
| TCF.TII | TII circular fit calibration data | | |

7.3 Algorithms

The detailed descriptions of the algorithms are formed in two documents:

- A) The Langmuir Probe (LP) algorithms can be found in [AD09], cf. Appendix J
- B) The Thermal Ion Imager algorithms can be found in [AD08], cf. Appendix I.

The S/C ephemeris and magnetic field vector data needed by the EFI algorithms are taken from various sources:

- The position is taken from Level 1b.Mag-L to co-locate plasma data with magnetic data (the ca. 7 m discrepancy between \mathbf{r}_{EFI} and \mathbf{r}_{VFM} is ignored). Interpolation in time is done using cubic Lagrange interpolation.
- The velocity is taken from Level 1b.Eph. The transformation of this from the ITRF to the NEC frame is given by

$$\mathbf{v}_{\text{NEC}} = \mathbf{R}_{\text{NEC} \leftarrow \text{ITRF}} \mathbf{v}_{\text{ITRF}} \quad (7.3-10)$$

where the transformation matrix $\mathbf{R}_{\text{NEC} \leftarrow \text{ITRF}}$ is defined in Appendix C.

- The transformation from the S/C frame to the NEC_{VFM} frame is given by $\mathbf{q}_{\text{ITRF} \leftarrow \text{S/C}} \otimes \mathbf{q}_{\text{NEC} \leftarrow \text{ITRF}}$, see also Eq. (6.4-340) in Section 6.4.2 (the difference between the NEC_{VFM} and NEC_{EFI} frame is less than 1/3" and is ignored).
- The magnetic field vector is taken from the Level 1b.Mag-H. \mathbf{B}_{NEC}

7.3.1 Illumination of LP Probes

The illumination of the LP probes by the Sun generates a photo-electric effect which disturbs the LP measurements. To estimate whether the probes are sunlit or not, the position of the Sun is computed in the S/C frame and converted to spherical coordinates which are looked up in the CCDB.LP.Sun tables. The shadow of the Earth is also taken into account. Let

\mathbf{r} = Level 1b.Mag-L. \mathbf{r} – S/C position, ITRF

\mathbf{r}_{Sun} = xl_sun(t) – position of Sun, ITRF, see [RD12] for xl_sun function

then if $\mathbf{r} \cdot \mathbf{r}_{\text{Sun}} < 0$ and $|\mathbf{r} \times \mathbf{r}_{\text{Sun}}| / |\mathbf{r}_{\text{Sun}}| < \text{CCDB.Constants.r}_E$ the S/C is in the shadow of the Earth and the probes are not illuminated. Otherwise compute position of the Sun in S/C frame:

$$\mathbf{s} = (\mathbf{q}_{\text{ITRF} \leftarrow \text{S/C}})^{-1} \times (\mathbf{r}_{\text{Sun}} - \mathbf{r}) \quad (7.3-20)$$

and convert \mathbf{s} to spherical coordinates (s, θ, ϕ). Make linear interpolations to determine illumination:

$$\text{illum}_k = \text{Interpol}_{\text{Lin}}(\text{CCDB.LP.Sun.Probe}_k, \theta, \phi) \quad (7.3-20)$$

k is the probe number (1 and 2), $\text{Interpol}_{\text{Lin}}$ is defined in Appendix E.

8 Position and Acceleration

8.1 GPS Receiver - GPSR

8.1.1 Introduction

Through the GPS antenna, the GPS receiver (GPSR) receives the signals from all of the antenna visible GPS satellites. The L1b processing corrects for known effects related to the Swarm instruments and satellite. The external errors e.g. due to the GPS segment are corrected in the orbit determination processing.

Eleven different input packet definitions from the ISP exists, these are

| | |
|-----|---|
| MDH | Measurement Data Header format |
| CAP | Carrier Phase data record |
| CAA | Carrier Amplitude data record |
| COP | Code Phase data record |
| GNA | GPS Nav Almanac data record |
| GNU | GPS Nav UTC and Ionosphere data record |
| MNS | Minimum Navigation Solution data record |
| IGC | IMT/GPST Correlation data record |
| GNE | GPS Nav Ephemeris data record |
| CS | Constellation Status record |
| AUX | Swarm Auxiliary data record |

However, for the GPS algorithms processing only seven of them are used. The collection of the data record from the CAP, CAA, COP, and GNE has to be repeated N times for the N viewed satellites with a 0.1 Hz/1 Hz update frequency.

8.1.2 Input and Output Parameters

| Inputs | | | | |
|---|-------|-------------------------------|---|------|
| Elements | | Description | Unit | |
| L E V E L 0 D A T A M N S | M | UTC.DAYS | Number of days since 1 st of January 2000 in the UTC time base | UTC |
| | D | | | |
| | H | UTC.MSEC | Number of milliseconds of day | UTC |
| | | UTC.USEC | Number of microseconds of milliseconds | UTC |
| | | FE_TEMP | Instrument temperature | K |
| | C | SV_ID | Space vehicle identifier | |
| | A | SIG | Signal type | |
| | P | NCO_PHASE | Carrier Cycle count and Carrier NCO phase | m |
| | C | SV_ID | Space vehicle identifier | |
| | A | SIG | Signal type | |
| | A | CNO | Carrier to noise power density ratio | dBHz |
| | | AMPL | Carrier amplitude | dBW |
| | C | SV_ID | Space vehicle identifier | |
| | O | SIG | Signal type | |
| | P | CC | Number of code chips counts since start of GPS week | |
| | | FP | Code phase fractional part | |
| | M | NMS | Navigation solution method | |
| | N | QUAL_IDX | Quality index | |
| | S | GDOP | Geometrical dilution of precision | |
| | | POS_X | Position in WGS 84, x coordinate | m |
| | | POS_Y | Position in WGS 84, y coordinate | m |
| | | POS_Z | Position in WGS 84, z coordinate | m |
| | | VEL_X | Velocity in WGS84, x velocity | m/s |
| | | VEL_Y | Velocity in WGS84, y velocity | m/s |
| | VEL_Z | Velocity in WGS84, z velocity | m/s | |

| Inputs | | | | |
|-----------------|-------------|---------------------------|---|-------------|
| Elements | | | Description | Unit |
| I G C | IMT | | Instrument measurement time representation of the synchronization time stamp. | Weeks and s |
| | GPST.SEC | | GPS time representation of the synchronization time stamp. | S |
| | GPST.SUBSEC | | Same as above, just in sub-seconds | s |
| G | SV_ID | | Space vehicle identifier | |
| N E | CRS | | Amplitude of the Sine Harmonic Correction term to the orbit radius | m |
| | CRC | | Amplitude of the Cosine Harmonic Correction term to the orbit radius | m |
| | CUS | | Amplitude of the Sine Harmonic Correction term to the argument of latitude | rad |
| | CUC | | Amplitude of the Cosine Harmonic Correction term to the argument of latitude | rad |
| | CIS | | Amplitude of the Sine Harmonic Correction term to the angle of inclination. | Rad |
| | CIC | | Amplitude of the Sine Harmonic Correction term to the angle of inclination. | Rad |
| | DELTAN | | Mean motion difference from computed value | rad/s |
| | M0 | | Mean Anomaly at reference time | rad |
| | E | | Eccentricity | |
| | SQRTA | | Square root of the semi major axis | \sqrt{m} |
| | OMEGA0 | | Longitude of ascending node of orbit plane at weekly epoch | rad |
| | I0 | | Inclination angle at reference time | rad |
| | OMEGA | | Argument of perigee | rad |
| | OMEGADOT | | Rate of right ascension | rad/s |
| TOE | | Reference time ephemeris | s | |
| IDOT | | Rate of inclination angle | rad/s | |

| Inputs | | | | |
|--|----------------------|-------------------------|---|------|
| Elements | | Description | Unit | |
| C C D B P S R | GPSR_r | | Position of GPSR antenna phase centre in S/C coordinate system | |
| | GPSR_q | | Transformation from S/C frame to GPSR antenna reference frame | |
| | G | Ant.Patt_L1 | Complex antenna radiation pattern representing the L1 C/A signal as function of azimuth and zenith angle | V |
| | | Ant.Patt_L2 | Complex antenna radiation pattern representing the L2 P(Y) signal as function of azimuth and zenith angle | V |
| | Ant.Code_CA | | Antenna code range pattern of C/A on L1 as function of azimuth and zenith angle | m |
| | Ant.Code_P1 | | Antenna code range pattern of P on L1 as function of azimuth and zenith angle | m |
| | Ant.Code_P2 | | Antenna code range pattern of P on L2 as function of azimuth and zenith angle | m |
| | ARP_r | | Position of antenna reference point (not used) | m |
| | Rx.Carr.L1_L2 | | Receiver carrier range bias for L2-L1 as a function of receiver temperature | m/C |
| | Rx.Code.P1_CA | | Receiver code range bias for L1 P(Y) - L1 C/A as a function of receiver temperature | m/C |
| | Rx.Code.P2_CA | | Receiver code range bias for L2 P - L1 C/A as a function of receiver temperature | m/C |
| | Rx.Cno.L1 | | Receiver C/No bias of L1 C/A as a function of receiver temperature | dB/C |
| | Rx.Cno.L2 | | Receiver C/No bias of L2 Y as a function of receiver temperature | dB/C |
| | Rx.No.L1 | | System noise density of receiver on L1 C/A as a function of receiver temperature | dB/C |
| | Rx.No.L2 | | System noise density of receiver on L2 Y as a function of receiver temperature | dB/C |
| | t_smooth | | The smoothing interval half width of the temperature smoothing | |
| GPS.L1 | | GPS L1 frequency, f_1 | Hz | |
| GPS.L2 | | GPS L2 frequency, f_2 | Hz | |
| ResIF_L1 | | Residual IF at L1 | | |

| Inputs | | | | |
|-------------------|------------------------------------|--|------------------------------|----------------|
| Elements | | Description | Unit | |
| | | ResIF_L2 | Residual IF at L2 | |
| | | F_CA | CA cod chip rate | Hz |
| | | F_P | P code chip rate | Hz |
| | | B_CA | CA code loop bandwidth | Hz |
| | | d_CA | CA early late spacing | |
| | | T_CA | CA coherent integration time | s |
| | | Constants.c | | Speed of light |
| STR output | $\mathbf{q}_{ITRF \leftarrow S/C}$ | Quaternion S/C attitude; output from the STR Instrument level processing | | |

| Outputs |
|---|
| RINEX Observation File <i>Version 3.0</i> |
| RINEX Navigation File <i>Version 3.0</i> |

For further definition of the RINEX format, see RD 11. The decision on the version of the RINEX format will be done in the requirements consolidation phase. The RINEX Observation and Navigation files are roughly organized as follows:

| | | | | |
|---|----------|----------------|--|---------------------------------------|
| R I N E X O b s e r v a t i o n F i l e | | Ant_bore | Antenna boresight | |
| | <i>H</i> | CoG_sat | Center of Gravity of the LEO satellite | m |
| | <i>e</i> | Ant_pos | Antenna position | m |
| | <i>a</i> | LEO_pos | Approximate LEO position in WGS84 | m |
| | <i>d</i> | Obs_type | Type of observations | |
| | <i>e</i> | Obs_scalef | Observation scale factor | |
| | <i>r</i> | AUX | Auxiliary information | |
| | | t_epoch | Time for each epoch | GPS |
| | | N_sat | Number of measured GPS satellites | |
| | | <i>D</i> | L1 | Phase information on the L1 frequency |
| | <i>a</i> | L2 | Phase information on the L2 frequency | Cycle |
| | <i>t</i> | C1 | Pseudo-range of the C/A code on the L1 frequency | m |
| | <i>a</i> | P1 | Pseudo-range of the P-code on the L1 | m |

| | | | | |
|-----------------------------|----------------------------|----------|--|------|
| I O N O r d | R e c o r d | | frequency | |
| | | P2 | Pseudo-range of the P-code on the L2 frequency | m |
| | | S1 | Raw signal strength on L1 – or SNR | |
| | | S2 | Raw signal strength on L2 – or SNR | |
| | | CH | Receiver channel number | |
| | | L_lock | Loss of lock indication | |
| | | P_signal | Signal strength (quality) | Watt |
| N A V I G A. | H e a d | ION_par | Ionospheric parameters from almanac | |
| | | UTC_par | UTC calculation parameters | |
| | | AUX | Auxiliary data information | |
| I G A. | D a t a | t_epoch | Time for each epoch | GPS |
| | | N_sat | Number of measured GPS satellites | |
| | | EPH | Ephemeris data of observed GPS satellites | |

8.1.3 GPSR Algorithm

The processing flow of algorithms is separated into three major steps:

- *L0 processing*, which comprises reading and checking of the raw binary level 0 instrument data.
- *L1a processing*, which comprises reformatting as well as interpretation and unit conversions of the L0 ISPs. The result is stored as L1a products.
- *L1b processing*, which comprises correction of the L1a data corresponding to the characterized distortions comprised in the Instrument Characterization Data Base (ICDB) which will be a part of the CCDB. The result is stored as RINEX 3.00 formatted ASCII data.

The overall data flow from L0 to L1b is show in Figure 8-1. An overview of the sequential walk-through of the data flow will be given below. For details a section number referring to AD11 is given and the associated algorithms are given in brackets in the sequential walk-through.

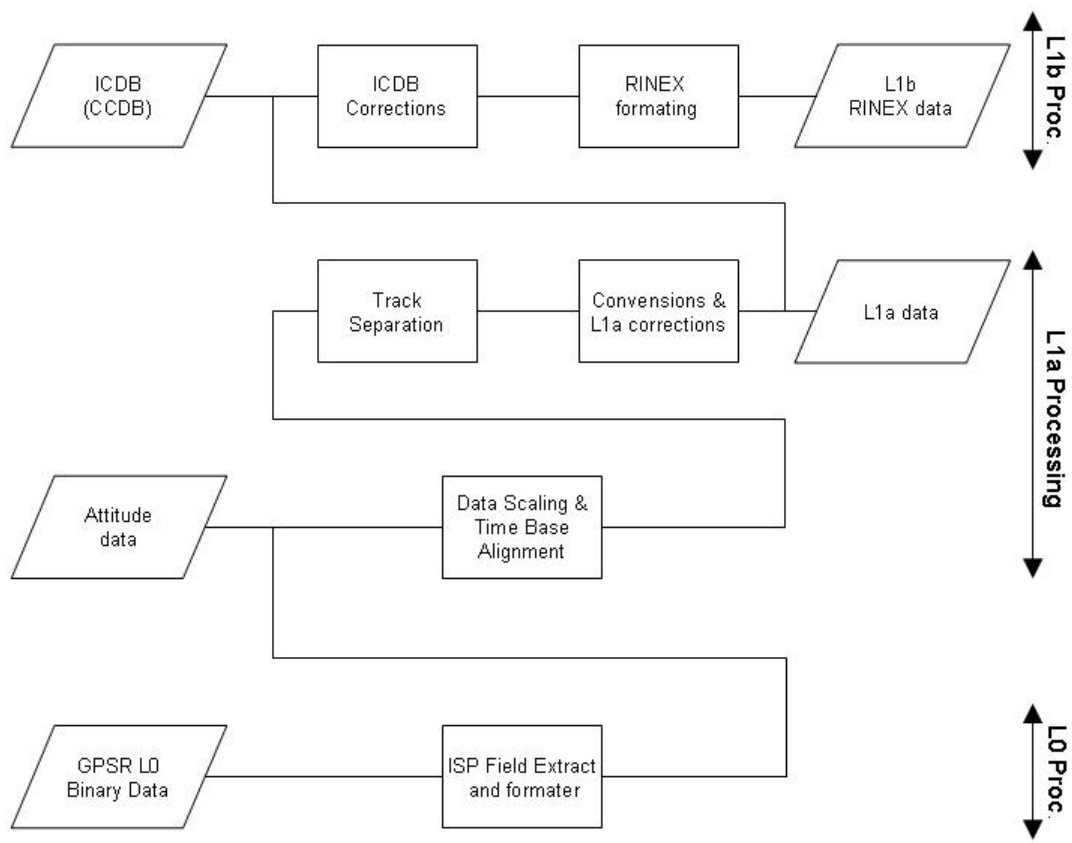


Figure 8-1 Level 0 to Level 1b processing flow for the GPSR.

1. First the level 0 to level 1a data processing, as defined in chapter 5 of this document, shall be performed. This includes also the following specific GPSR processing tasks.

- ISP are scaled into floating point values (§6.1.1)
- The instrument measurement time (IMT) shall be aligned to the GPS time (GPST) [GPSR§6.1.2]¹² and the data are time shall be stamped in all three time bases: UTC, GPST, and IMT.
- As an additional input the spacecraft attitude is needed. For this the result of the STR processing, chapter 6.4, i.e. the rotation of ITRF to S/C frame, shall be used. The algorithms defined by [AD11] (Section 6.2.1.2) need the attitude defined by yaw, roll and pitch at certain time stamps. Therefore the quaternion rotation from STR processing shall be transformed to roll, pitch, and yaw angles via the orbital reference frame. Let $M_{itrf2SC}$ be the rotation corresponding to $q_{ITRF-S/C}$, and $R = M_{itrf2SC} \times M_{orf2wgs}$ (eq-11 of [AD_11]), then

$$\begin{aligned}
 \text{pitch} &= \text{asin}(R_{3,1}) \\
 \text{roll} &= -\text{atan2}(R_{3,2}, R_{3,3}) \\
 \text{yaw} &= -\text{atan2}(R_{2,1}, R_{1,1})
 \end{aligned}
 \tag{8.1-10}$$

These are then interpolated to the required time stamps [GPSR§6.1.3].

¹² GPSR§x.y.z provides reference to section x.y.z of the GPSR L1b Algorithms Definition [AD11]

Note: In the requirements consolidation phase it should be considered whether the processing can be simplified by calculation of the quaternion already for the required time stamps and using quaternions for the further GPSR processing in [GPSR§6.2.1.2].

- Temperature data shall be smoothed (e.g. using a triangular weighting of the temperature measurements) [GPSR§6.2.2.1]
- Before further processing the GPSR data should be remapped to a track oriented mapping. This “track separation” parses through the data from carrier phase, carrier amplitude, carrier amplitude C/No, and the code phase, and separates the data into tracks.

The tracks are associated by the following criteria [GPSR§6.1.4]:

- ◇ Data from the same GPS satellite, i.e same PRN number
- ◇ Data that is measured on the same multi frequency channel (MF_chn)
- ◇ The data gap between samples is below 100s
- Provision of GPS Ephemeris Data. The GPS Ephemeris are to be taken from the related level 0 product, when available or alternatively from auxiliary data files to be downloaded from IGS

Next step are the 11a conversion and corrections. This conversion generates the level 1a data based on the demultiplexed, scaled, time correlated and track separated level 0 data. Further inputs to this processing are the spacecraft attitude information and the GPS Ephemeris Data. The 11a conversion and correction shall cover:

- GPS PVT: Position, velocity and time at the time of transmission shall be calculated for each GPS, ref. [GPSR§6.2.1.1]
- The azimuth, elevation and range to the LEO satellite shall be calculated for each GPS satellite based on the GPS PVT, the LEO PVT and the attitude information, ref. [GPSR§6.2.1.2].
- The data shall be merged with further data extracted from the level 0 products to GPS EPVT and LEO EPVT data sets that will be available as level 1a products. The detailed contents is to be defined during the design phase, for a first definition of the contents ref. [GPSR§5.2.1]
- Carrier range: Carrier range, in units of meters, shall be determined from the accumulated carrier phase reported by the instrument. It shall be corrected for downconversion scheme of the instrument and demodulated for the residual IFs, given in the CCDB ref. [GPSR§6.2.3.1]
- Code range: Code range, in units of meters, shall be determined from the chip counts and the fractional code phase reported by the instrument. Code range shall be reported for the C/A and P(Y) code on L1 and the P(Y) code on L2 depending on the tracking status of the instrument. Code range shall be reported at the selected code phase sample rate for the instrument.
- Code transmission time: The transmit time of the individual GPS signals shall be determined, This can be done from the code range by resolving the 1 ms (300 km) ambiguity of the C/A code and the 0.5 s (150000 km) ambiguity of the P codes. The

ambiguity is resolved based on the expected transmission time calculated from the GPST time stamp of the navigation solution and the range calculated from the ephemeris. For details ref. [GPSR§6.2.3.2]

- Pseudo Range: The code Pseudo Range (PR), in units of meters, shall be determined as the difference between the IMT timestamp of the code phase measurements and the GPS transmission time determined from the code phase samples. For details ref. [GPSR§6.2.3.3]
- Cycle slip detection and correction: All observations shall be checked and the time intervals that are corrupted by cycle slips shall be identified. If possible the cycle slips shall be repaired. The reported data shall be tagged with information on cycle slip detection and correction. For details refer to section 8.2.4 (MAUPRP section).
- Carrier smoothing: The code range shall be smoothed with the carrier range measurements. The algorithm requires that dual frequency code and carrier range measurements are available at identical sample instants. If only single frequency data is available, or if different sample rates are selected for code and carrier phase, this algorithm shall be bypassed. For details refer to [GPSR§6.2.3.4]. A check point where the smoothed code range is compared to the unsmoothed code range shall be introduced. If the difference exceeds a threshold, determined from the current C/No, the smoothing shall be discarded and the unsmoothed code range shall be reported. The reported data shall be tagged with the smoothing conditions used.

As a further step the observation data have to be corrected for instrument characteristics, including amplitude, C/No, phase, and group delay variations of the GPSR receiver and antenna patterns. These characteristics are available from the Characterisation and Calibration Data Base (CCDB). Note: the GPSR_r parameter of the CCDB contains the position of the GPSR antenna phase centre relative to the origin of the S/C. The characteristics are tabulated against azimuth and elevation for the GPS antenna and against temperature for the GPS receiver. These tables shall be used to correct the observation data, including

- ◇ Amplitude of L1 and L2 carriers
- ◇ C/No of L1 and L2 carriers
- ◇ Carrier range of L1 and L2
- ◇ Pseudoranges of CA, P1, and P2

The exact correction values are to be determined via interpolation. Where needed the level 1a data shall be transformed to the antenna coordinate system. For details refer to [GPSR§6.3.1].

The final step is the RINEX formatting. The output from the former algorithms steps together with further data extracted from the level 0 products shall be formatted into the RINEX 3.00 format.

8.2 Orbit Determination

8.2.1 Introduction

The Medium Accurate Orbit Determination MOD shall run automatically in a “black-box” solution, and fed with the output data from the GPSR (RINEX Observation files), IGS’ GPS orbits, and the Earth orientation parameters.

Because of the very high complexness of the parameter estimation of the orbit determination the algorithms are not trivial and are acquired after many years of experience. An existing “plug-and-play” orbit determination software does **not** exist. Two possibilities can be considered:

1. Perform some kind of smoothing or filtering of the already onboard navigational solution performed by the GPSR. These algorithms could be implemented in the L1b processor.
2. Using already developed orbit modeling software.

8.2.1.1 Filtering/Smoothing of Navigational Solution

GPS expert’s opinion is that filtering or smoothing of the navigational solution over an arc will achieve higher accuracy than 20m RMS. However, a problem will be to reach the accuracy of 1m RMS in all three directions. To smooth an orbit solution with accuracy of 20 RMS to 1m meter is a very challenging task, and perhaps not possible. By doing a smoothing the used algorithms can be included in the L1b processing and need no external and perhaps manual control.

8.2.1.2 Existing POD Software

Several POD software packages exist and some has been considered in consultation with experienced POD experts to be sure to deliver an orbit determination in an automatic processing of 1m accuracy for the MOD or even a manual processing of 10 cm accuracy for the POD. After many consultations and investigations of some of the software-packages we have decided to choose the Bernese 5.0 software. By the use of Bernese, it is guaranteed that the ~1m RMS requirement of the MOD will be reached. Some disadvantages might be:

- It is a more or less commercial package, and has to be paid – Contractor B-license has to be obtained through the Leica Geosystems company
- According to a statement by M. Rothacher (GFZ) (formerly programmer of parts of the software) Bernese is **not** documented according to ESA software standards and the algorithms are only sparsely documented.
- Primarily a GPS processing software and no commercial scripts for POD or MOD are available – hence Perl module scripts has to be written
- Highly sophisticated software that need experience to handle and set up

8.2.2 Input and Output Parameters

| Inputs | | | | |
|--------------------------|------------------------------|--|----------------|------------------------|
| Elements | | Description | Unit | Accuracy |
| RINEX Observation | Header | This part is roughly organized as mentioned in Section 8.1.2. This is stored only once per file. | | |
| | Data record | This part is roughly organized as mentioned in Section 8.1.2. The data record is repeated N times for N satellites in view for each epoch. | | |
| STR output | $q_{ITRF \leftarrow S/C}$ | Quaternion S/C attitude; output from the STR L1b processing (optional: Bernese may be run with or without attitude data) | | |
| External Data | sp3 | IGS GPS Satellite Ephemeris, minimum 'rapid' resolution is needed. | | <5cm |
| | clk | IGS high rate GPS satellite clocks and corrections. Same resolution as sp3. | s | <1 μ s |
| | erp | Earth rotation parameters, used for transformation between ITRF/ICRF. Same resolution as sp3. | mas mas/day | <0.1mas <0.2mas/day |
| | SAT_YYYY.CRX SATELLIT.I01 | GPS satellite problem file Satellite information file | | |
| | CONF | Bernese configuration files, e.g. leap seconds, phase center corrections, datum information, satellite information files. ¹³ | | |

| Outputs | | | |
|---------------|--------------------------------|------|--------|
| Elements | Description | Unit | Range |
| r_ITRF | Position vector in ITRF system | m | ~1m |
| v_ITRF | Velocity vector in ITRF system | m/s | ~1cm/s |

¹³ All Swarm specific configuration files to be delivered by DNSC, all other auxiliary data files are included in Bernese distribution. GPSUTC file must be updated in case of future introduction of leap seconds.

8.2.3 Orbit Determination Processing

The orbit determination is organized as sketched in Figure 8-2. Below is a cursory description of the individual processing steps necessary. For details, e.g. on Bernese directory structure and input/output files and formats, please see AD12.

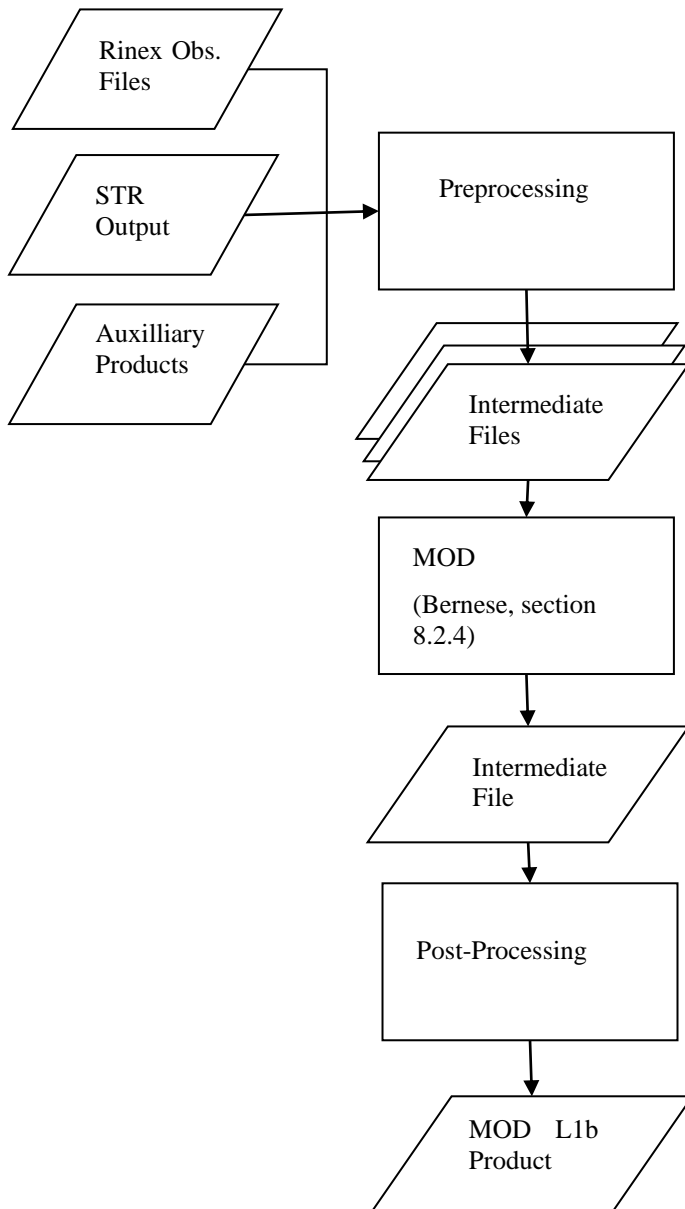


Figure 8-2 Orbit Determination Processing

Pre-processing:

Basically, pre-processing consists of downloading the necessary files, renaming according to Bernese standard and placing them in the relevant Bernese campaign sub-directories. Some possible exceptions:

1. Rinex observation files: if given as sub-daily (hourly) files these should be concatenated. This may be done in pre-processing or by the Bernese software.

2. Attitude data: the Bernese software may read attitude quaternions in Champ or Jason formats, or as native Bernese rotation matrix file. The attitude file should be reformatted to one of these options or an update of the Bernese READATT subroutine should be written to accept Swarm attitude files.

MOD processing:

The Medium accuracy Orbit Determination is carried out using the Bernese 5.0 software package, please see section 8.2.4. The output produced by Bernese is a precise orbit file SWNnyydd.pre containing

1. Header section (22 lines) containing processing information (time of first epoch, sample frequency, satellites processed).
2. Data section containing 3 lines for each epoch (each second):
 - a. Time of epoch
 - b. Satellite position
 - c. Satellite velocity

8.2.4 Bernese Software Orbit Determination Steps

In Figure 8-3 the overall processing of both the MOD and the Final POD are sketched. Bernese is a Fortran based software invented by the Astronomical Institute at the University of Bern, Switzerland. The current Version 5.0 consists of a graphical user interface (GUI) with a front-end for automatization called the Bernese Processing Engine (BPE). It can be installed on UNIX/Linux or Windows platforms.

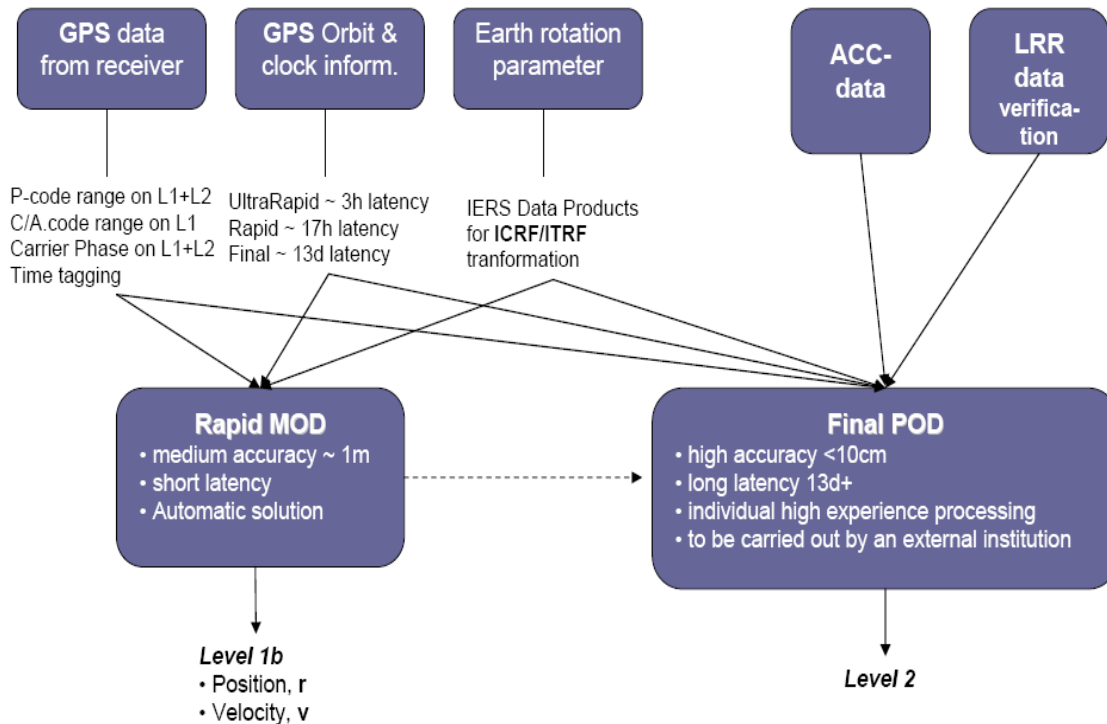


Figure 8-3 The overall processing of the orbit determination, both for the MOD and the final POD.

Several different programs in Bernese have to be run in order to receive the final position and velocity of the orbit determination. The overall dataflow is shown in Figure 8-4. In the top the IGS GPS orbits and clock, the ERP, the RINEX observation files and some Bernese specific auxiliary data are shown as input data. The rectangular boxes with hard edges show the individual programs that are executed and the boxes with round corners are the output from the programs. The orbit determination is performed in three steps, indicated by three dashed boxes:

- 1) the orbit part, where the GPS satellites orbits are estimated using a dynamical approach,
- 2) the pre processing, where an a priori orbit are generated,
- 3) the reduced-dynamic POD approach, where all the needed parameters are estimated and stochastic pulses from the GPS-estimated parameters are used as further input into the dynamic processing.

8.2.4.1 The Preliminary Processing

In the preliminary processing flow the main task is to convert the input data to a format readable for the Bernese Software.

8.2.4.2 The Orbit Part

The main task for the orbit part is to generate the GPS orbits. For this purpose the program ORBGEN which uses a dynamical process is used. Since this program is also used for the generation of a priori orbits and the final MOD orbit, the algorithmic background for this program is further described:

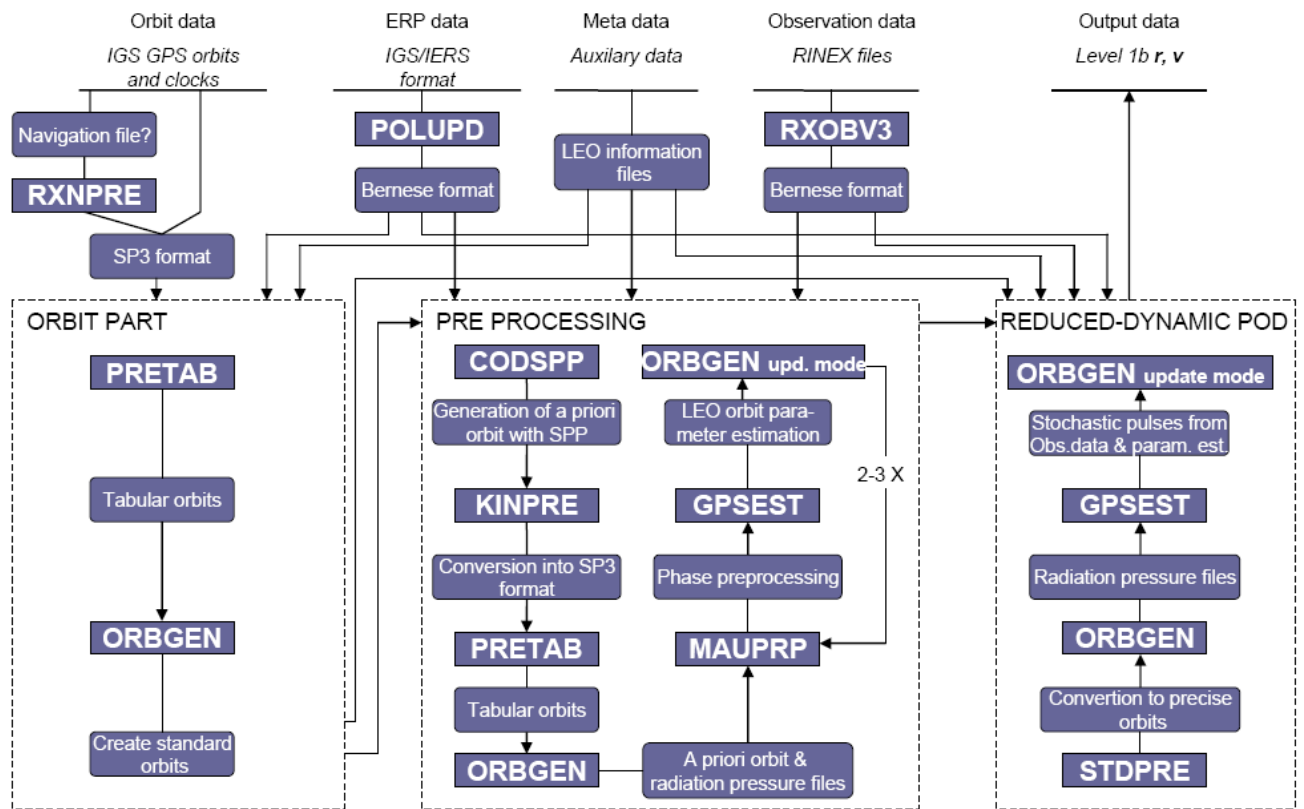


Figure 8-4 The overall processing of the MOD with the Bernese Software.

ORBGEN

The ORBGEN program integrates numerically the equation of motion, which basically is the main equation for estimation of a position and d velocity of a satellite. Each GPS orbit (each arc of the orbit) is a solution of the equation of motion given by

$$\ddot{\vec{r}} = -GM \frac{\vec{r}}{r^3} + \delta\vec{f}(t; \vec{r}, \dot{\vec{r}}, p_1, p_2, \dots, p_m),$$

$$\vec{r}(t_0) = \vec{r}(s_i(t_0)),$$

$$\dot{\vec{r}}(t_0) = \dot{\vec{r}}(s_i(t_0)),$$
(8.2-10)

where G is the universal constant of gravitation, $\delta\vec{f}$ is the perturbation accelerations, \vec{r} the geocentric position vector of the satellite, $\dot{\vec{r}}$ is the first time derivative, $\ddot{\vec{r}}$ its second time derivative of the satellite position, p_i , $i = 1, 2, \dots, m$ which is the unknown dynamical parameters of the orbit, and s_i is any one of the six classical Keplerian elements that uniquely describe the satellite orbit.

The force model used within Bernese includes the Earth's potential up to a selectable degree and order, the gravitational attractions of Sun and Moon as well as of the planets Jupiter, Venus, and Mars, the elastic Earth tidal corrections according to IERS 1996 conventions, pole tide, ocean tides, and general relativistic corrections.

When determining an orbit (ORBGEN are used both for the final determination of the reduced-dynamic POD and for the orbit determination for the GPS orbits, see Figure 8-4) first

the six parameters defining the position and velocity at the initial epoch t_0 of the arc has to be specified – these are called the inertial conditions. These are done in ORBGEN by use of the six osculating Keplerian orbital elements. The dynamical parameters used in Bernese are attributed into the radiation pressure model. The acceleration of the radiation pressure model, $\bar{\mathbf{a}}_{rp}$, is modelled in the following way:

$$\bar{\mathbf{a}}_{rp} = \bar{\mathbf{a}}_{MODEL} + \bar{\mathbf{a}}_D + \bar{\mathbf{a}}_Y + \bar{\mathbf{a}}_X, \quad (8.2-20)$$

where $\bar{\mathbf{a}}_{MODEL}$ is an a priori radiation pressure model, and

$$\begin{aligned} \bar{\mathbf{a}}_D &= (a_{D0} + a_{DC} \cos u + a_{DS} \sin u) \bar{\mathbf{e}}_D \\ \bar{\mathbf{a}}_Y &= (a_{Y0} + a_{YC} \cos u + a_{YS} \sin u) \bar{\mathbf{e}}_Y \\ \bar{\mathbf{a}}_X &= (a_{X0} + a_{XC} \cos u + a_{XS} \sin u) \bar{\mathbf{e}}_X \end{aligned} \quad (8.2-30)$$

where $a_{D0}, a_{DC}, a_{DS}, a_{Y0}, a_{YC}, a_{YS}, a_{X0}, a_{XC}, a_{XS}$ are the nine parameters of the radiation pressure model Bernese has to estimate, $\bar{\mathbf{e}}_D, \bar{\mathbf{e}}_Y, \bar{\mathbf{e}}_X$ are the three unit vectors 1) in the Sun direction, 2) along the spacecraft's solar-panel axis assuming nominal satellite attitude, and 3) that completes a right-handed orthogonal system, and finally u is the argument of latitude at time t ¹⁴. The a priori model is known for the Block I and Block II GPS satellites, but not for Swarm. Using ORBGEN only for the LEO orbit determination, the $\bar{\mathbf{a}}_{MODEL}$ term is set to zero.

Hence the minimum number of parameters to be estimated per arc is $n = 6 + 9 = 15$. However, this is only done in the dynamical process. In the reduced-dynamic approach, the orbit is additionally parameterized with so-called pseudo-stochastic parameters, characterizing instantaneous velocity changes at user-determined epochs in user-determined direction (typically all three directions). The attribute stochastic is justified because usually a priori weights (i.e., variances) are associated with these parameters. The attribute 'pseudo' is used because we are not allowing the orbits to adjust themselves continuously at every measurement epoch.

For the solution of the dynamical equation ORBGEN has to compute the partial derivatives of the position and velocity vector with respect to all orbit parameters. Because of the perturbation acceleration term $\delta\bar{\mathbf{f}}$ no analytical solution can be found for the partial derivatives. Since for longer arcs an analytical approximation is not sufficient in all cases, all partials computed by ORBGEN are found using numerical integration method. The procedure is to derive one set of differential equations, called variational equations, and one set of initial conditions, for each parameter. Then the resulting initial value problem will be solved by numerical integration.

If we write the dynamical equation as

$$\ddot{\bar{\mathbf{r}}} = -GM \frac{\bar{\mathbf{r}}}{r^3} + \delta\bar{\mathbf{f}}(t; \bar{\mathbf{r}}, \dot{\bar{\mathbf{r}}}, p_1, p_2, \dots, p_m) = \bar{\mathbf{f}}(t; \bar{\mathbf{r}}, \dot{\bar{\mathbf{r}}}, p_1, p_2, \dots, p_m) \quad (8.2-40)$$

then the variational equations can be derived by taking the derivative of the equation above with respect to the parameters, p . This gives the following initial value problem (variational equation and associated initial conditions):

¹⁴ u is the sum of the two Kepler elements: the mean anomaly, M , and the argument of the orbits perigee, ω , for a nominal satellite attitude.

$$\ddot{\vec{\mathbf{r}}}_p = \mathbf{A}\vec{\mathbf{r}}_p + \vec{\mathbf{f}}_p \quad (8.2-50)$$

$$\begin{aligned} \vec{\mathbf{r}}_{0,p} &= \vec{\mathbf{r}}_p(s_i(t_0)) \\ \vec{\mathbf{v}}_{0,p} &= \vec{\mathbf{v}}_p(s_i(t_0)) \end{aligned} \quad (8.2-60)$$

where it is assumed that there are no velocity-dependent forces. \mathbf{A} is a 3×3 matrix with $A_{p,ik} = \partial \vec{\mathbf{f}}_i / \partial \vec{\mathbf{r}}_k$ for element i, k and $\vec{\mathbf{f}}_p$ is the explicit derivative of $\vec{\mathbf{f}}$ with respect to the parameter p (equal to zero for osculating elements). The initial conditions are zero for the dynamical parameters.

In the orbit part, ORBGEN creates standard GPS orbits using a dynamical approach. These orbits serve as input to almost every program used in the further MOD processing.

8.2.4.3 The Pre Processing

In the pre processing the RINEX observation files are processed. Together with the processed GPS orbits and the Bernese internal auxiliary data, all these data serves as input in the pre processing for generation of good a priori LEO orbits. It will also be used for the final reduced dynamic MOD processing. The main programs in the pre processing are, CODSP, ORBGEN, MAUPRP, and GPSEST.

In the pre processing the GPS observations are used as input and in basically every program the GPS observation equations are used. Four basic GPS observation equations are currently used. Two for the code pseudo-ranges and two for the phase pseudo-ranges – each pseudo-range can use two frequencies F , both L_1 and L_2 with frequency f_1 and f_2 .

If the signal reception time (GPS time system) is called t and the reading of the receiver clock at signal reception is called t_k , then the error of the receiver clock (with respect to GPS time) is given by

$$\delta_k = t_k - t. \quad (8.2-70)$$

Further we define the geometrical distance between GPS satellite i , at the emission time $t - \tau$, and receiver k , at reception time t , as

$$\rho_k^i = |\vec{\mathbf{r}}_k(t) - \vec{\mathbf{r}}^i(t - \tau)| = c\tau, \quad (8.2-80)$$

with τ being the signal travel time from GPS satellite to receiver, c the velocity of light, $\vec{\mathbf{r}}_k$ the position of the LEO satellite, and $\vec{\mathbf{r}}^i$ the position of the i 'th GPS satellite.

Using the known codes modulated onto the GPS carriers, the receiver measures the pseudo-range

$$P_k^i = c((t + \delta_k) - (t - \tau + \delta^i)), \quad (8.2-90)$$

with δ^i being the error of the GPS satellite clocks at signal emission time $t - \tau$. P_k^i is called the pseudo-range because it is biased by satellite and receiver clock errors. Writing Eqn. (4) in terms of geometrical distance for each frequency the position of the LEO satellite can be introduced

$$P_{Fk}^i = \rho_k^i + c\delta_k - c\delta^i. \quad (8.2-100)$$

To achieve phase pseudo-ranges the GPS receiver measures the difference between two phases. The basic form of the observation equation is

$$\psi_{Fk}^i(t) = \phi_{Fk}(t) - \phi_F^i(t - \tau) + n_{Fk}^i, \quad (8.2-110)$$

where $\psi_{Fk}^i(t)$ is the phase measurement (in cycles) at epoch t and frequency F , $\phi_{Fk}(t)$ is the phase generated by the receiver oscillator, $\phi_F^i(t - \tau)$ is the phase of the carrier at emission time, and n_{Fk}^i is an unknown integer number of cycles, the so-called initial phase ambiguity. Using a Taylor series expansion of first order on the $\phi_F^i(t - \tau)$ term and taken the receiver and GPS satellite clock errors into account, the phase observation equation can be written as

$$\psi_{Fk}^i(t) = (\delta_k - \delta^i) f_F + \mathcal{I}_F + n_{Fk}^i. \quad (8.2-120)$$

By multiplying this equation by the wavelength λ_F , we receive the phase observation in meters

$$L_{Fk}^i = \rho_k^i + c\delta_k - c\delta^i + \lambda_F n_{Fk}^i. \quad (8.2-130)$$

The phase measurement and the code pseudo-ranges are affected by both systematic and random error. All relevant systematic errors should carefully be modeled in the used GPS software, but traditionally two of them are included in the observation equations, namely the tropospheric refraction $\Delta\rho_k^i$ and ionospheric refraction I_k^i . Taken this into account, the four basic observation equations can be written as

$$P_{1k}^i = \rho_k^i + c\delta_k - c\delta^i + I_k^i + \Delta\rho_k^i \quad (8.2-140a)$$

$$P_{2k}^i = \rho_k^i + c\delta_k - c\delta^i + \frac{f_1^2}{f_2^2} I_k^i + \Delta\rho_k^i \quad (8.2-140b)$$

$$L_{1k}^i = \rho_k^i + c\delta_k - c\delta^i - I_k^i + \Delta\rho_k^i + \lambda_1 n_{1k}^i \quad (8.2-140c)$$

$$L_{2k}^i = \rho_k^i + c\delta_k - c\delta^i - \frac{f_1^2}{f_2^2} I_k^i + \Delta\rho_k^i + \lambda_2 n_{2k}^i \quad (8.2-140d)$$

Due to the frequency dependence the ionospheric refraction, the L_2 is written as the squared fraction between the two frequencies f_1 and f_2 . This is the four basic GPS observables that are also used in the Bernese software.

For LEO orbit modeling the tropospheric refraction is automatically disabled, since the received signal is out of the troposphere. To eliminate the ionospheric refraction one can take advantages of the dual frequencies the GPSR in Swarm delivers. It is possible to form a linear combination between the two frequencies called the Ionosphere-Free linear combination, L_3 , which is defined for the phase measurement as

$$L_3 = \frac{1}{f_1^2 - f_2^2} (f_1^2 L_1 - f_2^2 L_2). \quad (8.2-150)$$

The same is true for the corresponding combination of code measurements. By this linear combination the ionospheric refraction is canceled.

CODSPP

The main task of CODSPP is to compute the receiver clock corrections. The receiver clock error has to be known with accuracy better than 1µs. It would be possible to introduce the receiver clock error as unknown parameters during the final least-squares adjustment in program GPSEST, but this would increase the number of parameters considerably. Fortunately, it is possible to compute the clock correction, together with the coordinates of the LEO, a priori with sufficient accuracy (< 1µs) using code measurements. This procedure is called Single Point Positioning (SPP).

The linearised observation equation to compute the receiver clock correction and a priori position for every epoch in CODSPP is given by

$$l_i = \frac{-1}{\rho_k^i} (\vec{r}^i - \vec{r}_0) \cdot (\vec{r}_k - \vec{r}_0) - \Delta t + \vec{v}_k, \tag{8.2-160}$$

where \vec{r}_0 the initial condition, Δt is the receiver clock error in length, i.e. $\Delta t = c\delta_k$, and \vec{v}_k is the residual. The term, l_i , is the so-called observed minus computed pseudorange (O-C) and is calculated for each observation of an epoch introducing the GPS satellite orbits, GPS satellite clocks, and the a priori position of the LEO. Based on these O-C values the receiver clock correction and the positions for the LEO for this particular epoch is obtained by majority voting. After correcting the O-C values for all observations for the receiver clock corrections the residual are analyzed for outliers. If an observation of an epoch exceeds a specified threshold the current epoch is marked both in phase and code observations.

The above equation can be written in general terms of matrices and is solved with least squares adjustment. The coefficients of the equation are computed using the initial coordinate vector. The a priori coordinates may not be accurate enough or even not known and for that reason the equation are solved iteratively. Note also that the equation has four unknowns and can then only be solved with a minimum of four GPS satellites available for the particular epoch. If fewer than four satellites are available CODSPP (and also all further processing) cannot compute the SPP and clock correction and therefore this particular epoch will be deleted.

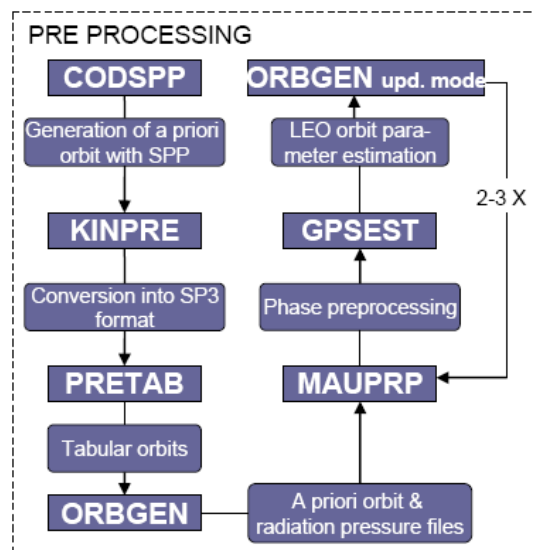


Figure 8-5 The Pre Processing of the Bernese orbit determination.

ORBGEN

The important output from this process here is the generation of the radiation pressure model for the LEO satellite. For this purpose the orbit integration has to be based on a recent gravity model (EIGEN2) including the Colombo parameters with a degree and order of minimum 70. The integration step has to be selected to 1 min in order to achieve the lowest RMS values.

MAUPRP

The following tasks are accomplished by MAUPRP:

- (1) Marking of observations due to the following reasons in order to exclude them from the preprocessing and the data analysis:
 - observations at low satellite elevation,
 - epochs with unpaired observations (L_1 without L_2 or vice versa),
 - small pieces of observations.
- (2) Perform a non-parametric screening to identify big outliers.
- (3) Compute an epoch-difference solution as a reference for the cycle slip detection.
- (4) Check all the observations and find the time intervals which are corrupted by cycle slips.
- (5) If possible, repair the cycle slips.
- (6) Check for clock events.

The phase measurement of the GPS receiver yields a value between 0 and 1 cycle (0 and 2π). After turning on the receiver an integer counter is initialized. During tracking, the counter is incremented by one whenever the fractional phase changes from 2π to 0. Thus, for every epoch the accumulated phase is the sum of the directly measured fractional phase and the integer count. The initial integer number of cycles between the GPS satellite i and receiver k is unknown and has to be estimated (see observation equations). In case of

$$n_{Fk}^i(t_2) - n_{Fk}^i(t_1) \neq 0, \quad (8.2-170)$$

a cycle slip has occurred between time t_1 and t_2 . MAUPRP uses n cycle slip detection and correction algorithm witch is as followed:

If we define the epoch-difference of the L_1 residual as r_1 and that for L_2 as r_2 , it is written for two different GPS satellites as

$$\begin{aligned} r_1 &= b_1 \lambda_1 + (I_k^{ij}(t_2) - I_k^{ij}(t_1)) + (\delta_k(t_2) - \delta_k(t_1)) \\ r_2 &= b_2 \lambda_2 + \frac{f_1^2}{f_2^2} (I_k^{ij}(t_2) - I_k^{ij}(t_1)) + (\delta_k(t_2) - \delta_k(t_1)), \end{aligned} \quad (8.2-180)$$

where the values b_1 and b_2 are integers used to test whether a no-cycle slip hypothesis ($b_1 = b_2 = 0$) holds. The residual in L_3 linear combination is computed as

$$r_3 = \frac{f_1^2}{f_1^2 - f_2^2} r_1 - \frac{f_2^2}{f_1^2 - f_2^2} r_2 = \beta_1 r_1 + \beta_2 r_2. \quad (8.2-190)$$

One of the two conditions in the no-cycle slip conditions are then

$$|r_3| \leq 3g \sqrt{(\beta_1 \sigma_1)^2 + (\beta_2 \sigma_2)^2}, \quad (8.2-200)$$

where the factor g is $\sqrt{2^2}$ caused by the growth in standard derivation by a factor $\sqrt{2}$ by forming every difference (two satellites and two epochs). σ_1 and σ_2 is the a priori RMS error of the zero difference observable. The other no-cycle slip condition is linked to the ionospheric refraction behavior. If the mean value m fulfills

$$m = \frac{1}{2} \left(r_1 + \frac{f_2^2}{f_1^2} r_2 \right) \leq M_{ion} \quad (8.2-210)$$

where M_{ion} is the maximum ionospheric change from epoch to epoch (specified by the user of MAUPRP), and the condition in Eqn. (8.2-210) hold, then the no-cycle slip hypothesis is accepted as true.

In the opposite case a search over the values b_1 and b_2 is performed. All combinations of

$$\begin{aligned} b_{1p} &= INT\left(\frac{r_1}{\lambda_1}\right) + p, & p &= -J_1, \dots, -1, 0, 1, \dots, J_1 \\ b_{2q} &= INT\left(\frac{r_1}{\lambda_1} - \frac{r_2}{\lambda_2}\right) + q, & q &= -J_2, \dots, -1, 0, 1, \dots, J_2 \end{aligned} \quad (8.2-220)$$

are formed. INT is the nearest integer and the search ranges J_1, J_2 has to be specified by the user. If one combination meets the no-cycle slip hypothesis, this pair is assumed to be the cycle slip correction. If no combination is found a new ambiguity parameter should be introduced in the parameter estimation program GPSEST. Too many ambiguity parameters (and few GPS satellite observation per epoch) would result in large RMS errors in the other parameter estimated.

In the non-parameters screening of phase observation high-rate precise GPS clocks correction are essential needed. Also due to the rapidly changing GPS satellite geometry as seen by the LEO several time interval criterions have to be reduced. The screening may be iterated when an improved a priori orbit gets available in the final pre-processing.

GPSEST

GPSEST is the main estimation program for the adjustment of the model parameters. It sets up the linearized observation equations in the Gauss-Markoff Model of full rank and solves the normal equations using Least-Squares Estimation. Since the observation equations are linearized by a Taylor series expansion around 0, the use of good a priori positions are essential to adapt a globally extremum and not a local.

Table 8-1 summarizes the adjustable parameters implemented in GPSEST relevant for processing a LEO orbit. The parameterization as a function of time has three different forms: A) A parameters may be constant over the entire computed arc. This may be the case for ex. antenna offset or patterns. B) A parameter may be represented as a pies-wise linear function in time. This is the case for e.g. the ionosphere parameters and the radiation pressure parameters. C) A parameters may be valid for a single observation epoch only. This is the case for most of the main relevant parameters for a LEO determination, e.g. coordinates, ambiguity resolution after a cycle slip, the stochastic orbit parameters etc.

The constant parameter are either set by the user or estimated once at the beginning of the arc. The piece-wise linear parameter functions in the time interval between t_1 and t_2 are

parameterized either by the values in time t_1 and t_2 (two biases) or by the function in t_1 and its time derivative (bias and tilt terms) at equidistant nodal points. The parameter spacing can be defined by the user. Epoch parameters are set up for each epoch. Due to their large number it is generally necessary to pre-eliminate them epoch wise e.g. in CODSPP or MAUPRP. This is possible because epoch-parameters, by definition, are not directly correlated – physical correlations are neglected. Due to the large number of coordinate parameters including other epoch parameter, a back-substitution step is necessary to resolve the parameters with the smallest RMS possible. This is done by solving the normal equations for the parameters, but not for the coordinates, and insert them back into the observation equation which then are successively solved for each epoch.

In the use of GPSEST in the pre-processing the main relevant estimated parameters are the epoch specific coordinates, the phase ambiguities and the stochastic ionospheric parameters. If, however, some of the pre-estimated parameters are not well estimated, these may also go into the parameter estimation. But the use of the pseudo-stochastic parameters shall not be introduced in this step. To keep the generation of the a priori orbit as dynamical as possible, the stochastic pulses are first introduced in the reduced-dynamic processing step. 15 min pulses may, however, be used if the RMS of the a priori orbit is worse than some meters.

| Parameter | Description |
|--|---|
| Epoch specific coordinates | Estimation of the position of the LEO assigned to each epoch. |
| Phase Ambiguities | One initial phase ambiguity parameter has to be assigned for each continued data-locked satellite. Also if a cycle slip occurs that MAUPRP could not repair a new ambiguity parameter is introduced. Resolved ambiguities may be introduced in subsequent program runs. |
| Stochastic ionospheric parameters | Epoch- and satellite-specific ionosphere parameters may be introduced, together with a priori weights, to support ambiguity resolution. |
| Radiation pressure parameters | A total of nine parameters per arc may be introduced, three in each of the three orthogonal directions. Constant and periodic once-per-revolution terms may be introduced. |
| Pseudo-Stochastic Orbit Parameters | Velocity changes in pre-determined directions at user defined epochs may be introduced. Up to three directions, radial, along-track and out-of-plane, may be defined per epoch. |
| Receiver clock corrections | Estimation using code and phase information if for some reason the CODSPP estimates are not good or not estimated. |
| Receiver antenna phase center variations | Antenna phase center variations may be modeled using different techniques. Model parameters may be determined. |

Table 8-1 Parameter types implemented in GPSEST, relevant for LEO orbit determination.

ORBGEN

In the last step of the pre-processing ORBGEN reads the orbit parameters element file written by GPSEST and updates the standard orbit by numerical integration. It is essential that the orbit models used for the generation of the a priori orbit and for updating of the orbit are identical.

In order to an additional a priori orbit improvement, the last three steps in the pre-processing (MAUPRP -> GPSEST -> ORBGEN) have to be iterated 2-3 times. Some of the constraints and rejection criteria in MAUPRP and GPSEST may slightly be sharpened in order to archive the smallest RMS value on the a priori orbit. The importance of a very reliable a priori orbit, an effective data editing, and orbit adjustment was also a main conclusion in formatting the MOD on CHAMP. This is exactly the task of this iterative step-wise approach in the pre-processing by Bernese.

8.2.4.4 The Reduced-Dynamic Processing

The final step in the orbit determination of the LEO satellite is the reduced-dynamic processing step. Due to the dynamical model implementation in ORBGEN (which is not optimized for LEO's) it is generally preferable to estimate the orbit using the reduced-dynamic approach and not a kinematic approach. However, a kinematic solution is possible using GPSEST for a kinematic point positioning and hereafter the KINPRE to convert the output into a precise orbit file, but some dynamics will be introduced since the a priori orbit (which also is essential for a good kinematic approach) is generated by the use of dynamic parameters.

Essential the reduced-dynamic orbit determination is an orbit improvement process where orbital parameters are refined using observations. This is done by ORBGEN and GPSEST and involves three steps

1) Preparation of a priori orbit information:

A priori orbit as well as the partial derivatives of the orbit positions with respect to the parameters to be estimated are generated with program ORBGEN by numerical integration of the equations of motion and of the variational equations. The information is written to a standard orbit and a radiation pressure file.

2) Estimation of improvements for orbit parameters:

Program GPSEST reads the a priori orbit and the derivatives from these two files, builds up the normal equations in a loop over all observations, and solves the equation system to obtain the parameter improvements. The improved orbital parameters are written to an element file referring to the start epoch of the a priori orbit (osculation epoch).

3) Update of orbit:

ORBGEN reads the element file written by GPSEST and integrates the orbit numerically based on the improved orbit parameters. The output is a standard orbit for a specified time interval.

The input data from to the reduced-dynamic processing is the RINEX observation files, the ERP data, Bernese internal auxiliary data, the processed GPS orbits from the Orbit Pert, and the a priori Leo orbit from the Pre Processing part.

ORBGEN

The same procedure has to be followed as in the pre processing. Not only the equations of motion but also the so-called variational equations, which are the derivatives of satellite positions with respect to orbit parameters, have to be integrated numerically for orbit improvement. The integration process writes the polynomial coefficients for the satellite, each component, and each integration subinterval into the standard orbit file and those for all the partials into a radiation pressure file.

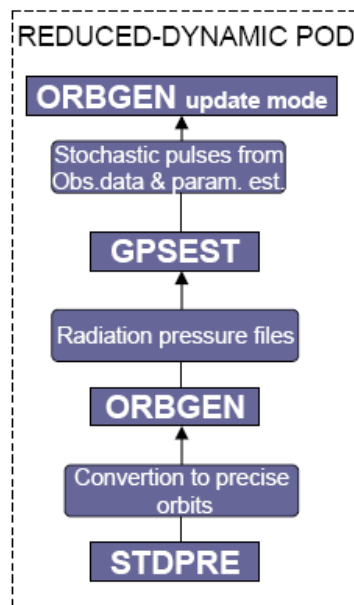


Figure 8-6 The Reduced-Dynamic approach in the orbit determination.

GPSEST

The actual orbit improvement has to be set up in program GPSEST. It is recommended using data spans shorter than one day. The main difference in this run of GPSEST compared with that of the pre processing is the use of the pseudo-stochastic orbit parameters pulses. They have to be set up for all three directions: radial, along-track, and out-of-plane. It is recommended for LEO POD to use around 6 min pulses in all three directions. If, however, the RMS in some of the directions, radial for instance, is remarkable worse, higher pulses frequencies may be added additional in the radial direction. It is important that the stochastic pulses epoch have to coincide with the integration interval boundary in ORBGEN.

8.3 Accelerometer – ACC

8.3.1 Introduction

The Level 1b instrument processing of the ACC is described in [AD13] and briefly repeated here. In case of discrepancies, this document shall take precedence.

8.3.2 Input and Output Parameters

| Inputs | | | | | |
|---------------------------------|---|--|--|-----------|-----------------------|
| Element | | Description | Unit | Range | |
| L e v e l 1 a | A C | a_{lin} | Acceleration in translation | eu | $0 - 2^{24}-1$ |
| | | a_{ang} | Acceleration in rotation | eu | $0 - 2^{24}-1$ |
| | C | p_{lin} | Translational position of proof mass | m | $\pm 10^{-5}$ |
| | | p_{ang} | Rotational position of proof mass | rad | $\pm 6 \cdot 10^{-4}$ |
| | T | Temperatures, vector of length 6 | °C | -50 – 100 | |
| | V_{pLTC1043} | LTC1043 positive voltage | V | 0 – 6 | |
| | V_{nLTC1043} | LTC1043 negative voltage | V | -6 – 0 | |
| | U_{pol} | Polarization voltage | V | 0 – 12 | |
| | Mode | Instrument mode | | 1 – 7 | |
| | ALSwitch | Angular/Linear switch | | 0, 1 | |
| | ADNR | Acceleration data not ready flags, 3x2 matrix | | 0, 1 | |
| | HDNR | Housekeeping data not ready flag | | 0, 1 | |
| | A O C S | Prop_HK | Cold gas system pressures | Bar | -30 – 60 |
| | | | Cold gas system temperatures | °C | |
| Accumulated thruster on-time | | | s | | |
| Mag_HK | | Magneto torquer currents telemetry | A | ± 20 | |
| Thru_HK | | Thruster firing telemetry | | | |
| Bus.State | Bus states – for heater switching | | | | |
| C C D B | S t r u c t u r e | ACC_r | Position of ACC sensor in S/C frame | m | ± 5 |
| | | ACC_q | Transformation of S/C to ACC sensor frames | | ± 1 |
| | SC_CoG | Parameters to calculate CoG of S/C | | | |
| | SC_Cross Section | Structure for estimating effective cross sections, 2-D look-up table as function of azimuth and elevation, providing outward normal vectors in S/C frame | | | |

| Inputs | | | | |
|-------------|---|--|-------------------------|----------------|
| Element | | Description | Unit | Range |
| A C C | SC_Mass | Parameters to calculate actual mass of S/C | | |
| | SC_RadP | Structure for estimating effective radiation properties, 2-D look-up table as function of azimuth and elevation, S/C frame | | |
| | SC_Uplift | Look-up table (1-D) for estimate of atmospheric up-drift depending on altitude | | |
| | Daa | ACC delay between angular acceleration measurement time and time stamp, vector | s | ± 1 |
| | Dla | ACC delay between linear acceleration measurement time and time stamp, vector | s | ± 1 |
| | t_C | Duration of ADC conversion | s | ± 1 |
| | t_AD | Delay of ADC analogue part and digital filter | s | ± 5 |
| | Aao | Bias of angular acceleration | rad/s ² | $\pm 10^{-2}$ |
| | Aaot | Angular acceleration bias as function of temperatures, vector | rad/s ² °C | $\pm 10^{-4}$ |
| | Aao_tab | Look-up table (LUT1d) of a priori biases of angular acceleration as function of time | rad/s ² | $\pm 10^{-3}$ |
| | Aas | Scale of angular acceleration | rad/s ² eu | $\pm 10^{-9}$ |
| | Aast | Angular acceleration scale as function of temperatures, vector | rad/s ² eu°C | $\pm 10^{-11}$ |
| | Aas_tab | Look-up table (LUT1d) of a priori scales of angular acceleration as function of time | rad/s ² eu | $\pm 10^{-10}$ |
| | Lao | Bias of linear acceleration | m/s ² | $\pm 10^{-4}$ |
| | Laot | Linear acceleration bias as function of temperatures, vector | m/s ² °C | $\pm 10^{-6}$ |
| | Lao_tab | Look-up table (LUT1d) of a priori biases of linear acceleration as function of time | m/s ² | $\pm 10^{-5}$ |
| | Las | Scale of linear acceleration | m/s ² eu | $\pm 10^{-11}$ |
| | Last | Linear acceleration scale as function of temperatures, vector | m/s ² eu°C | $\pm 10^{-13}$ |
| | Las_tab | Look-up table (LUT1d) of a priori scales of linear acceleration as function of time | m/s ² eu | $\pm 10^{-12}$ |
| | T ₀ | “Standard” temperature of ACC instrument | °C | 0 – 30 |
| N_Invalid | Numbers of neighbouring measurements to be flagged in cases of outliers | | 0 – 10 | |

| Inputs | | | | | |
|-------------------------------|---|---|---|---|--------|
| Element | | Description | Unit | Range | |
| | N_Invalid _{xxx} | | Numbers of neighbouring or subsequent measurements to be removed in cases of S/C events invalidating ACC measurements | 0 – 100 | |
| | L i m i t s | <i>Structure holding limits for outlier detection and/or rejection</i> | | | |
| | | Aa_lim | | Absolute limit of angular acceleration | eu |
| | | La_lim | | Absolute limit of linear acceleration | eu |
| | | T_Range | | Range of temperatures | °C |
| | | n _{sigma} | | σ-factor for detecting outliers | 1 – 10 |
| | | N _{window} | | Number of samples in outlier detection fits | 1 – 60 |
| | | degree | | Polynomial degree in outlier detection fits | 1 – 8 |
| | Thermi stor_ Weights | wT12 | Weight of temperature 1 wrt temperatur 2 | | 0 – 1 |
| | | wT34 | Weight of temperature 3 wrt temperatur 4 | | 0 – 1 |
| | | wT56 | Weight of temperature 5 wrt temperatur 6 | | 0 – 1 |
| | Apply Correc tion | Radiation Pressure | Flag indicating if solar radiation pressure estimate is subtracted from Level 1b data | | 0, 1 |
| | | Gravity Gradient | Flag indicating if gravity gradient estimate is subtracted from Level 1b data | | 0, 1 |
| | | Centri-fugal | Flag indicating if centrifugal acceleration estimate is subtracted from Level 1b data | | 0, 1 |
| | C o n s t a n t s | c | | Speed of light (=299,792,458 m/s) | m/s |
| GM _E | | Earth's gravitational constant (=3.986004418 10 ¹⁴ m ³ /s ²) | m ³ /s ² | | |
| P _{Sun} | | Mean radiation pressure of solar flux (~1366 W/m ²) | W/m ² | | |
| r _E | | Mean radius of Earth (~6.372·10 ⁶ m) | m | | |
| r | | Position of CoG, ITRF, at ACC time instants (cubic interpolation of Level 1b.Eph. r) | m | ±10 ⁷ | |
| v | | Velocity of CoG, ITRF, at ACC time instants (cubic interpolation of Level 1b.Eph. v) | m/s | ±10 ⁴ | |
| q _{ITRF←S/C} | | Attitude of S/C, S/C → ITRF transformation at ACC time instants | | ±1 | |
| q̇ _{ITRF←S/C} | | Time derivative of q _{ITRF←S/C} | s ⁻¹ | ±1 | |

| Outputs | | | | |
|---|--------------------------------------|--|------------------------|---------------------|
| Element | | Description | Unit | Range |
| L e v e l 1 b . A C C | t | Time, UTC | s | |
| | a | Pre-processed linear acceleration data ¹⁵ | m/s ² | ±10 ⁻⁴ |
| | a_{ang} | Pre-processed angular acceleration data | rad/s ² | ±10 ⁻² |
| | p | Position of proof mass within ACC cavity | m | ±10 ⁻⁵ |
| | p_{ang} | Angular position of proof mass within ACC cavity | rad | ±10 ⁻³ |
| | Temp | Vector of 6 temperatures of the ACC | °C | -50 – 100 |
| | V_{pLTC1043} | LTC1043 positive voltage | V | 0 – 6 |
| | V_{nLTC1043} | LTC1043 negative voltage | V | -6 – 0 |
| | U_{pol} | Polarization voltage | V | 0 – 12 |
| | a_{centr} | Centrifugal acceleration | m/s ² | ±10 ⁻⁷ |
| | a_{GG} | Gravity gradient acceleration | m/s ² | ±10 ⁻⁷ |
| | a_{Sun} | Acceleration due to Solar radiation pressure | m/s ² | ±10 ⁻⁷ |
| | e_{Sun} | Direction to the Sun, unit vector, S/C frame | | ±1 |
| | A_{Xxx} | Cross section normal vectors of the S/C, Xxx = head, down, left, right | m ² | 0 – 10 |
| | K_{Earth} | Normalized downwards reflectivity | m ² | ±0.1 |
| | m_{S/C} | Mass of S/C | kg | 300 – 500 |
| | r_{CoG} | Center of gravity, S/C frame | m | ±2 |
| | P_{Gas} | Pressure of gas tanks | Pa | 0 – 10 ⁷ |
| | T_{Gas} | Temperature of gas tanks | °C | -50 – 70 |
| | Thru_Acc_On | Accumulated thruster on time | s | 0 – 10 ⁵ |
| Flags_{ACC} | Flags related to the ACC measurement | | 0 – 2 ¹⁸ -1 | |
| Flags_{Platform} | Flags related to the S/C platform | | 0 – 63 | |

8.3.3 ACC Algorithms

8.3.3.1 Overview

The intrinsic ACC processing is described in [AD13], cf. Appendix L. The Level 1a data comprising the acceleration vectors (linear and rotational) in engineering units (eu) and the required house-keeping information (e.g. temperatures and polarization voltage) in physical units. The Level 1a data shall (optionally, i.e. user selectable) be stored as Level 1a Products.

The processing of Level 1a data to Level 1b ACC data is sketched in Figure 8-7 below.

¹⁵ All accelerations in Level 1b.ACC are provided in the S/C frame.

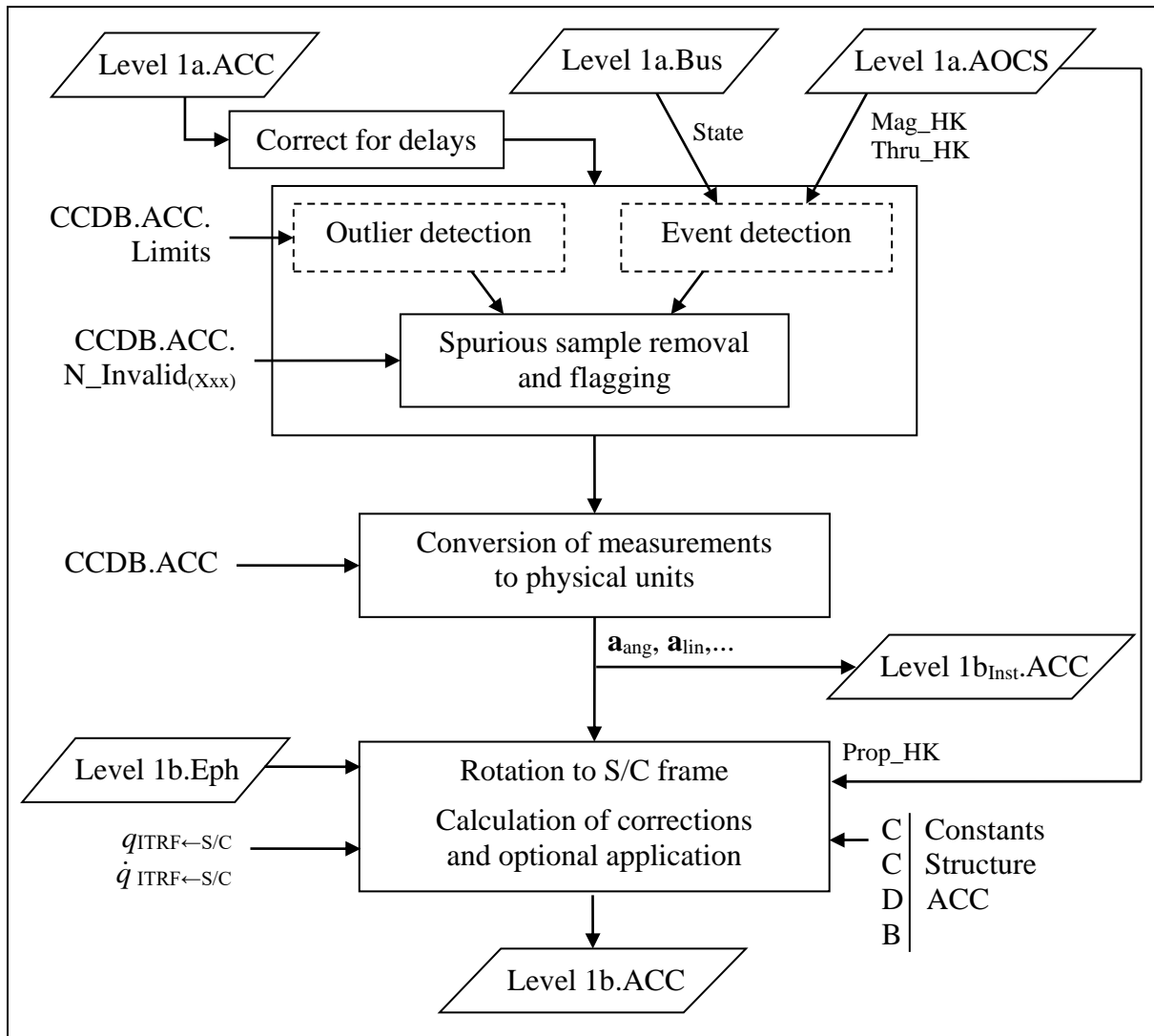


Figure 8-7 ACC Processing Overview

It consists of the following tasks:

- Correct for delays
- Identification of spurious samples, flag measurements accordingly
- Determine satellite events with possible impact on ACC measurements (e.g. thruster firing, magnetic torquer operation, heater switching) and flag ACC measurements accordingly
- Conversion of ACC measurements (and their linear estimates) from engineering units (eu) to physical units
- Rotation of accelerations from ACC frame to S/C frame
- Calculate and possibly (depending on processor configuration) apply correctional terms

8.3.3.2 Outlier and Event Detection

The ACC outlier detection is described in [AD13]. This method is to be applied to the accelerations and temperatures. Initially these quantities are checked to be within the corresponding CCDB.ACC.Limits values – the acceleration components shall be numerically less than the corresponding Aa_Lim and La_Lim values. Then, the (remaining) measurements are checked not to deviate significantly from linear prediction of the adjacent samples. The principle is to make N+1 linear fits of the N adjacent samples (excluding the target sample itself) and if $n \cdot \sigma_k \geq |x - x_{est,k}|$ for all k – for all N+1 linear fits – then the target sample is characterized as spurious. In this:

- N = CCDB.ACC.Limits.N_{window}
- n = CCDB.ACC.Limits.n_{sigma}
- k = index of linear fit, k = 0..N
- σ_k = sigma of linear fit k
- x = target sample (measurement)
- $x_{est,k}$ = estimate of linear fit k at target sample

In case a sample is detected as an outlier, additionally CCDB.ACC.N_invalid samples before and after are flagged

S/C events causing distortion of the ACC measurements are detected and the affected ACC samples plus a number of subsequent samples are flagged. The list of events is given in Table 8.3-1 below. The column “**Xxx**” is the CCDB.ACC.N_Invalid suffix, where N_Invalid_{xxx} is the number of subsequent samples to flag. Thruster activation is computed using the State_{Thruster} function described in Section 6.1.1, Eq. (6-1.16) using zero for the st (settling time) parameter.

| Description | Level 1a Source | Xxx | Comment |
|---------------------|-----------------|------|-----------------------------|
| Thruster activation | AOCS.Thru_HK | Thru | After activation has ceased |
| Heater switching | Bus.State | Heat | |

Table 8.3-1 S/C Events Affecting ACC Measurements

8.3.3.3 Conversion of Measurements to Physical Units

The calibration parameters of the ACC are applied to convert the acceleration measurements in engineering units to physical units. Both raw measurements as well as estimated values of the linear regressions are to be converted. The conversion is described in Section 6.3 of [AD13] with the modification that the temperatures are not weighted equally but using CCDB.Acc.Thermistor_Weights.wT12, wT34, and wT56 respectively such that

$$T_X = wT12 T_1 + (1-wT12) T_2 \tag{8.3-4}$$

$$T_Y = wT34 T_3 + (1-wT34) T_4 \tag{8.3-6}$$

$$T_Z = wT56 T_5 + (1-wT56) T_6 \tag{8.3-8}$$

T_X, T_Y, and T_Z are multiplied onto the respective components of CCDB.ACC.Laot and CCDB.ACC.Last. However, for the angular acceleration parameters, T_Y is multiplied onto

the x-components of CCDB.ACC.Aaot and CCDB.ACC.Aast, T_z onto the y-components, and T_x onto the z-components.

With respect to delays contained in CCDB.ACC.Daa (angular) and CCDB.ACC.Dla (linear), only the delay of the linear x-component is used, i.e. Dla₁. All measurements (including temperatures and voltages) are corrected using this delay, i.e. the common time-stamp is:

$$t_{out,ACC} = t_{0,ACC} + CCDB.ACC.t_C/2 - CCDB.ACC.t_AD - CCDB.ACC.Dla_1 \quad (8.3-10)$$

No interpolations (e.g. to account for differences in the delays) are performed.

8.3.3.4 Rotation to S/C Frame

The linear and angular accelerations (measured and estimated values) are rotated to the S/C frame by means of the CCDB.Structure.ACC_q:

$$\mathbf{a}_{lin,S/C} = CCDB.Structure.ACC_q^{-1} \times \mathbf{a}_{lin,ACC} \quad (8.3-12)$$

$$\mathbf{a}_{ang,S/C} = CCDB.Structure.ACC_q^{-1} \times \mathbf{a}_{ang,ACC} \quad (8.3-15)$$

where $\mathbf{a}_{...,ACC}$ are the accelerations in the ACC frame (from Level 1b_{Inst}) and $\mathbf{a}_{...,S/C}$ are the accelerations in the S/C frame (going to Level 1b).

8.3.3.5 Corrections and Cross Sections

The correctional terms of the accelerations are described next. Whether these are applied to the Level 1b acceleration data or not depends on the values of the CCDB.ACC.ApplyCorrection elements (see Eq. (8.3-120)). The actual state of these are noted in the Flags_{ACC}.

The corrections are as follows:

- Calculate bias due to centrifugal acceleration, for background information see [AD13].
 - Calculate the center of gravity in the S/C frame, \mathbf{r}_{CoG} , see Appendix E.
 - Calculate deviation of ACC proof mass position from center of gravity

$$\mathbf{r}' = CCDB.Structure.ACC_r - \mathbf{r}_{CoG} \quad (8.3-30)$$

- Calculate the angular velocity relative to Earth

$$\vec{\omega}_{S/C,ITRF} = \begin{pmatrix} \omega_x \\ \omega_y \\ \omega_z \end{pmatrix} = \begin{pmatrix} 2(\dot{q}_1 q_4 - \dot{q}_2 q_3 + \dot{q}_3 q_2 - \dot{q}_4 q_1) \\ 2(\dot{q}_2 q_4 - \dot{q}_3 q_1 + \dot{q}_1 q_3 - \dot{q}_4 q_2) \\ 2(\dot{q}_3 q_4 - \dot{q}_1 q_2 + \dot{q}_2 q_1 - \dot{q}_4 q_3) \end{pmatrix} \quad (8.3-40)$$

where \mathbf{q} and $\dot{\mathbf{q}}$ are $\mathbf{q}_{ITRF \leftarrow S/C}$ and $\dot{\mathbf{q}}_{ITRF \leftarrow S/C}$ respectively.

- Correct for angular velocity of Earth:

$$\vec{\omega} = \vec{\omega}_{S/C,ITRF} - \mathbf{q}_{ITRF \leftarrow S/C}^{-1} \times (0 \ 0 \ 2\pi/86400)^T \quad (8.3-45)$$

- Calculate centrifugal acceleration

$$\mathbf{a}_{centr} = -\vec{\omega} \times (\vec{\omega} \times \mathbf{r}') \quad (8.3-50)$$

- Calculate bias due to gravity gradient. For this, transformation via the local NEC frame is needed. \mathbf{a}_{GG} in S/C frame is computed follows, where \mathbf{r}' is the deviation of ACC proof mass position from center of gravity, cf. Eq. (8.3-30), \mathbf{r} is the position of

center of gravity in ITRF, and $\mathbf{q}_{\text{NEC} \leftarrow \text{ITRF}}$ is the quaternion representation of the $\mathbf{R}_{\text{NEC} \leftarrow \text{ITRF}}$ ITRF \rightarrow NEC(\mathbf{r}) transformation matrix, cf. Appendix C:

$$\mathbf{q}_{\text{NEC} \leftarrow \text{S/C}} = \mathbf{q}_{\text{ITRF} \leftarrow \text{S/C}} \otimes \mathbf{q}_{\text{NEC} \leftarrow \text{ITRF}} \quad (8.3-56)$$

$$\mathbf{r}'_{\text{NEC}} = \mathbf{q}_{\text{NEC} \leftarrow \text{S/C}} \times \mathbf{r}' \quad (8.3-58)$$

$$\mathbf{a}_{\text{GG}} = \frac{-\text{CCDB.Constants.GM}_E}{|\mathbf{r}|^3} \mathbf{q}_{\text{NEC} \leftarrow \text{S/C}}^{-1} \times \begin{pmatrix} \mathbf{r}'_{\text{NEC},x} \\ \mathbf{r}'_{\text{NEC},y} \\ -2\mathbf{r}'_{\text{NEC},z} \end{pmatrix} \quad (8.3-60)$$

- Calculate acceleration vector due to radiation pressure of solar flux.
 - Determine if the Sun is visible. Let $\mathbf{r}_{\text{Sun}} = \text{x1_sun}(t)$ (see [RD12]), then if $\mathbf{r} \cdot \mathbf{r}_{\text{Sun}} < 0$ and $|\mathbf{r} \times \mathbf{r}_{\text{Sun}}|/|\mathbf{r}_{\text{Sun}}| < \text{CCDB.Constants.r}_E$ the S/C is in the shadow of the Earth, and $\mathbf{a}_{\text{Sun}} = \mathbf{0}$. Otherwise proceed with the following steps.

- Determine the line of sight of the Sun in the S/C frame: let \mathbf{s} be the position of the Sun in the S/C frame (then $\mathbf{e}_{\text{Sun}} = \mathbf{s}/|\mathbf{s}|$, which is also stored in Level 1b.ACC):

$$\mathbf{s} = \mathbf{q}_{\text{ITRF} \leftarrow \text{S/C}}^{-1} \times (\mathbf{r}_{\text{Sun}} - \mathbf{r}) \quad (8.3-65)$$

- Determine the optical reflectivity properties for direction of incidence of solar radiation, θ and φ are obtained by converting \mathbf{s} to spherical coordinates:

$$\mathbf{K} = \text{Interpol}_{\text{lin}}(\text{CCDB.Structure.SC_RadP}, \theta, \varphi) \quad (8.3-70)$$

- Calculate the radiation pressure

$$\mathbf{FT} = \text{CCDB.Constants.P}_{\text{Sun}} \mathbf{K} / \text{CCDB.Constants.c} \quad (8.3-80)$$

- Calculate the mass of the spacecraft, Mass, (also stored in Level 1b.ACC): see Appendix E.

- Calculate acceleration vector due to radiation pressure

$$\mathbf{a}_{\text{Sun}} = \frac{\mathbf{FT}}{\text{Mass}} \quad (8.3-100)$$

- Calculate the downward reflectivity of the S/C:

$$\mathbf{K}_{\text{Earth}} = \text{Interpol}_{\text{lin}}(\text{CCDB.Structure.SC_RadP}, \theta_E, \varphi_E) \quad (8.3-102)$$

where θ_E and φ_E are the spherical coordinates of $\mathbf{r}_E = -\mathbf{q}_{\text{ITRF} \leftarrow \text{S/C}}^{-1} \times \mathbf{r}$.

The corrections calculated above are used to generate the Level 1b accelerations from the instrument Level 1b data, \mathbf{a} and \mathbf{a}_{ang} :

$$\text{Level 1b.ACC.}\mathbf{a} = \mathbf{a} - A_{\text{centr}} \mathbf{a}_{\text{centr}} - A_{\text{Sun}} \mathbf{a}_{\text{Sun}} - A_{\text{GG}} \mathbf{a}_{\text{GG}} \quad (8.3-120)$$

$$\text{Level 1b.ACC.}\mathbf{a}_{\text{ang}} = \mathbf{a}_{\text{ang}} \quad (8.3-130)$$

where A_{XXX} are the respective CCDB.ACC.ApplyCorrection flags (zero or one).

The cross sections of the S/C are provided as outward (from S/C) pointing normal vectors with lengths corresponding to projected surface areas. The vectors are calculated by linear interpolations in the CCDB.Structure.SC_CrossSection table. The interpolations are

performed for the angles (θ and φ) of the spherical representation of the following vectors (orbit frame):

$$\begin{aligned} \mathbf{Head} &= \mathbf{q}_{ITRF \leftarrow S/C}^{-1} \times \mathbf{v} \\ \mathbf{Left} &= \mathbf{q}_{ITRF \leftarrow S/C}^{-1} \times -(\mathbf{v} \times \mathbf{r}) \\ \mathbf{Right} &= \mathbf{q}_{ITRF \leftarrow S/C}^{-1} \times (\mathbf{v} \times \mathbf{r}) \\ \mathbf{Down} &= \mathbf{q}_{ITRF \leftarrow S/C}^{-1} \times (\mathbf{v} \times (\mathbf{v} \times \mathbf{r})) \end{aligned}$$

I.e.

$$\text{Level 1b.ACC.A}_w = \text{Interpol}_{\text{in}}(\text{SC_CrossSection}, \theta_w, \varphi_w) \quad (8.3-140)$$

where $w = \text{Head, Left, Right, Down}$, and $\text{Interpol}_{\text{in}}$ is given in Appendix E.

8.3.3.6 Flags

The flags of the Level 1b.ACC product are as listed below. The values of $\text{Flags}_{\text{ACC}}$ and $\text{Flags}_{\text{Platform}}$ are obtained by summing the values of all applicable conditions.

| Value | Condition |
|---------------------------------|---|
| Flags_{ACC} | |
| 1 | \mathbf{a}_{Sun} correction applied |
| 4 | \mathbf{a}_{GG} correction applied |
| 8 | $\mathbf{a}_{\text{centr}}$ correction applied |
| 16 | U_{Pol} detected as outlier |
| 64 | Temperature detected as outlier |
| 128 | Proof mass angular position (\mathbf{p}_{ang}) detected as outlier |
| 256 | Proof mass linear position (\mathbf{p}) detected as outlier |
| 512 | Angular acceleration (\mathbf{a}_{ang}) detected as outlier |
| 1024 | Linear acceleration (\mathbf{a}) detected as outlier |
| Flags_{Platform} | |
| 4 | Heater switching |
| 8 | Level 1a.Bus.State telemetry missing |
| 16 | Thruster firing |
| 32 | Level 1a.AOCS.Thru_HK telemetry missing |

Appendix A

Abbreviations and Acronyms

| | |
|-------|--|
| ACC | Accelerometer |
| ADC | Analogue to Digital Converter |
| AOCS | Attitude and Orbit Control System |
| ASM | Absolute Scalar Magnetometer |
| CCDB | Characterisation and Calibration Data Base |
| CHU | Camera Head Unit |
| CDC | Compact Detector Coil |
| CSC | Compact Spherical Coil |
| CRF | Common Reference Frame of the STR |
| DNSSC | Danish National Space Center |
| EADS | European Aeronautic Defence and Space |
| EESS | End-to-End System Simulator |
| EFI | Electric Field Instrument |
| ESA | European Space Agency |
| eu | engineering unit |
| GNSS | Global Navigation Satellite System |
| GPS | Global Positioning System |
| GPSR | GPS/GNSS Receiver |
| ICRF | International Celestial Reference Frame |
| IMDD | Instrument Measurement Data Definition |
| ISP | Instrument Source Packet |
| ITRF | International Terrestrial Reference Frame |
| NEC | North-East-Centre reference frame |
| N/A | Not Applicable |
| PPS | Pulse Per Second |
| S/C | Spacecraft |
| SRD | System Requirements Document |
| STR | Star Tracker |
| TBC | To Be Confirmed |
| TBD | To Be Defined |
| UTC | Universal Time Coordinated |
| VFM | Vector Field Magnetometer |

Appendix B

Quaternions

A quaternion is a 4 dimensional hyper complex number. In this document, we use normalized quaternions to describe rotations. A rotation θ (degrees) around a unit vector \mathbf{e} is described by the quaternion:

$$\mathbf{q} = (e_x \sin(\theta/2), e_y \sin(\theta/2), e_z \sin(\theta/2), \cos(\theta/2)) \quad (\text{B-10})$$

Example: the 30° rotation around the vector $\mathbf{e} = (1/\sqrt{2}, 1/\sqrt{2}, 0)$ is depicted in Figure B - 1 as the rotation of the blue frame A into the red frame B – \mathbf{z}_B is tilted out of the \mathbf{y}_A - \mathbf{z}_A frame towards the reader. This rotation is given by the quaternion $\mathbf{q}_{B \leftarrow A} = (\sin(30^\circ/2)/\sqrt{2}, \sin(30^\circ/2)/\sqrt{2}, 0, \cos(30^\circ/2)) \approx (0.183, 0.183, 0, 0.966)$.

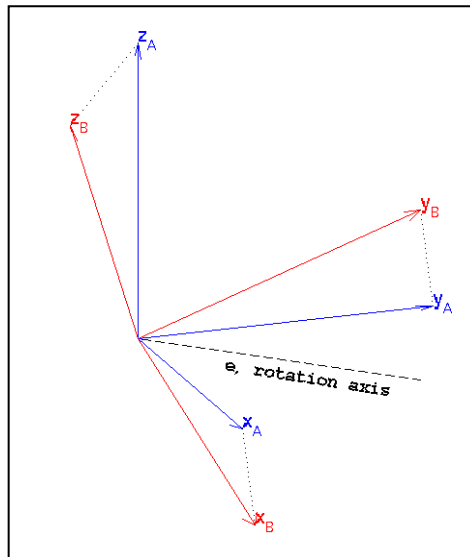


Figure B - 1 A 30° Rotation

To transform the representation of a vector, \mathbf{v} , from frame A to frame B, calculate Eq. (B-20) and extract the first three components (the fourth component is 0):

$$\mathbf{v}^B = (\mathbf{q}_{B \leftarrow A}^* \otimes (v_x^A, v_y^A, v_z^A, 0) \otimes \mathbf{q}_{B \leftarrow A})_{1..3} \quad (\text{B-20})$$

where

$$\mathbf{q}^* \equiv \mathbf{q}^{-1} = (-q_1, -q_2, -q_3, q_4) \quad (\text{B-30})$$

The multiplication (\otimes) of quaternions is most elegantly written using the “complex” form of quaternions:

$$\mathbf{q} = q_1 \mathbf{i} + q_2 \mathbf{j} + q_3 \mathbf{k} + q_4 \quad (\text{B-40})$$

where $\mathbf{i}, \mathbf{j}, \mathbf{k}$ are the “complex” unit vectors such that:

$$\mathbf{i}^2 = \mathbf{j}^2 = \mathbf{k}^2 = \mathbf{ijk} = -1 \quad (\text{B-50})$$

$$\mathbf{ij} = -\mathbf{ji} = \mathbf{k} \quad (\text{B-60})$$

The full formula for multiplication is given by:

$$\mathbf{p} \otimes \mathbf{q} = \begin{pmatrix} p_1 q_4 + p_2 q_3 - p_3 q_2 + p_4 q_1 \\ -p_1 q_3 + p_2 q_4 + p_3 q_1 + p_4 q_2 \\ p_1 q_2 - p_2 q_1 + p_3 q_4 + p_4 q_3 \\ -p_1 q_1 - p_2 q_2 - p_3 q_3 + p_4 q_4 \end{pmatrix}^T \quad -\mathbf{ji} = \mathbf{k} \quad (\text{B-70})$$

In the example of Figure B - 1 the transformation of the vector (0, 0, 1) from frame A to frame B would yield: $\approx (-0.354, 0.354, 0.866)$.

A more detailed description including transformations between quaternions and rotation matrices (*direction cosines*) is given in Section 5.4 of [AD10]. See also [RD5].

Appendix C

Reference Frames

C.1 Definitions

The table below summarises the definitions of the relevant Swarm reference frames.

| Name | Origin | Orientation | Description |
|-------------|---------------------------------|--|--|
| ACC | ACC sensor | TBD | ACC sensor frame |
| ASM | ASM sensor | X along boom axis (forward) Y along S/C Y Z downwards (tilted) | ASM sensor frame |
| CRF | VFM sensor | Aligned with S/C axes, but fixed w.r.t. optical bench | Common reference frame of the STR. See Section C.2 below |
| GPSR | GPSR antenna reference center | TBD | Reference frame for the GPSR |
| ICRF | Barycenter of Solar System | | Inertial, International Celestial reference frame |
| ITRF | Center of Earth | X along Greenwich meridian Y along 90° E meridian Z towards North pole | International Terrestrial reference frame |
| NEC | Reference position | N towards North E towards East C towards center of Earth | Local North-East-Center reference frame, position dependent. See Section C.3 |
| S/C | Bottom center of face-plate | X nominal flight direction Y sideways (“right”) Z downwards (nadir) | S/C reference frame |
| S T R | Center of corresponding CHU CCD | Z along boresight of CCD X and Y along CCD axes | Reference frames of the three STR CHUs |
| TIIH | Centers of TII H and V sensors | TBD | TII H-sensor frame |
| TIIV | | TBD | TII V-sensor frame |
| VFM | VFM sensor | Z along boom axis (backwards) Y along S/C Y X downwards (tilted) | VFM sensor frame |

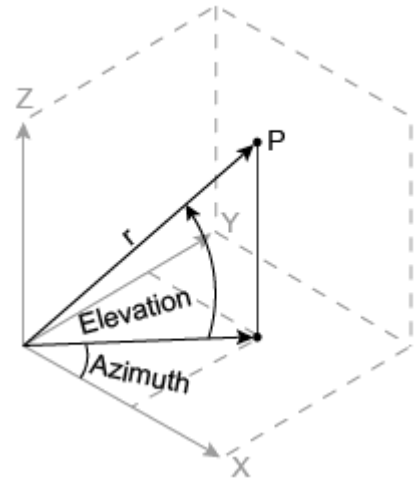
Spherical coordinates

Spherical coordinates are given as radius (r), elevation (θ), and azimuth (φ) as depicted in the figure on the right. The quantities may be computed as:

$$r = \sqrt{x^2 + y^2 + z^2}$$

$$\theta = \text{atan2}(z, \sqrt{x^2 + y^2})$$

$$\varphi = \text{atan2}(y, x)$$



C.2 STR Common Reference Frame (CRF)

The common reference frame of the STR is fixed w.r.t. the optical bench with origin at the center of the VFM sensor and oriented in the general direction of the S/C frame, i.e. CRF_x is in the general flight direction, CRF_z is in the general nadir direction, and CRF_y forms a right handed system.

C.3 North East Center (NEC)

The NEC frame is defined in Section 3.7.2.3 of Swarm System Requirements Document, [SW-RS-ESA-SY-001]. At position \mathbf{r} , the NEC frame unit vectors are:

$$\mathbf{e}_{\text{center}} = -\mathbf{r} / |\mathbf{r}| \quad (\text{C-10})$$

$$\mathbf{e}_{\text{east}} = \begin{cases} \mathbf{a} / |\mathbf{a}|, \mathbf{a} = \mathbf{e}_{\text{center}} \times (0 \ 0 \ 1)^T \\ (0 \ 1 \ 0)^T, \text{ if } |\mathbf{a}| = 0 \end{cases} \quad (\text{C-20})$$

$$\mathbf{e}_{\text{north}} = \mathbf{e}_{\text{east}} \times \mathbf{e}_{\text{center}} \quad (\text{C-30})$$

Hence, the rotation matrix, $\mathbf{R}_{\text{NEC} \leftarrow \text{ITRF}}$, is (with \mathbf{r} given in ITRF):

$$\mathbf{R}_{\text{NEC} \leftarrow \text{ITRF}} = \begin{pmatrix} \mathbf{e}_{\text{north}} \\ \mathbf{e}_{\text{east}} \\ \mathbf{e}_{\text{center}} \end{pmatrix} \quad (\text{C-40})$$

Appendix D

B-Splines

A polynomial spline is a piecewise polynomial function. In its most general form a polynomial spline, $S: [a,b] \rightarrow \mathfrak{R}$, consists of polynomial pieces $PP_i: [t_i, t_{i+1}] \rightarrow \mathfrak{R}$, where $a = t_0 < t_1 < t_2 < \dots < t_{k-1} < t_k = b$. I.e. $S(t) = PP_i(t)$ for $t_i \leq t < t_{i+1}$, $i = 0 \dots k-1$. The given $k+1$ points t_i are called knots.

A B-spline of degree n is composed of basis B-splines, $b_{i,n}$, of degree n :

$$S(t) = \sum_{i=0}^{k-n-1} P_i b_{i,n}(t), t \in [t_0, t_k] \quad (D-10)$$

The P_i are called *control points* or *de Boor points*. The $m-n$ basis B-splines of degree n can be defined using the *Cox-de Boor recursion formula*

$$b_{i,0}(t) = \begin{cases} 1 & \text{if } t_i \leq t < t_{i+1} \\ 0 & \text{otherwise} \end{cases} \quad (D-20)$$

$$b_{i,j}(t) = \frac{t - t_i}{t_{i+j} - t_i} b_{i,j-1}(t) + \frac{t_{i+j+1} - t}{t_{i+j+1} - t_{i+1}} b_{i+1,j-1}(t) \quad (D-30)$$

Cubic B-splines with uniform knot-vector is the most commonly used form of B-spline. The *blending* function can easily be precalculated, and is equal for each segment in this case. Put in matrix-form, it is:

$$S_i(t) = \begin{pmatrix} t^3 & t^2 & t & 1 \end{pmatrix} \begin{pmatrix} -1 & 3 & -3 & 1 \\ 3 & -6 & 3 & 0 \\ 3 & 0 & 3 & 0 \\ 1 & 4 & 1 & 0 \end{pmatrix} \begin{pmatrix} P_{i-1} \\ P_i \\ P_{i+1} \\ P_{i+2} \end{pmatrix} \quad (D-40)$$

Note though, this is not globally the case for the application here due to reduction of edge effects and potential gaps in the time series (see Section **Knots** below), hence the middle matrix of Eq. (D-40) must be computed from the preceding formulas directly.

8.3.3.7 Derivative

The derivative of a degree n B-spline, $dS(t)/dt$, is a degree $n-1$ B-spline. Let P'_i be the control points of $dS(t)/dt$, then:

$$P'_i = \frac{n(P_i - P_{i-1})}{t_{i+n} - t_i} \quad (D-50)$$

where $P_{-1} = P_{k-n} \equiv 0$.

8.3.3.8 Knots

The knots for the cubic B-splines are constructed in a special way to avoid oscillation effects near the end points of the data segment. The interior knots are equidistantly spaced according to the given *Knot_Space* parameter except at the ends where up to three additional knots are inserted (in either end) using the method specified below. Three external knots on either side

of the data segment are also used. In the event of gaps in the data segment, some knots may need to be removed; the algorithm for this is given at the end of this section.

The regular (no gaps) knot sequence is defined as follows. Let:

| | |
|---|--|
| ks | Given knot spacing |
| t_0, \dots, t_{n-1} | Time-instants of data samples |
| T | Nominal sampling rate (typical value of $t_{i+1} - t_i$) |
| $k_{-4}, k_{-3}, \dots, k_{m+2}, k_{m+3}$ | Time-instants of knots – k_0, \dots, k_{m-1} are the interior knots, i.e. $k_{-1} < t_0 < k_0$ and $k_{m-1} < t_{n-1} < k_m$. |
| k_0' | First, “regular” interior knot offset before insertion of extra knots. $k_0' = \text{mod}(t_{n-1} - t_0, ks)/2$ |
| x' | Number of additional, interior knots (to add in both ends): 0 if $ks < 1.5 T$ 1 if $1.5 T \leq ks < 1.8 T$ 2 if $1.8 T \leq ks < 2.75 T$ 3 otherwise Though limited such that $x' \leq (n-5)/2$. |
| x | Number of initial, non-equidistant knots: $x = \left\lfloor \frac{x' ks - k_0' + T/2}{ks - T} \right\rfloor + 1$ |
| Δks | Increase in knot spacing between x initial knots. $\Delta ks = 2 \frac{k_0' + (x - x')ks + T/2 - (x + 1)T}{x(x + 1)}$ |

Then the knots are given by:

| k_i | for... |
|--|--|
| $t_0 + T/2 + i T$ | $i = -4, -3, -2, -1, 0$ and $i < m-1$ |
| $(t_0 + t_{n-1})/2$ | $i = 0$, iff $m = 1$ |
| $k_{i-1} + T + i \Delta ks$ | $i = 1, 2, \dots, x-1$ and $k_i \leq (t_0 + t_{n-1})/2$ |
| $k_{i-1} + ks \{= t_0 + k_0' + (i-x')ks\}$ | $i = x, x+1, \dots, m-x-1$ |
| $k_{i+1} - T - (m - i - 1) \Delta ks$ | $i = m-2, m-3, \dots, m-x$ and $k_i > (t_0 + t_{n-1})/2$ |
| $t_{n-1} + T/2 + (i - m) T$ | $i = m-1, m, m+1, m+2, m+3$ and $i > 0$ |

Knots failing the conditions marked in blue are discarded from the knot sequence, i.e. the knot sequence is shortened. This only happens for very short time segments ($t_{n-1} - t_0$ is small).

If there are gaps in the data sequence, some knots may need to be removed since there can be no more than 3 knots between data points and there can be no more than 3 more knots than data points to the left or right of any point on the time-line. This is ensured by the following

algorithm where i is the index of t ($i = 0 \dots n-1$) and j is the index of k , $j = -3, -2, \dots, m+2$ (note: $t_{n-1} < k_{m+2}$):

```

lead = 0
i = 0
j = -3
j0 = j
while((i < n) and (j < m+3))
    if(ti > kj)
        j = j + 1
        lead = lead + 1
    else
        if(lead > 4)
            % There are lead-4 knots too many.
            Replace the knots kj0, ..., kj-1 by p=(j-j0-lead+4) new knots
            computed as the means of kj0, ..., kj-1 divided in p parts
            (if p=3 and mod(j-j0,3)=1 make middle section of k's one
            larger, if mod(j-j0,3)=2 make outer sections one larger)
            lead = 3
        elseif(lead > 0)
            % lead can not be negative
            lead = lead - 1
        endif
        j0 = j
        i = i+1
    endif
endwhile
if(lead + m + 3 - j > 4)
    Repeat the above backwards,
    i.e. start with i = n-1 and j = m+2 and count these downwards
    if(lead > 0) by the end of the while-loop
    remove ceil(lead/2) exterior knots from both ends
endif
endif

```

8.3.3.9 Collocation Matrix

The cubic B-splines used in this document are estimated by construction of collocation matrices via the `spsc01` MATLAB function listed on the following pages.

8.3.3.10 Damping of Second Derivatives (Acceleration)

The matrix for the second derivative damping, Λ , is using equidistant time-instants (t_{acc}) at $1/5$ of the regular knot-spacing though at least the nominal sampling period, i.e. $dt_{acc} = \max(ks/5, T)$. t_{acc} is centered in the data interval $t_0 \dots t_{n-1}$, i.e. $t_{acc0} = t_0 + dt_{acc}$, where $dt_{acc} = \text{mod}(t_{n-1} - t_0, dt_{acc})/2$, and $t_{acc_i} = t_{acc0} + i * dt_{acc}$. If dt_{acc} is smaller than $1/4$ of the nominal sampling rate, dt_{acc} is increased by $dt_{acc}/2$. Now the second differences of the rows of the collocation matrix, `spscol(knots, sp_order, t_acc)`, are divided by dt_{acc}^2 , weighted, and squared to produce Λ . The weights are all one except near the edges where they decay slowly to zero over a period, denoted width, of 90 (nominal) samples. If the total period of $t_0 \dots t_{n-1}$ is less than $180 T + 2 dt_{acc}$, width is reduced to $(t_{n-1} - t_0)/2 - dt_{acc}$. The weights, w_{ii} , are computed as follows with $width_{max} = 90 * T$.

| w_{ii} | for ... |
|---|----------------------------------|
| $(\frac{1}{2} - \cos(\pi * (t_{acc_i} - t_0)/width)/2) * width/width_{max}$ | $t_{acc_i} \leq t_0 + width$ |
| $(\frac{1}{2} - \cos(\pi * (t_{n-1} - t_{acc_i})/width)/2) * width/width_{max}$ | $t_{acc_i} \geq t_{n-1} - width$ |
| 1 | otherwise |

The complete calculation within MATLAB is as follows:

```

dt_acc = max(ks/5, T);
dt0_acc = mod(t(end) - t(1), dt_acc)/2;
if(dt0_acc < T/4)
    dt0_acc = dt0_acc + dt_acc/2;
end
t_acc = (t(1) + dt0_acc : dt_acc : t(end))';
if(numel(t_acc) > 2) % To be absolutely safe
    Gacc = diff(spcol(knots, sp_order, t_acc, 'sparse'), 2, 1) / dt_acc^2;
    width_max = 90 * T;
    width = min((t(end) - t(1))/2, width_max);
    t_acc([1 end]) = [];
    w_slow = (1 - cos(pi*(t_acc(t_acc <= t(1) + width) - t(1))/width))/2 *
        width / width_max;
    W = spdiags([w_slow; ...
        ones(size(Gacc,1) - 2*numel(w_slow), 1); ...
        w_slow(1^6min(size(Gacc,1)-end,end):-1:1)], ...
        0, size(Gacc,1), size(Gacc,1))
    Lambda = Gacc' * W * Gacc;
else
    Lambda = 0;
end

```

¹⁶ "min" function to safeguard against $size(Gacc,1) < 2 * numel(w_slow)$

```

function colloc = spcol(knots,k,tau,varargin)
%SPCOL B-spline collocation matrix.
%
% COLLOC = SPCOL(KNOTS,K,TAU) is the matrix
%
% [ D^m(i)B_j(TAU(i)) : i=1:length(TAU), j=1:length(KNOTS)-K ] ,
%
% with D^m(i)B_j the m(i)-fold derivative of B_j,
% B_j the j-th B-spline of order K for the knot sequence KNOTS,
% TAU a sequence of sites,
% both KNOTS and TAU are assumed to be nondecreasing, and
% m(i) is the integer #{ j<i : TAU(j) = TAU(i) }, i.e., the 'cumulative'
% multiplicity of TAU(i) in TAU.
%
% This means that the j-th column of COLLOC contains values and, perhaps,
% derivatives, at all the entries of the vector TAU, of the j-th
% B-spline of order K for the sequence KNOTS, i.e., the B-spline
% with knots KNOTS(j:j+K).
% The i-th row of COLLOC contains the value at TAU(i) of the m(i)-th
% derivative of all these B-splines, with m(i) the number of earlier
% entries of TAU that equal TAU(i) .
%
% Example:
% tau = [0,0,0,1,1,2]; % therefore, m equals [0,1,2,0,1,0]
% k = 3; knots = augknt(0:2,k); % therefore, knots equals [0,0,0,1,2,2,2]
% colloc = spcol(knots,k,tau)
%
% has the 6 entries of COLLOC(:,j) contain the value, first, and second
% derivative of B_j at 0, then the value and first derivative of B_j
% at 1, and, finally, the value of B_j at 2, with B_j the j-th B-spline of
% order k for the knot sequence knots; e.g., B_2 is the B-spline with
% knots 0,0,1,2.
%
% You can use COLLOC to construct splines with prescribed values and,
% perhaps, also some derivatives, at prescribed sites.
%
% Example:
% a = -pi; b = pi; tau = [a a a 0 b b]; k = 5;
% knots = augknt([a,0,b],k);
% sp = spmak(knots, ( spcol(knots,k,tau) \ ...
% [sin(a);cos(a);-sin(a);sin(0);sin(b);cos(b)] ) .') )
%
% provides the quartic spline, on the interval [a,b] with just one interior
% knot, at 0, that interpolates the sine function at a,0,b, but also matches
% its first and second derivative at a, and its first derivative at b .
%
% COLLOC = SPCOL(KNOTS,K,TAU,ARG1,ARG2,...) provides the same or a related
% matrix, depending on the optional arguments ARG1, ARG2, ... .
%
% If one of the optional arguments is 'slvblk', then COLLOC is in the al-
% most block-diagonal format (specialized for splines) required by SLVBLK.
%
% If one of the optional arguments is 'sparse', then COLLOC is a sparse
% matrix.
%
% If one of the optional arguments is 'noderiv', then multiplicities are
% ignored, i.e., m(i) = 0 for all i.
%
% The B-spline recurrence relations are used to generate the entries of the
% matrix.
%
% Example:
% t = [0,1,1,3,4,6,6,6]; x = linspace(t(1),t(end),101);
% c = spcol(t,3,x); plot(x,c)
%
% uses SPCOL to generate, in c(:,j), a fine sequence of values of the
% j-th quadratic B-spline for the given knot sequence t.

```



```

%
% See also SLVBLK, SPARSE, SPAPI, SPAP2, BSPLINE.

% Copyright 1987-2003 C. de Boor and The MathWorks, Inc.
% $Revision: 1.21 $

if ~isempty(find(diff(knots)<0))
    error('SPLINES:SPCOL:knotsdecreasing',...
        'The knot sequence KNOTS should be nondecreasing.')
end
if ~isempty(find(diff(tau)<0))
    error('SPLINES:SPCOL:TAUdecreasing', ...
        'The point sequence TAU should be nondecreasing.')
end

% Compute the number n of B-splines of order K supported by the given
% knot sequence and return an empty matrix in case there aren't any.

npk=length(knots); n=npk-k;
if n<1, warning('SPLINES:SPCOL:noBsplines', ...
    'There are no B-splines for the given input.')
    colloc = zeros(length(tau),0); return
end

% Settle the options:
slvblk=0; noderiv=0;
for j=4:nargin
    argj = varargin{j-3};
    if ~isempty(argj)
        if ischar(argj)
            if argj(1)=='s', slvblk=1;
                if length(argj)>1, if argj(2)=='p', slvblk=2; end, end
            elseif argj(1)=='n', noderiv=1;
                else error('SPLINES:SPCOL:wronginarg2',...
                    ['The second optional argument should be 'sl', ',...
                    ''sp'', 'n'', or a number.'])
            end
        else
            switch j % for backward compatibility
                case 4, slvblk=1;
                case 5, noderiv=1;
            end
        end
    end
end

% If NODERIV==0, remove all multiplicities from TAU and generate repetitions
% of rows instead of rows containing values of successive derivatives.
nrows = length(tau); tau = reshape(tau,1,nrows);
if noderiv
    index = 1:nrows; m = ones(1,nrows); nd = 1; pts = tau;
else
    index = [1 find(diff(tau)>0)+1];
    m = diff([index nrows+1]); nd = max(m);
    if nd>k
        error('SPLINES:SPCOL:multtoohigh',...
            'Point multiplicity should not exceed the given order %g.',k);
    end
    pts = tau(index);
end

%set some abbreviations
kml = k-1;

% augment knot sequence to provide a K-fold knot at each end, in order to avoid
% struggles near ends of basic interval, [KNOTS(1) .. KNOTS(npk)] .
% The resulting additional B-splines, if any, will NOT appear in the output.

```

```

[augknot,addl] = augknt(knots,k); naug = length(augknot)-k;
pts = pts(:); augknot = augknot(:);

% For each i , determine savl(i) so that K <= savl(i) < naug+1 , and,
% within that restriction,
%     augknot(savl(i)) <= pts(i) < augknot(savl(i)+1) .

savl = max(sorted(augknot(1:naug),pts), k);

b = zeros(nrows,k);

% first do those without derivatives
index1 = find(m==1);
if ~isempty(index1)
    pt1s = pts(index1); savls = savl(index1); lpt1 = length(index1);
    % initialize the b array.
    lpt1s = index(index1); b(lpt1s,1) = ones(lpt1,1);

    % run the recurrence simultaneously for all pt1(i) .
    for j=1:kml
        saved = zeros(lpt1,1);
        for r=1:j
            tr = augknot(savls+r)-pt1s;
            tl = pt1s-augknot(savls+r-j);
            term = b(lpt1s,r)./(tr+tl);
            b(lpt1s,r) = saved+tr.*term;
            saved = tl.*term;
        end
        b(lpt1s,j+1) = saved;
    end
end

% then do those with derivatives, if any:
if nd>1
    indexm=find(m>1);ptss=pts(indexm);savls=savl(indexm);lpts=length(indexm);
    % initialize the bb array.
    %temp = [1 zeros(1,kml)]; bb = temp(ones(nd*lpts,1),:);
    bb = repmat([1 zeros(1,kml)],nd*lpts,1);
    lptss = nd*[1:lpts];

    % run the recurrence simultaneously for all pts(i) .
    % First, bring it up to the intended level:
    for j=1:k-nd
        saved = zeros(lpts,1);
        for r=1:j
            tr = augknot(savls+r)-ptss;
            tl = ptss-augknot(savls+r-j);
            term = bb(lptss,r)./(tr+tl);
            bb(lptss,r) = saved+tr.*term;
            saved = tl.*term;
        end
        bb(lptss,j+1) = saved;
    end

    % save the B-spline values in successive blocks in bb .

    for jj=1:nd-1
        j = k-nd+jj; saved = zeros(lpts,1); lptsn = lptss-1;
        for r=1:j
            tr = augknot(savls+r)-ptss;
            tl = ptss-augknot(savls+r-j);
            term = bb(lptss,r)./(tr+tl);
            bb(lptsn,r) = saved+tr.*term;
            saved = tl.*term;
        end
        bb(lptsn,j+1) = saved; lptss = lptsn;
    end
end

```

```

end

% now use the fact that derivative values can be obtained by differencing:

for jj=nd-1:-1:1
    j = k-jj;
    temp = repmat([jj:nd-1].',1,lpts)+repmat(lptsn,nd-jj,1); lptss=temp(:);
    for r=j:-1:1
        temp = repmat((augknot(savls+r)-augknot(savls+r-j)).'/j,nd-jj,1);
        bb(lptss,r) = -bb(lptss,r)./temp(:);
        bb(lptss,r+1) = bb(lptss,r+1) - bb(lptss,r);
    end
end

% finally, combine appropriately with b by interspersing the multiple
% point conditions appropriately:
dtau = diff([tau(1)-1 tau(:).', tau(nrows)+1]);
index=find(min(dtau(2:nrows+1),dtau(1:nrows))==0); % Determines all rows
% involving multiple tau.
dtau=diff(tau(index));index2=find(dtau>0)+1; % We need to make sure to
index3=[1 (dtau==0)]; % skip unwanted derivs:
if ~isempty(index2)
    index3(index2)=1+nd-m(indexm(1:length(indexm)-1));end
b(index,:)=bb(cumsum(index3),:);

% ... and appropriately enlarge savl
index = cumsum([1 (diff(tau)>0)]);
savl = savl(index);
end

% Finally, zero out all rows of b corresponding to TAU outside the basic
% interval, [knots(1) .. knots(npk)] .

index = find(tau<knots(1)|tau>knots(npk));
if ~isempty(index)
    b(index,:) = 0;
end

% The first B-spline of interest begins at KNOTS(1), i.e., at augknot(1+addl)
% (since augknot's first knot has exact multiplicity K). If addl<0 ,
% this refers to a nonexistent index and means that the first -addl columns
% of the collocation matrix should be trivial. This we manage by setting
savl = savl+max(0,-addl);

if slvblk % return the collocation matrix in almost block diagonal form.
    % For this, make the blocks out of the entries with the same
    % SAVL(i) , with LAST computed from the differences.
    % There are two issues, the change in the B-splines considered because of
    % the use of AUGKNOT instead of KNOTS , and the possible drop of B-splines
    % because the extreme TAU fail to involve the extreme knot intervals.

    % SAVL(j) is the index in AUGKNOT of the left knot for TAU(j) , hence the
    % corresponding row involves B-splines to index savl(j) wrto augknot, i.e.,
    % B-splines to index savl(j)-addl wrto KNOTS.
    % Those with negative index are removed by cutting out their columns (i.e.,
    % shifting appropriately the blocks in which they lie). Those with index
    % greater than n will be ignored because of last .

    last0 = max(0,savl(1)-max(0,addl)-k); % number of cols in trivial first block
    if addl>0 % if B-splines were added on the left, remove them now:
        width = km1+k;cc = zeros(nrows*width,1);
        index = min(k,savl-addl);
        temp = +repmat(nrows*[0:km1],nrows,1);
        cc(repmat([1-nrows:0]+nrows*index).',1,k)+repmat(nrows*[0:km1],nrows,1)=b;
        b(:)=cc(repmat([1-nrows:0].',1,k)+repmat(nrows*(k+[0:km1]),nrows,1));
        savl=savl+k-index;
    end
end

```

```

ds=(diff(sav1));
index=[0 find(ds>0) nrows];
rows=diff(index);
nb=length(index)-1;
last=ds(index(2:nb));
if addl<0 nb=nb+1; rows=[0 rows]; last=[last0 last]; end
if slvblk==1
    colloc=[1 nb rows k last n-sum(last) b(:).'];
else % return the equivalent sparse matrix (cf BKBRK)
    nr = (1:nrows).'; nc = 1:k; nrnc = nrows*k;
    ncc = zeros(1,nrows); ncc(1+cumsum(rows(1:(nb-1)))) = last;
    ncc(1) = last0; ncc = reshape(cumsum(ncc),nrows,1);
    ijs = [reshape(repmat(nr,1,k),nrnc,1), ...
           reshape(repmat(ncc,1,k)+repmat(nc,nrows,1), nrnc,1), ...
           reshape(b,nrnc,1)];
    index = find(ijs(:,2)>n);
    if ~isempty(index), ijs(index,:) = []; end
    colloc = sparse(ijs(:,1),ijs(:,2),ijs(:,3),nrows,n);
end
else % return the collocation matrix in standard matrix form
    width = max([n,naug])+kml+kml;
    cc = zeros(nrows*width,1);
    cc(repmat([1-nrows:0].',1,k)+ ...
        repmat(nrows*sav1.',1,k)+repmat(nrows*[-kml:0],nrows,1))=b;
    % (This uses the fact that, for a column vector v and a matrix A ,
    % v(A(i,j))=v(A(i,j)), all i,j.)
    colloc = reshape(cc(repmat([1-nrows:0].',1,n) + ...
        repmat(nrows*(max(0,addl)+[1:n]),nrows,1)), nrows,n);
end

```

Appendix E

Miscellaneous Functions

This Appendix contains the description of some miscellaneous functions.

E.1 Table Look-Up Function, $\text{Interpol}_{\text{Lin}}$

The linear interpolation function, $\text{Interpol}_{\text{Lin}}$, is defined in the following for one and two dimensions. It uses the LUT1d and LUT2d look-up tables defined in [AD03]:

| <i>Id</i> | <i>Name</i> | <i>Type</i> | <i>Description</i> |
|-----------|--------------------------------------|------------------|--------------------------------|
| LUT1d | <i>One-dimensional look-up table</i> | | |
| | m | integer | Number of entries in x and v. |
| | x | vector, length m | Nodes (keys) |
| | v | vector, length m | Function values |
| LUT2d | <i>Two-dimensional look-up table</i> | | |
| | n | integer | Number of entries in y and lut |
| | y | vector, length n | Nodes (keys) |
| | Lut | vector, length n | 1-d look-up tables |

Now:

$$\text{Interpol}_{\text{Lin}}(\text{T1}, x') = v_i + \frac{x' - x_i}{x_{i+1} - x_i} (v_{i+1} - v_i) \quad (\text{E-10})$$

where

- T1 is of type LUT1d
- x' is the key-value for the look-up
- x and v are elements (vectors) of T1
- i is the index such that $x_i \leq x' \leq x_{i+1}$, it is an error if i does not exist

The two dimensional case is very similar:

$$\text{Interpol}_{\text{Lin}}(\text{T2}, x', y') = F_i + \frac{y' - y_i}{y_{i+1} - y_i} (F_{i+1} - F_i) \quad (\text{E-20})$$

where

- T2 is of type LUT2d
- x' and y' are the key-values for the look-up
- y are the nodes (keys) of T2
- i is the index such that $y_i \leq y' \leq y_{i+1}$, it is an error if i does not exist
- $F_i = \text{Interpol}_{\text{Lin}}(\text{T2.Lut}_i, x')$ is the values of one-dimensional look-ups

E.2 Symmetric Finite Impulse Response Filter, Filter

Filter is the function applying a given set of filter coefficients (FIR_FP) onto a time-series. A range check and an outlier or jump detection method is build into Filter. Generally, the time-series shall be equidistantly spaced in order to preserve the filter characteristics; hence gaps in the time-series – up to a specified length – are filled by linear interpolation. The filter coefficients are defined in [AD03]:

| <i>Id</i> | <i>Name</i> | <i>Type</i> | <i>Description</i> |
|-----------|---|-------------------|---|
| FIR_FP | <i>Finite Impulse Response filter coefficients, symmetric</i> | | |
| | n | Integer, ≥ 0 | Number of entries in b ; $n = 0$ means no filter |
| | b | vector, length n | Filter coefficients, right-hand side, b_2, \dots, b_n are mirrored to left-hand side coefficients |
| | lim | real | Threshold for outlier or jump detection |
| | range | vector | Allowed range of input data |
| | T_nom | real | Nominal sampling period, seconds |
| | Max_Gap_Size | real | Maximum length of data gap to be filled by interpolation, seconds |

Now, Filter(FIR_FP, \mathbf{t}^{in} , \mathbf{x}^{in}) returns the time-series y :

$$y_i = \frac{b_1 x'_i + \sum_{j=2}^{n'} b_j (x'_{i+j-1} + x'_{i-j+1})}{b_1 + 2 \sum_{j=2}^{n'} b_j} \quad (\text{E-100})$$

where

\mathbf{t}^{in} and \mathbf{x}^{in} are the input vectors of data time-instants and values

$i = 1, 2, \dots, k$; k is the length of the equidistant, gap-filled time-series \mathbf{t}, \mathbf{x} (and hence also the length of y)

b is the filter coefficients of FIR_FP

\mathbf{t} is the vector of output time instants, i.e. a version of \mathbf{t}^{in} with gaps shorter than Max_Gap_Size filled with equidistant points. Formally, let $\tilde{\mathbf{t}} \subseteq \mathbf{t}^{\text{in}}$ be the time-instants of $\tilde{\mathbf{x}}$ (see below), then $\tilde{\mathbf{t}} \subseteq \mathbf{t}$, and for $i \geq j$, $i = 1 \dots k$:

$$t_i = \begin{cases} \tilde{t}_j + \frac{m}{m_0} (\tilde{t}_{j+1} - \tilde{t}_j) & \text{if } \tilde{t}_{j+1} - \tilde{t}_j > 1.5 T_{\text{nom}} \text{ and } \tilde{t}_{j+1} - \tilde{t}_j \leq \text{Max_Gap_Size,} \\ \tilde{t}_j & \text{otherwise} \end{cases} \quad \text{where } m_0 = \left\lfloor \frac{\tilde{t}_{j+1} - \tilde{t}_j}{T_{\text{nom}}} + 0.5 \right\rfloor, m = 0 \dots m_0 - 1 \quad (\text{E-105})$$

\mathbf{x}' is the vector of gap-filled data corresponding to the time-instants \mathbf{t} .

\mathbf{x}' is computed by linear interpolation in time (to the instants \mathbf{t}) of \mathbf{x} , where \mathbf{x} are the “good” values of \mathbf{x}^{in} . Let $\tilde{\mathbf{x}} \subseteq \mathbf{x}^{\text{in}}$ for which $\tilde{x}_i \in \text{range}$ then \mathbf{x} is the subset of

\tilde{x} for which (the second part of (E-110) distinguishes between single outliers and jumps):

$$|\tilde{x}_i - \tilde{x}_{i-1}| \leq \text{lim} \text{ or } |\tilde{x}_{i+1} - \tilde{x}_{i-1}| > \text{lim} \quad (\text{E-110})$$

n' is the *running* filter width, which is reduced compared to n (of FIR_FP) near the ends of the time-series and around jumps within the time-series. If there are no jumps:

$$n' = \begin{cases} i & \text{if } i < n \\ n & \text{if } n \leq i \leq k - n + 1 \\ k - i + 1 & \text{if } i > k - n + 1 \end{cases} \quad (\text{E-120})$$

If there is a jump from \tilde{x}_{m-1} to \tilde{x}_m , i.e. if $|\tilde{x}_m - \tilde{x}_{m-1}| > \text{lim}$ and $|\tilde{x}_{m+1} - \tilde{x}_{m-1}| > \text{lim}$, then n' is defined near m as:

$$n' = \begin{cases} m - i & \text{if } m - n < i < m \text{ and } i \geq m/2 \\ i - m + 1 & \text{if } m \leq i < m + n - 1 \text{ and } i \leq (k + m)/2 \end{cases} \quad (\text{E-130})$$

with m being the index of the jump closest to i . The two last conditions of Eq. (E-130) ensure consistency near the ends of the time-series – if nearer the ends than any jump, Eq. (E-120) is used.

If $n = 0$, $y_i = x'_i$ (also the case, if $n = 1$).

If any gap or outlier is detected, all affected y_i are flagged, i.e. all y_i which are n samples or closer to the gap/outlier. If a jump is detected, all affected y_i are flagged (with a different flag).

Filter(FIR_FP, x) may also be applied to time-series of vectors in which case Eq. (E-100) is applied to each component of x individually.

E.3 S/C Mass and CoG Calculation

The functions to calculate the S/C mass and CoG are given below.

Input Data

The following input data from Level 1a.AOCS.Prop_HK and Level 1a.AOCS.Thru_HK are used:

- P_A – Pressure of tank A
- P_B – Pressure of tank B
- $V_{A,j}$ – Thermistor voltages, tank A, $j = 1, \dots, 5$
- $V_{B,j}$ – Thermistor voltages, tank B, $j = 1, \dots, 5$
- V_i – Reference voltage
- t_{thrus} – Time of last thruster operation

The following characterization parameters are used:

| Element | Type | Description | |
|--------------------------------|------------|--|---|
| CCDB. Bus. Tank | Thermistor | Array of calibration coefficients for the tank thermistors, order: A1, B1, A2, B2, ..., A5, B5 | |
| | K1 | real | Thermistor circuit calibration factor. Volt |
| | K2 | real | Thermistor circuit calibration factor. Ohm/Volt |
| | K3 | real | Thermistor circuit calibration factor. Volt |
| | a | real | Steinhart coefficient 1 |
| | b | real | Steinhart coefficient 2 |
| | c | real | Steinhart coefficient 3 |
| Vcal | real | Nominal reference voltage | |
| CCDB. Structure. SC_Mass | Dry | real | Spacecraft dry Mass |
| | Fuel | LUT2d | Look-up table providing mass of fuel depending on pressure and temperature. x: pressure [bar] y: temperature [°C] v: mass [kg] |
| | wT | vector | Weights for temperature average, length 5 |
| | a | real | Filter coefficient for mass |
| CCDB. Structure. SC_CoG | Dry | vector | CoG of dry spacecraft |
| | TankA | vector | CoG of dry tank A |
| | TankB | vector | CoG of dry tank B |
| | dL | real | Variation of tank CoG in x-direction depending on pressure |

The Level 1a.AOCS.Xxx_HK, CCDB.Structure.SC_Yyy, and CCDB.Bus.Tank.Thermistors prefixes are omitted in the following if the element is unambiguous.

Algorithm

Compute the tank temperatures ($X = A$ and B , $j = 1, 2, \dots, 5$):

$$T_{j,X} = 1 / (a + b \ln(R_{j,X}) + c (\ln(R_{j,X}))^3) - 273.15 \quad (\text{E-194})$$

where

$$R_{j,X} = K2 \, dV_{j,X} / (K1 - dV_{j,X}) \quad (\text{E-196})$$

and

$$dV_{j,X} = V_{X,j} - (V_i - \text{CCDB.Bus.Tank.Vcal}) - K3 \quad (\text{E-198})$$

Calculate weighted tank temperatures ($X=A$ and B):

$$T_X = \frac{\sum_{j=1}^5 wT_j T_{j,X}}{\sum_{j=1}^5 wT_j} \quad (\text{E-200})$$

Calculate fuel mass per tank by linear interpolation in look-up table ($X=A$ and B):

$$\tilde{m}_X = \text{Interpol}_{\text{Lin}}(\text{Fuel}, P_X, T_X) \quad (\text{E-210})$$

Calculate fuel mass

$$\tilde{m}_{\text{fuel}} = \tilde{m}_A + \tilde{m}_B \quad (\text{E-220})$$

The mass should not have changed since time of last thruster operation (i.e. variations are mainly due to HK data noise). In order to reduce this noise filter fuel mass using parameter a from CCDB.SC_Mass as follows

$$m_{\text{fuel}} = \begin{cases} \tilde{m}_{\text{fuel}} & \text{if first packet after thruster operation} \\ a m_{\text{fuel, previous}} + (1-a) \tilde{m}_{\text{fuel}} & \text{otherwise} \end{cases} \quad (\text{E-230})$$

Adapt tank X (A and B) masses accordingly

$$m_X = \frac{m_{\text{fuel}}}{\tilde{m}_{\text{fuel}}} \tilde{m}_X \quad (\text{E-240})$$

Calculate spacecraft mass:

$$\text{Mass} = m_A + m_B + \text{CCDB.SC_Mass.Dry} \quad (\text{E-250})$$

Calculate centre of gravity of tanks (X=A and B):

$$\mathbf{CoG}_X = \text{CCDB.SC_CoG.TankX} - (\text{CCDB.SC_CoG.dL P}_X \ 0 \ 0)^T \quad (\text{E-260})$$

Calculate centre of gravity of spacecraft:

$$\mathbf{r}_{\text{CoG}} = \frac{\text{SC_Mass.Dry SC_CoG.Dry} + m_A \mathbf{CoG}_A + m_B \mathbf{CoG}_B}{\text{Mass}} \quad (\text{E-270})$$

E.4 Aberrational Correction

The method for the correction of the relativistic aberration is described in “Attitude Correction for Relativistic Aberration” [Attitude Correction for Relativistic Aberration.pdf](#) (next pages). The inertial reference frame ($v s n$) – Vernal, Summer, North – is orientated identical to ($x y z$) of the ICRF. The velocity vector of the observer is with respect to the Stars, i.e. it shall include S/C orbit velocity as well Earth velocity.

Attitude Correction for Relativistic Aberration

Troelz Denver, August 2005

Background

When a scene (e.g. a star field) is observed by an observer moving at high velocities tangential to the scene direction, the apparent position of the scene objects (e.g. stars) will shift towards the motion direction. The measurements of a sensor determining the position of scene objects will therefore be shifted in the forward direction of motion. On the contrary, the measurements of a sensor determining its own position based on scene objects will be shifted in the backward direction. When the sensor velocity is not orthogonal to the observed scene, the correction magnitude will decrease by sinus to the angle between the velocity vector and the vector to the scene.

Procedure

Let an attitude of a sensor, A , be defined as a orthogonal 3 x 3 matrix:

$$\bar{A} = [\bar{x} \quad \bar{y} \quad \bar{z}] = \begin{bmatrix} vx & vy & vz \\ sx & sy & sz \\ nx & ny & nz \end{bmatrix}$$

such that the three columns in A defines the orientation of the sensor axes (called x , y and z) in an inertial reference frame with axes called v , s and n . The sensor frame is defined such that the z -axis is equal to the pointing direction and the x and y are selected such that an arbitrary right-handed coordinate system is realized.

Furthermore, let the velocity of the sensor, v , be defined as:

$$\bar{v} = \begin{bmatrix} vv \\ vs \\ vn \end{bmatrix}$$

such the three elements define the velocities along each of the three axes of the inertial reference frame. The element units are m/s.

First of all, a vector to perform the correction about, v_r , is derived as the cross product between the observation direction and the velocity vector.

$$\bar{v}_r = \frac{\bar{v} \times \bar{z}}{c}$$

where the speed of light, c , is given in the same units as the elements of v (m/s). Since $|v_r|$ is proportional to sinus to the angle between v and z , the magnitude dependency of this angle is already included in the figure.

In the following description, it is applied that the rotations about different system axes do commute for small angular motions. The correction for each of the system axes is performed. The new z -axis is found from adding the correction to the original axis:

$$\vec{\hat{z}} = \vec{z} + \vec{z} \times \vec{v}_r$$

Similar, the two other system axes will be corrected accordingly:

$$\vec{\hat{x}} = \vec{x} + \vec{x} \times \vec{v}_r$$

and

$$\vec{\hat{y}} = \vec{y} + \vec{y} \times \vec{v}_r$$

The attitude at this stage formed by the three independently corrected system axes will not be orthogonal. Again, it is used that rotations about system axes will commute for small angular motions.

First of all, the corrected attitude z -axis is formed by the estimated z -axis by a simple normalization:

$$\vec{z}' = \frac{\vec{\hat{z}}}{|\vec{\hat{z}}|}$$

The corrected attitude y -axis is formed by the z -axis and the previously estimated x -axis:

$$\vec{y}' = \frac{\vec{z}' \times \vec{\hat{x}}}{|\vec{z}' \times \vec{\hat{x}}|}$$

Finally, the corrected attitude x -axis is found to realize the right-handed coordinate frame:

$$\vec{x}' = \vec{y}' \times \vec{z}'$$

The corrected attitude, A' , given as

$$\vec{A}' = [\vec{x}' \quad \vec{y}' \quad \vec{z}']$$

will now be orthogonal.

Appendix F

ASM Algorithm Descriptions

The description of the Swarm ASM Level 1b processing algorithms supplied by the instrument manufacturer is contained in [AD05]: “Swarm ASM level 1B algorithms”, [SW-CEA-AUT-ALGO1B-001 4-0.pdf](#).

Appendix G

VFM Algorithm Description

The description of the Swarm VFM instrument and the Level 1b processing algorithms supplied by the instrument manufacturer is contained in [AD06]: “Vector Field Magnetometer for the Swarm Project, Users Manual”, [SW-MA-DTU-VF-5001_2 UserManual.pdf](#)

Appendix H

STR Algorithm Description

The description of the Swarm STR instrument and the Level 1b processing algorithms supplied by the instrument manufacturer is contained in [AD07]: “micro Advanced Stellar Compass User’s Manual”, [ASC-DTU-MA-3001 v2.0 User Manual.pdf](#).

Appendix I

EFI-TII Algorithm Description

The Swarm EFI instrument package consists of the Thermal Ion Imager (TII) and the Langmuir Probe (LP) instruments. The description of the TII Level 1b processing algorithms supplied by the instrument manufacturer is contained in [AD08]: “Swarm CEFI Level 1b Processor Definition“, [SW-TN-UOC-EF-003.pdf](#), version 1.14.

Appendix J

EFI-LP Algorithm Description

The Swarm EFI instrument package consists of the Thermal Ion Imager (TII) and the Langmuir Probe (LP) instruments. The description of the LP Level 1b processing algorithms supplied by the instrument manufacturer is contained in [AD09]: “Swarm CEFI-LP Level 1b Algorithms”, [SW-TN-IRF-EF-003_level1b_algorithms.pdf](#), version 2.6.

Appendix K

GPSR Algorithm Description

The description of the Swarm GPSR Level 1b processing algorithms supplied by the instrument manufacturer is contained in [AD11]: “Swarm GPSR TE-12 Instrument L1b Algorithms Definition”, [SW-TN-SES-GP-0018_6.pdf](#).

Appendix L

ACC Algorithm Description

The description of the Swarm ACC instrument Level 1b processing algorithms supplied by the instrument manufacturer is contained in [AD13]: “Accelerometer Instrument Level 1b Algorithms Definition”, [SW-DF-VZL-AC-0001 3 4 L1B Algorithm.pdf](#).